THE DEVELOPMENT OF CONNECTIVITY AND THE NATURE OF SYNAPTIC TRANSMISSION BETWEEN AVIAN SONG CONTROL NUCLEI

Thesis by

Richard Daniel Mooney

In Partial Fulfillment of the Requirements
for the Degree of
Doctor of Philosophy

California Institute of Technology
Pasadena, California

1991

(Defended January 11, 1991)

ACKNOWLEDGMENTS

I would like to extend my special appreciation to Mark Konishi. He has been a great advisor in every sense of the word. Beyond creating a stimulating and productive environment in which to work, he ultimately taught me by example. I know that I will continue to profit by his example for the rest of my life.

I would also like to thank the Caltech biology faculty in general, especially Drs. Van Essen, Patterson, and Anderson. All of these people provided me with guidance and advice that have only grown more valuable in hindsight.

Dr. Scott Fraser, equipped with more ideas and technical expertise than I ever knew what to do with, was even more valuable as a friend and teacher. I am extremely grateful for his willingness to discuss and explain ideas to me. His patience and advice are truly appreciated.

Dr. Gilles Laurent, who was deluged with several of my manuscripts shortly after his arrival, responded with many helpful comments. Gene Akutagawa provided superb technical training, and was boundless in his enthusiasm for birdsong.

My many fellow students have been greatly appreciated. I would especially like to thank Larry Proctor for writing software, and for our many interesting conversations, helpful to my work. Derek Stemple has been a great friend and has always amazed and benefited me with his incredible intellectual breadth. Moreover, he never tired of my jokes. Mahendra Rao was also a helpful collaborator in the initial stages of the project. Finally, I would like to thank Allison Doupe for her scientific support and great friendship.

ABSTRACT

Song is a learned vocalization unique to passerine birds. Young songbirds hear and memorize their father's song and then, as they mature, match their own song to the memorized model using auditory feedback. Song is controlled by a specialized neural circuit in the songbird's brain. The primary song control circuit is involved in vocal motor control, and is essential to song production in the adult. An "accessory" portion of the circuit appears unnecessary for adult song production, but is required for normal song development. The discrete nature of the song circuit, plus the stereotyped nature of song development, promise that the acquisition and refinement of a learned behavior can be understood on a cellular level.

The robust nucleus of the archistriatum (RA), located in the songbird's caudal forebrain, is part of the primary pathway, and projects to motoneurons innervating the vocal musculature. RA is innervated by nucleus HVc, another primary structure, and by nucleus MAN, part of the accessory pathway.

This study examines the changes in connectivity and the nature of synaptic transmission between these nuclei during development. MAN terminals were present within RA fifteen days after hatching, although HVc axons did not enter the nucleus until ten days later. The physiology of MAN and HVc synapses within RA was examined in an *in vitro* brain slice preparation. Before day 25, stimulation of MAN, but not HVc, fibers evoked excitatory synaptic potentials from virtually all RA neurons. MAN EPSPs were glutamatergic and activated NMDA-receptors on RA neurons. In slices prepared from male birds 40 to 70 days old, stimulation of MAN and HVc fibers evoked synaptic responses from most RA neurons. The properties of MAN EPSPs resembled those observed before day 25. Unlike the MAN EPSPs, HVc

EPSPs were largely mediated by non-NMDA glutamate receptors. Both EPSPs could be enhanced for long periods of time by certain patterns of electrical stimulation.

Therefore, connections important to song development form before those essential to adult song production. These two pathways exhibit distinct pharmacological properties that may be related to their specific roles in song acquisition and production.

TABLE OF CONTENTS

LIST OF ILLUSTRATIONS

CHAPTER 1. INTRODUCTION

SONG AND ITS BEHAVIORAL SIGNIFICANCE

The acquisition and refinement of motor patterns is fundamental to the behavioral development of most vertebrates. Many behaviors are purely innate; although they may require practice in order to be perfected, they do not require an external model to develop correctly. Most locomotor skills, such as walking in terrestrial animals, and swimming in aquatic animals, are innate. In contrast, many other vertebrate behaviors are acquired by copying or imitating an external model. The songs of certain birds of the order Passeriformes fall into this latter category.

Recent scientific interest in birdsong stems from two important observations. The first is that young songbirds learn their songs from other birds. The second is that song is controlled by specialized groups of neurons within the bird's central nervous system. These two features offer promise that the neuronal mechanisms involved in song learning and production can be elucidated.

Song refers to a specific type of vocalization produced by passerine (perching) birds. Song can be distinguished from other avian vocalizations, such as calls, in that it is often produced spontaneously, without any triggering stimulus, and that it is accompanied by a specific body posture (Konishi 1985). Many other birds, such as chickens (Galliformes) and doves (Columbiformes), produce complex vocalizations (such as crowing and cooing) that may be functionally equivalent to passerine song, but differ in that they are innate (Marler and Peters 1981). A fundamental feature of passerine song is that it is a learned behavior.

Song may function both to establish and maintain a certain territory, and to attract and retain a mate (Catchpole 1982). As McDonald (1989) asserts, these functions need not be mutually exclusive. Field experiments have demonstrated that male Great tits (*Parus major*) will refuse to enter territories in which the recorded songs of other Great tits are being broadcast (Krebs 1977). Furthermore, male Scott's seaside sparrows (*Ammodramus maritimus peninsulae*), muted at the onset of their breeding season by rupture of the interclavicular air sac, fail to acquire mates and establish territories (McDonald 1989). When males were muted later in the breeding season, after having already established territories and acquired mates, both mates and territories were lost. These losses usually were recouped when the air sac healed and the birds began to sing again. McDonald's results, although striking, do not determine whether the loss of the female mate is a direct result of muting, or follows as an indirect consequence of the muted males' reduced territories. Regardless of its primary function, birdsong is a necessary behavioral prerequisite to successful reproduction in most passerine species. The variable issue in any given case is whether song functions in intrasexual selection (i.e., repulsive interactions between males and the acquisition of territory), or in intersexual selection (i.e., to attract females) (Catchpole 1982).

Certain estrildid finches, including the zebra finch (*Taeniopygia guttata*) and the Bengalese finch (*Lonchura striata*), sing primarily to attract females, not to establish territories (Hall 1962). In these species, females exhibit more copulation displays in response to the songs of conspecific males of their own race, than to either conspecific song of a different race, or to heterospecific song (Clayton and Prove 1989). When exposed only to conspecific song of their same race, female estrildids respond most strongly to

the longest and most complicated songs (Clayton and Prove 1989). Therefore, the songs of zebra and Bengalese finches may serve as heterospecific isolating mechanisms, as well as to increase the male's reproductive success by heightening female receptivity (Clayton and Prove 1989).

SONG LEARNING AND DEVELOPMENT

The stereotypy of the adult or "full" song belies the fundamentally plastic nature of its development. Song progresses through several distinct phases before attaining its stable adult form. Immelmann (1969) has characterized this developmental progression in the zebra finch. Although zebra finch songs develop more rapidly than do those of many other species, the basic sequence is similar in most other songbirds. The earliest song produced by the male zebra finch begins around thirty days after hatching, and may develop continuously from the young bird's begging calls. This stage, called subsong, can be distinguished by both its rambling quality and its low volume. Over the next several weeks, subsong yields to plastic song, which is louder and contains certain elements that are repeated more frequently. Plastic song also marks the first construction of individual song phrases, which are more elaborate acoustic structures containing several individual song syllables. The species-specific nature of the song becomes quite apparent during plastic song, but the overall duration of the song, as well as its constituent syllables, may continue to vary from one bout of singing to the next. The variability of the plastic song declines over the next several weeks, and the song becomes highly stereotyped in its acoustical structure between eighty and one hundred days after hatching. At this point, the song is fixed, or "crystallized," and can remain unchanged almost indefinitely. In the zebra finch, less than two months

pass between the initial onset of song and the attainment of its final, crystallized form.

A key feature of song is that it is a learned behavior. Male zebra finches normally copy the acoustic structures of their father's song (Immelmann 1969). Two sets of experiments illustrate that the bird's early auditory experience influences the song it subsequently produces. First, songbirds raised in complete acoustic isolation generate a song that differs noticeably from the wild-type song. Such isolate song consists of a smaller total number of syllables, and the syllable type is of a more simple variety, than those normally found in the wild-type song (Immelmann 1969; Price 1979). In another manipulation, zebra finch eggs were placed in the nests of Bengalese finches, a related species that produces a song distinct from that of the zebra finch (Immelmann 1969). Upon maturation, the male zebra finches raised in these nests produced a song resembling that of their Bengalese foster fathers.

Song learning occurs in two distinct phases. In the first of these stages, commonly referred to as the sensory phase of song acquisition, the young bird listens to and memorizes the tutor song, a term that denotes the song ultimately copied by the young songbird. The second or sensorimotor phase refers to the stage in which the bird vocally reproduces the tutor song.

The sensory phase can occupy a rather limited period early in the bird's life. Young zebra finches, initially raised by their natural fathers, then acoustically isolated after day thirty-five, developed song copies as complete as those produced by birds that were never isolated from their fathers (Bohner 1990). Therefore, in certain conditions, young zebra finches exhibit the capacity to learn their father's song in a relatively short period of time. Some evidence suggests that the duration of the sensory phase may be regulated by the quality of the young bird's auditory experience. Young zebra finches isolated from their

natural fathers between days 35 and 60 days of age, but subsequently exposed to a *new* song model, will copy elements of the new model (Eales 1985). The colonial breeding habits of the zebra finch may increase the probability that young zebra finches will copy portions of songs produced by males other than their natural fathers, and consequently, this fact may explain how individual differences in song arise (Bohner 1983; Williams 1990). Nevertheless, sensory acquisition remains limited to the early portions of the zebra finch's life.

The sensory phase of song acquisition often ends before sensorimotor learning actually begins. Species such as the Swamp Sparrow (*Zonotrichia georgiana*) can experience a gap as long as eight months between the end of the sensory phase and the first renditions of plastic song (Marler and Peters 1981). These observations, as well as isolation experiments (Bohner 1990), suggest that young birds commit the tutor song to memory during the sensory phase. Once this memorization process is complete, song development will progress normally without any further exposure to the tutor song. The vocal refinement that characterizes sensorimotor learning can be achieved purely from memory.

Although songbirds no longer need to hear the tutor song during sensorimotor learning, they still must be able to listen to their own vocalizations for their songs to develop normally. White-crowned sparrows (*Zonotrichia leucophrys*) and zebra finches deafened before the onset of subsong produced highly aberrant songs as adults, even when deafening occurs after the sensory phase is normally over (Konishi 1965; Price 1979). Even the song of birds raised in acoustic isolation are degraded by early deafening, suggesting that birds still listen to their own vocalizations during sensorimotor learning, even when a tutor model is absent during sensory acquisition (Konishi and Nottebohm 1969). In contrast, non-passerines still produce a complete

repertoire of species-specific vocalizations as adults despite early deafening (Konishi 1963).

One hypothesis is that in sensorimotor learning, songbirds use auditory feedback to match their own vocalizations to the auditory memory formed during sensory acquisition (Konishi 1965). In normal situations, a young bird matches its own song to the memorized tutor model. When birds are raised in acoustic isolation, however, auditory feedback is still used to match the bird's song to an innate pattern. In either situation, songbirds correct errors in their vocal output through the use of auditory feedback. The internal standard that a bird uses to identify these vocal errors is called the template (Konishi 1965).

Song no longer depends intimately on auditory feedback with the onset of crystallization. Zebra finch as well as white-crowned sparrow song does not change once crystallization occurs, even when birds are subsequently deafened (Konishi 1965; Price 1979). Songbirds require an intact auditory system for both sensory acquisition and the subsequent vocal modification of sensorimotor learning, but not for the short-term maintenance of the stable, crystallized song.

NEURAL MECHANISMS: THE SONG CONTROL SYSTEM

The discovery of a discrete, vocal-control circuit within the songbird brain greatly advanced our understanding of the neural mechanisms controlling song. This circuit was first delineated in the canary through a combination of anatomical and behavioral (lesion) techniques (Nottebohm et al., 1976). Subsequent work in the canary and the zebra finch has elucidated a complex circuit that includes at least five forebrain nuclei, two thalamic nuclei, one midbrain nucleus, and one hindbrain nucleus (Bottjer et al., 1989; Gurney 1981; Nottebohm et al., 1982; Okuhata and Saito 1987). These brain nuclei,

collectively referred to as the song control system, are represented schematically in Figure 1. Although the song system is quite complex, it can be more readily comprehended when viewed as the combination of two functionally distinct pathways. The primary pathway includes those song control nuclei that are essential to song production in the adult bird. These include the nucleus interfacialis (NIf), the nucleus hyperstriatum ventrale, pars caudale (HVc), the nucleus robustus archistriatalis (RA), and the nucleus nervi hypoglossi, pars tracheosyringealis (nXIIts). NIf, HVc, RA, and nXIIts form a serial, descending chain of nuclei that, by way of motoneurons in nXIIts, are connected to the muscles of the avian vocal organ, or syrinx. The accessory pathway includes several nuclei that make anatomical connections to the primary nuclei, but are not essential to normal song production in the adult bird. These consist of area X of the lobus parolfactorius, the medial nucleus of the dorsolateral thalamus (DLM), the magnocellular nucleus of the anterior neostriatum (MAN), and the thalamic nucleus uvaeformis (Uva).

The primary song pathway

Two different observations indicate that the primary pathway plays a direct role in the elaboration of song. First, the lesioning of NIf, HVc, or RA, or the sectioning of the hypoglossal nerve, results in the loss of most or all of the syllables constituting the adult song (McCasland 1987; Nottebohm et al., 1976; Simpson and Vicario 1990). Bilateral lesions of HVc can exert extremely specific effects on the song: when presented with a female canary, a male canary with bilateral HVc lesions displayed all of the postures associated with singing, but failed to open its bill, and remained mute (Nottebohm et al., 1976).

Figure 1. Schematic of the song control circuit.

A parasagittal view of the songbird brain, in which various song control nuclei are depicted in black. The descending vocal motor control pathway includes nucleus HVc, nucleus RA, and the hypoglossal nucleus (nXIIts). Motoneurons located in nXIIts innervate the muscles of the syrinx, the avian vocal organ. Other song control nuclei include area X, which receives afferent input from HVc; nucleus MAN, which provides afferent input to RA; and the thalamic nucleus DLM, which interconnects X and MAN. Auditory regions are represented by cross-hatching. This includes Field L, the primary telencephalic recipient of ascending auditory projections from the thalamus, which makes axonal projections to regions contiguous with HVc and RA. The thalamic nucleus Uva and the telencephalic nucleus NIf are not shown in this diagram for the sake of clarity.

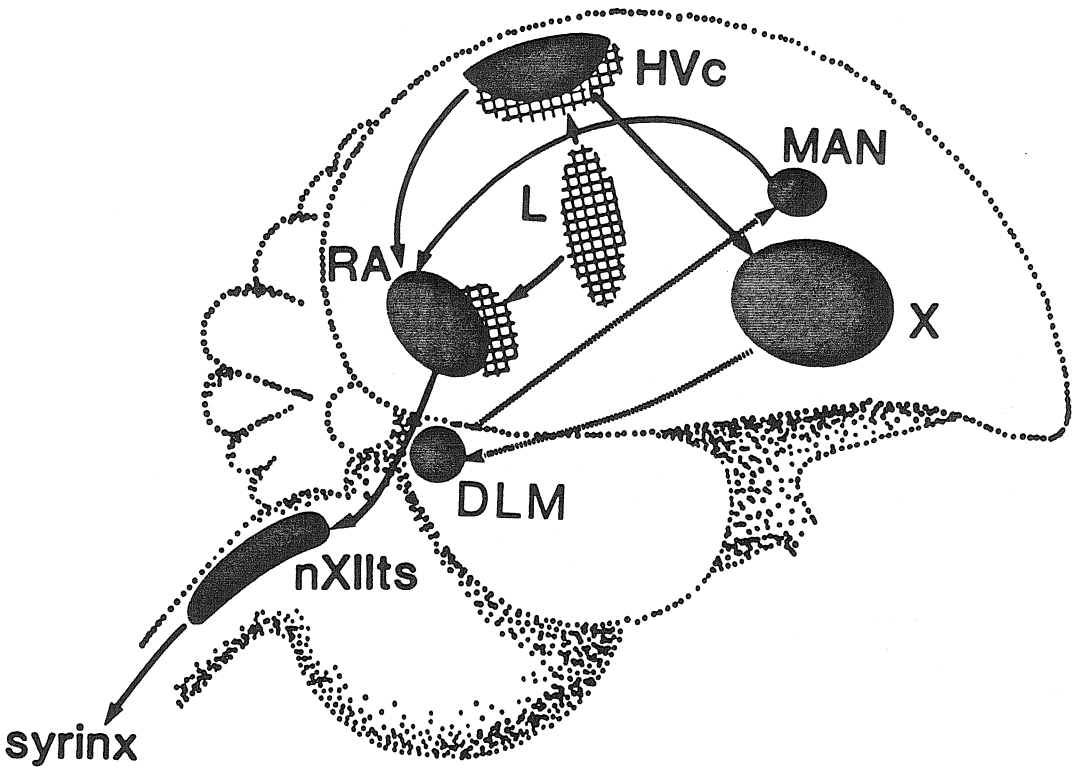
HVc
MAN
L
RA
X
DLM
nXIIts
syrinx

The second observation was made when chronic electrophysiological recordings were obtained from the primary song nuclei in singing birds (McCasland 1987). NIf, HVc, and RA all exhibited a marked increase in patterned activity immediately preceding the onset of each song syllable. Audible elements in the song were preceded by heightened neural activity in each of these nuclei, while diminished activity preceded periods of silence. Finally, the latency between the increased activity in a given area and the actual utterance of the corresponding sound was greatest for NIf, next longest for HVc, and shortest for RA, consistent with their anatomical relationship. These observations support the idea that NIf, HVc, RA, and nXIIts form a descending pathway that is directly involved in vocal motor control during song.

The accessory song pathway

Besides the innervation it supplies to RA, HVc also sends axonal projections to area X (Nottebohm et al., 1976). Area X in turn projects to the dorsolateral nucleus of the medial thalamus (DLM), which in turn projects back into the forebrain, where it innervates the lateral lobe of MAN (Bottjer, Halsema et al. 1989; Okuhata and Saito 1987). Neurons within the lateral part of MAN are connected to the primary pathway via their axonal terminations on RA neurons (throughout this thesis, I will refer to lateral MAN simply as MAN, unless otherwise stated) (Gurney 1981; Nottebohm et al., 1982). The accessory pathway can be viewed as a loop that begins in HVc, travels through the thalamus, and circles back onto the descending vocal motor control pathway at the level of RA.

After song crystallization, lesions made within the accessory pathway have no immediate effects on the quality of the bird's song. Electrolytic and chemical lesions of area X do not alter the songs produced by adult

canaries and zebra finches (Nottebohm et al., 1976; Sohrabji et al., 1990). Similarly, lesions of zebra finch MAN made either in the late plastic stages of song, or following song crystallization, do not cause any deterioration in song quality (Bottjer et al., 1984). At present, no data exist on the effects of DLM lesions in adult songbirds, or on the question of whether MAN and X lesions exert deleterious effects on song over longer time periods (> 5 weeks). These experiments do reveal that, in adult birds, MAN and X do not play an immediate role in the motor control of song.

Experimental evidence suggests that MAN and X exert fundamental effects on song development, even though they are not essential to normal song production in the adult. Lesioning either MAN or X during the early stages of sensorimotor learning markedly disrupts normal song development. Before day 65 in the zebra finch, MAN lesions are followed by severe, irreversible deterioration in the song quality (Bottjer et al., 1984). X lesions in zebra finches younger than 45 days old also disrupt song development by arresting the refinement of song syllables (Sohrabji et al., 1990). Unlike MAN lesions, however, X lesions are not accompanied by any pronounced degradation of song syllable quality (Sohrabji et al., 1990).

NEUROTRANSMISSION WITHIN THE SONG SYSTEM

To date, our knowledge of the specific neurotransmitters acting within the song system has been limited primarily to immunohistochemical studies, which were recently reviewed by Ball (Ball 1990). Immunostaining has indicated that various neuropeptides, including substance P, vasoactive intestinal peptide (VIP), methionine-enkephalin (MET), cholecystokinin (CCK), as well as nicotinic cholinergic receptors, are present within the song system (Ball et al., 1988; Ryan et al., 1981; Watson et al., 1988). Receptor-binding

assays have also detected muscarinic cholinergic receptors (Ryan and Arnold 1981), as well as adrenergic receptors (Barclay and Harding 1988), within certain song control nuclei. Finally, HPLC studies suggest that dopamine, acetylcholine, and norepinephrine may also act within the song system (Sakaguchi and Saito 1989). These studies imply that a variety of neuromodulatory systems are present within the song system, and that these may interact with primary excitatory and inhibitory neurotransmitters to shape the activity of neurons within individual song control nuclei. Still lacking, however, is a physiological description of how these different systems interact and more importantly, what the identities of the primary neurotransmitters within the song system really are. Until such a description is provided, the wealth of data provided by neurochemical approaches cannot be integrated into a more complete perspective relating neurotransmission to the song behavior itself.

TOWARDS A CELLULAR MODEL OF SONG LEARNING

One major goal of modern neurobiology is to discover the cellular mechanisms responsible for the acquisition of learned behaviors. The first step towards this goal depends on establishing that the behavior of interest is actually learned. The second step requires the delineation of the neural circuit mediating the behavior. The third step requires actually analyzing the cellular properties within the circuit, and characterizing how these properties change over the period in which the behavior is being learned.

Clearly, as discussed in the previous sections, the song system satisfies the first two requirements. Song is a complex, yet highly stereotyped, learned behavior. The song control nuclei that mediate singing are well delineated from surrounding brain regions, and their basic interconnections are known. The third requirement, an analysis of the cellular properties of song

control neurons over the course of song development, has remained largely unfulfilled.

Despite the wealth of analysis at the behavioral level, as well as the substantial anatomical description of the song system, little is actually known about the detailed physiology of song system neurons. The physiological nature of synaptic connections between different song control areas, as well as synaptic transmission between neurons within individual song control nuclei, are probably the most poorly understood aspects of the song system. However, an explicit knowledge of synaptic properties within the song system will be an essential prerequisite to the understanding of every aspect of song from sensory acquisition to the production of the crystallized behavior.

The present experiments constitute an initial step in the pursuit of the cellular mechanisms relevant to song learning and production. My strategy was to develop an acute *in vitro* brain slice preparation in which the synapses formed between presynaptic axons originating in MAN and HVc and postsynaptic neurons in RA could be examined systematically at different stages in the development of song. The birdsong brain slice preparation permitted detailed intracellular analyses of synaptic physiology, as well as anatomical descriptions of the structure of pre- and postsynaptic elements.

I focused on RA because by virtue of the synaptic input from HVc and MAN, it is an important site of convergence between the primary and accessory pathways of the song circuit. One hypothesis is that these two pathways interact during song development to stabilize the motor program most closely matching the tutor model. RA is the last telencephalic locus where such interaction may occur, since it projects directly onto the hypoglossal motoneurons innervating the syringeal musculature. Therefore, knowledge of the time when MAN and HVc first establish connections with RA neurons, as

well as the physiological properties of their synaptic terminations within RA, may be especially relevant to changes in the bird's behavioral capacity to learn and produce song.

Another reason for focusing on RA is that, like other song control nuclei, it develops into a markedly sexually dimorphic structure in the adult zebra finch (Nottebohm and Arnold 1976). The sexual dimorphism of the song system is under the control of steroid hormones, which act during a distinct and limited critical period early in the bird's life (Gurney 1981; Konishi and Akutagawa 1988). Previous studies have shown that hormones influence the pattern of HVc axonal projections to RA in a sexually dimorphic fashion (Konishi and Akutagawa 1985). Differential innervation of RA might be the cause of the great differences in RA cell number between the adult male and female. Detecting changes in other afferent inputs to RA near the closure of the critical period might reveal mechanisms responsible for sexual differentiation in the song system.

These experiments were not intended to define the end state of the circuit in the mature animal after the behavioral consolidation of song crystallization was completed, but rather to examine circuit properties in the juvenile brain, when song plasticity was most pronounced. The first step was to characterize the physiological properties of RA neurons, as well as their synaptic responses to afferents arising from MAN and HVc, at the very onset of song learning. I then examined the same pathway in brain slices prepared from increasingly older animals, to characterize any changes in synaptic transmission that might be correlated with the behavioral development of song.

The experimental body of this thesis consists of three sections. In the first section, anatomical techniques were used to image the presynaptic axons from MAN and HVc, as well as the postsynaptic neurons in and near RA,

at different developmental stages. In the second section, an *in vitro* brain slice preparation was developed to examine the physiological properties of the MAN and HVc synapses within RA. In the first part of this section, the intrinsic properties of postsynaptic RA neurons were studied, and in the second part, the synaptic responses evoked from these neurons by MAN and HVc fiber stimulation were characterized. Pharmacological manipulations identified characteristics that differed between the synapses that MAN and HVc make within RA. In the third and final section, different patterns of electrical stimulation applied to the MAN and HVc fiber pathways *in vitro* were used to determine whether either pathway could exhibit use-dependent changes in synaptic strength.

CHAPTER 2. THE ANATOMICAL DEVELOPMENT OF CONNECTIVITY BETWEEN THREE FOREBRAIN SONG CONTROL NUCLEI

ABSTRACT

This chapter provides an anatomical description of the development of connections between several song control nuclei. In the adult male zebra finch, the song control nucleus RA receives afferent input from two other forebrain song control nuclei, HVc and MAN. Previous studies have shown that HVc axons arrive at the dorsal border of RA as early as day fifteen, but do not enter the nucleus until ten to fifteen days later. The present study examines this "waiting" phenomenon in more detail, and contrasts it with the development of axonal projections from MAN to RA. The waiting compartment, or the area immediately dorsal to RA where HVc axons ramify before entering the nucleus, was studied with an *in vitro* brain slice preparation. Neurons within this region were stained intracellularly, and their responses to electrical stimulation in HVc were noted. Other anterograde and retrograde connections were also revealed by tracing early projections from HVc and MAN. Finally, RA neuronal morphology was characterized immediately before and after the ingrowth of HVc axons into the nucleus. MAN terminals were present within the male and female RA by day fifteen, and persisted there throughout adult life. Before day twenty-five, however, RA-projecting HVc axons were restricted to the area dorsal to RA. This contrasts with the projection from HVc to area X, which appears to be established by day twenty. Neurons in the region immediately dorsal to RA, within the waiting compartment, had dendrites oriented in the same plane as the HVc axon terminals, and extended axon collaterals dorsally towards HVc. Electrical stimulation in HVc evoked EPSPs from neurons within

the waiting compartment. RA neurons possessed many adult characteristics by day twenty, but in the male, continued to grow in a process that might involve the episodic elaboration of dendritic growth cones. The observation that MAN and HVc axons enter RA at different stages may relate directly to their specialized roles in song development.

INTRODUCTION

A clear relationship exists between the extreme sexual dimorphism of the adult song system and the contrasting abilities of male and female birds to produce song (Nottebohm and Arnold 1976). In the zebra finch, the adult female song nuclei are reduced in total volume, cell size, and number when compared to the male (Bottjer et al., 1986; Gurney 1981; Konishi and Akutagawa 1987). The behavioral consequence of this extreme sexual dimorphism is that males produce song, whereas female do not (Gurney 1982).

The hormonal experience of the young bird influences the architecture of the adult song system. Female zebra finch chicks implanted with estrogen develop masculinized song systems, and can produce song in adulthood (Gurney 1981; Gurney and Konishi 1980). These effects are limited to a posthatch critical period, and beyond day 45, the female song system becomes refractory to the masculinizing effects of estrogen (Konishi and Akutagawa 1988).

The mechanism by which estrogen acts is still unknown, but in nucleus RA, its major effect is to prevent cell death. Despite the striking degree of sexual dimorphism in the adult RA, the male and female zebra finch begin posthatch life with a similar complement of RA neurons (Konishi and Akutagawa 1985; Konishi and Akutagawa 1990). The sexual differentiation of RA begins

twenty-five to thirty days after hatching, when RA neurons atrophy and die in the female, but survive and grow in the male (Konishi and Akutagawa 1987).

Anatomical evidence suggested that estrogen might rescue RA neurons through an innervation-dependent mechanism. RA-projecting HVc axons were labeled with tritiated-proline at different developmental stages (Konishi and Akutagawa 1985). In the male, HVc terminals accumulated along RA's dorsal border as early as day fifteen, but remained there until day twenty-five, after which time they entered the nucleus. Although their development was similar to the male's before day 25, the female's HVc axons remained restricted from RA during the period of cell death, and even in adulthood, provided RA with little or no innervation. Therefore, RA's sexual dimorphism may arise from differential innervation by axons originating in HVc. In support of this interpretation, when RA-projecting HVc axons were severed on one side of the brain in a 15 day old male finch, the RA neurons on the cut side atrophied and died, whereas the RA neurons on the uncut side developed normally (Konishi and Akutagawa 1987). The male's steroidal milieu apparently cannot maintain RA neurons deprived of afferent input.

The development of the MAN axonal projection to RA is less well characterized. Although MAN axons are known to innervate the adult RA, it is not known when they first enter the nucleus. Clarifying the role of innervation in the sexual differentiation of RA depends on knowing when and how MAN axons form connections with RA.

In this study, I examined the development of connectivity between MAN, HVc, and RA. MAN axons were labeled with anterograde tracers, such as DiI, and their terminal fields imaged both with conventional epifluorescent and confocal microscopy. The MAN pathway was traced before the period of sexual differentiation occurred, and throughout the period of cell death in the female.

The projection between HVc and RA was also studied in animals less than twenty-five days of age, and special attention was focused on the HVc terminals situated along RA's dorsal border. Employing an *in vitro* slice preparation, neurons within this plexus of HVc terminals were stained with Lucifer Yellow or biocytin, and their responses to the electrical stimulation of the HVc fiber tract were noted.

MATERIALS AND METHODS

Fixed brain DiI

HVc axon terminals were labeled with DiI (1,1'-dioctadecyl-3,3,3',3'-tetramethylindocarbocyanine perchlorate, Molecular Probes, Inc.) in either fixed whole brain or in fixed parasagittal brain slices. Birds were deeply anesthetized with a lethal dose of Equithesin (>0.06 ml), and perfused transcardially with warmed (40°C), heparinized saline for five minutes, followed by fixative (4% paraformaldehyde and 0.1% glutaraldehyde in 0.025 M phosphate buffer) for another thirty minutes.

To label HVc axons in the whole brain, the fixed head was placed in a stereotaxic apparatus and small pressure injections (WPI Pico Pump) of 25% (w/v) DiI in absolute ethanol were placed in HVc through a glass micropipette (tip diameter ~10μm). To label HVc axons in fixed brain slices, a 500 μm thick parasagittal slice of fixed brain tissue containing HVc and RA was cut on a vibratome and placed in a Sylgard dish on the fixed stage of an upright microscope. Small pressure injections of DiI were made into HVc after locating it under transillumination. The injection size was tightly controlled by monitoring the efflux of the dye from the micropipette tip under epifluorescent illumination. Tissue was then stored in fixative at 37°C for 2 to 4 weeks.

MAN terminals were labeled by injection of either concentrated DiI or DiI crystals into the whole, fixed brain. After fixation as above, the head was mounted in a stereotaxic apparatus and blocked transversely just anterior of MAN. The brain was rotated to expose the rostral face of MAN and small pressure injections were placed in the nucleus. The brain subsequently was stored in fixative for 6 to 10 weeks at 37°C.

In vivo DiI

In vivo, stereotactic injections of DiI were made into the MAN or HVc of birds anesthetized with Equithesin (0.04 to 0.05 ml), or a combination of Metofane and ketamine. One hundred nanoliters of a 1% (w/v) solution of DiI in absolute ethanol were injected into the target area with a 1 µl Hamilton syringe. Survival times varied, but optimal anterograde transport usually required a 96-hour survival time after the injection, as opposed to 24 to 48 hours for retrograde transport. Vibratome sections 50 to 200 µm thick were prepared from tissue following fixation as outlined above.

DiI-Mediated Photoconversion of DAB

In certain cases, the fluorescence emitted by the DiI-labeled material was used to photooxidize diaminobenzidine (DAB) in order to produce a permanent, light opaque stain. The protocol was similar to that outlined elsewhere (Sandell and Masland 1988), except that an Olympus IMT-2 inverted microscope with a 100 Watt Mercury lamp was used. In most cases, tissue was illuminated with a 6.3x Zeiss Neofluar objective. After the photoconversion was finished, sections were washed, mounted on gelatin-coated slides, air-dried, dehydrated in 100% ethanol, cleared in xylene, and coverslipped with Permount.

WGA-HRP

Birds were anesthetized with 0.02 to 0.04 ml of Equithesin injected intramuscularly. The bird was placed in a stereotaxic apparatus, the scalp retracted, and a small window was made in the skull overlying HVc. A glass electrode (Haer Ω-dot borosilicate capillary glass, 1.2 mm diameter, with fiber), with a tip diameter of ~15 μm, was filled by capillarity with a 2% (w/v) solution of WGA-HRP (Sigma) in 0.1 M Tris hydrochloride. Relying on stereotactic coordinates, the electrode was positioned in HVc, and the WGA-HRP solution was iontophoresed from the pipette tip with positive current (~4 μA) pulses five seconds in duration every ten seconds. Total injection times varied from two to six minutes in length.

After a twenty-four to thirty-six hour survival period, the bird was anesthetized with an overdose of Equithesin, perfused transcardially first with warmed (37°C), 0.9% saline, then with cooled (4°C) 2% paraformaldehyde and 2% glutaraldehyde in 0.05M phosphate buffer (PB), followed by cooled (4°C) 10% sucrose in 0.05M PB. The brain was then removed and allowed to sink overnight in 30% sucrose in 0.05M PB. Sections 30 to 90 μm thick were cut with a freezing microtome and collected in 0.05M PB on ice, rinsed three times with distilled water, and then incubated for thirty minutes in a tetramethyl benzidine/sodium nitroferrocyanide mixture in acetate buffer (Mesulam 1978). Hydrogen peroxide was added at a final concentration of 0.006%, and the reaction closely monitored. The reaction ultimately was quenched in 0.01M sodium acetate buffer chilled to 4°C. In some cases, ammonium molybdate was used to stabilize the reaction product (Marfurt et al., 1988). Sections were mounted out of acetate buffer, air-dried, cleared in xylene, and coverslipped with Permount. Alternate sections were stained with Neutral Red to determine more accurately the exact location of the labeled material.

Intracellular recordings *in vitro*

Complete details of the *in vitro* brain slice preparation are described in the following chapter. In brief, birds were deeply anesthetized with a series of ketamine injections (3 injections of 0.02 to 0.04 ml each) and Metofane™ (Pitman-Moore, Inc.) inhalation. The brain was removed rapidly after decapitation and placed in ice-cold ACSF, blocked along the sagittal midline, and vibratome-sectioned at 400 μm thickness in the parasagittal orientation. After allowing one to three hours to equilibrate in an interface chamber, slices were transferred to a semisubmersion chamber warmed to 35°C, and perfused with oxygenated ACSF at a rate of 3 to 5 ml/min. The recording electrode was positioned on a micromanipulator (Leitz) over the area of interest with the aid of a dissecting microscope (Wild). Small hyperpolarizing (or depolarizing, with Lucifer Yellow) current pulses (0.1 to 0.5 nA, 100msec in duration, at 0.8 Hz) were passed through the recording electrode as it was lowered through the slice. Increases in electrode impedance signalled that the electrode tip was contacting a cell membrane, at which point diminishing the amplifier's capacitance compensation caused the electrode to ring and usually effected penetration. Successful penetration was accompanied by a rapid shift in membrane potential to a level between -40 and -70 mV. Synaptic responses and action potentials were stored on a videocasette recorder (Sony SLO 1800) in pulse-code format (Neuro-Corder DR-484), and analyzed, both on- and off-line, with the aid of digital oscilloscope software written by Larry Proctor for a MASSCOMP Graphics workstation. Bipolar tungsten electrodes were used to deliver brief (100 μsec), focal, extracellular electrical stimuli to fiber tracts within the slice preparation.

Intracellular staining techniques: Biocytin

Intracellular staining with biocytin (Sigma) was achieved by impaling neurons with 80 to 150 MΩ electrodes filled with 2% biocytin in 2 molar potassium acetate (Horikawa and Armstrong 1988). Biocytin was iontophoresed from the electrode with 0.6 to 1.5 nA depolarizing current pulses, one second in duration, at a frequency of 0.5 Hz. Optimal fills were obtained within 15 to 30 minutes, after which time the slices were placed in 4% paraformaldehyde in 0.025M phosphate buffer (4°C) for at least 12 hours.

Following fixation, slices were vibratome-sectioned to 100 μm thickness after being embedded in a polymerized gelatin-albumin mixture (Quick-embed). Sections were rinsed twice in 0.025M phosphate buffered saline (PBS), pH=7.40, and then permeabilized for 20 to 45 minutes in 0.25% Triton and 2% bovine serum albumin (BSA fraction V, Sigma) in PBS. Following a 15-minute rinse in PBS, sections were incubated for 6 to 12 hours in a solution of Avidin D HRP (Vector Labs, Inc.), diluted 1:100 in 2% BSA in PBS at 4°C. After rinsing again with PBS, sections were incubated in a 0.05% DAB solution in PBS for 1 hour, and then hydrogen peroxide was added to the DAB solution at a final concentration of 0.02%. Sections were monitored until a strong reaction product was visible. The sections were subsequently rinsed with PBS, mounted on gelatin-coated slides, air-dried, cleared with xylene, and coverslipped with Permount. Stained cells were reconstructed with the aid of a a camera lucida and a 100x Zeiss oil immersion objective (n. a. = 1.3).

Intracellular staining techniques: Lucifer Yellow

A solution of 5 to 10% Lucifer Yellow CH (Aldrich) in 1.0 to 0.5M lithium chloride was also used for intraneuronal staining (Stewart 1978). In some cases, the Lucifer Yellow solution also contained formaldehyde at a final

concentration of 3.7%. Electrodes were identical to those employed with biocytin, except that the impedance was typically 100 to 200 MΩ. In some instances, the tips of the higher-impedance electrodes were gently broken against the nylon grid on which the slice was resting in order to pass more current. Upon impalement, 1 to 2 nA hyperpolarizing current pulses (2.5 Hz, 1:1 duty cycle) were passed through the electrode for 10 to 30 minutes. After filling several cells, slices were fixed in 4% paraformaldehyde in 0.025M PBS and stored at 4°C. Slices were resectioned on a vibratome to a thickness of 200 μm, mounted on gelatin-subbed slides or #1 thickness coverslips, and air-dried.

Confocal microscopy

Confocal images were generated on a Biorad 600 scanning laser confocal system mated to a Zeiss Axiovert microscope with infinity-corrected optics. Either rhodamine (for DiI), or fluorescein (for Lucifer Yellow) filter sets were used. High-magnification images of Lucifer Yellow-filled neurons and individual DiI-labeled terminals were obtained with a 63x Zeiss Neofluar objective (n. a. = 1.25, infinity-corrected) under oil immersion. Lower-magnification images of whole terminal fields were generated with 5x, 10x, and 20x Zeiss Neofluar objectives. A Kalman filter was used to enhance the signal to noise ratio of individual optical sections, and in some cases edge-enhancement software was used to heighten contrast. Figures in which whole neurons are illustrated represent the two-dimensional projection of 5 to 20 separate optical sections, made in 0.25 to 2.5 μm increments along the z axis. In some cases, separate confocal images were made of the same area under brightfield and epifluorescent illumination, and then merged to form a single image showing both anatomical landmarks and fluorescently labeled structures.

RESULTS

MAN axonal projections to RA before day 25

MAN terminals were present within RA as early as fifteen days after hatching in both sexes. DiI was injected into the MAN of seven zebra finches younger than twenty-five days posthatch age. Birds included one twelve day, two fifteen-day, one seventeen-day, and one twenty-day old female, as well as two fifteen-day old males. Regardless of the sex or age of the bird in which MAN was injected, the whole extent of RA was filled with fluorescent label when examined three to four days later (see Figure 2a).

Confocal images were made of the DiI-labeled fluorescent material within RA. Single optical sections revealed a dense, fibrous meshwork, punctuated by characteristic "holes" of ten to twenty microns diameter, in which label was absent (see Figure 2b). Nuclei and nucleoli were found in these "holes" when the same optical section was examined under phase contrast optics, suggesting that the holes were formed by RA cell bodies. Higher magnification images of individual fibers indicated occasional branches and small swellings along their length (see Figure 2b).

MAN axonal projections to RA after day 25

After day twenty-five, the distribution of MAN terminals expanded or contracted, depending on the sex of the bird, as RA underwent sexual differentiation. The MAN in five birds (two males and three females) greater than twenty-five days of age was injected with DiI, either in fixed or living brain tissue. Again, in all cases, MAN injections labeled terminals within RA.

The three female birds were fifty, seventy, and greater than ninety days of age. At these ages, RA was already substantially atrophied. The

Figure 2. MAN terminals within RA before day 25.

a) A confocal image of anterograde label within RA following an injection of DiI into the MAN of a fifteen day old male zebra finch. The white, oval structure in the center of the figure is the mass of MAN terminals filling RA. Section is in coronal orientation, with dorsal to the top and medial to the right; the cerebellum is visible to the right of the medial edge of the forebrain. Scale bar equals 400 μm.

b) A higher magnification confocal image of DiI-labeled MAN axon terminals within RA. Note the periodic swellings along the length of individual processes, which may be synaptic varicosities. Scale bar equals 10 μm.

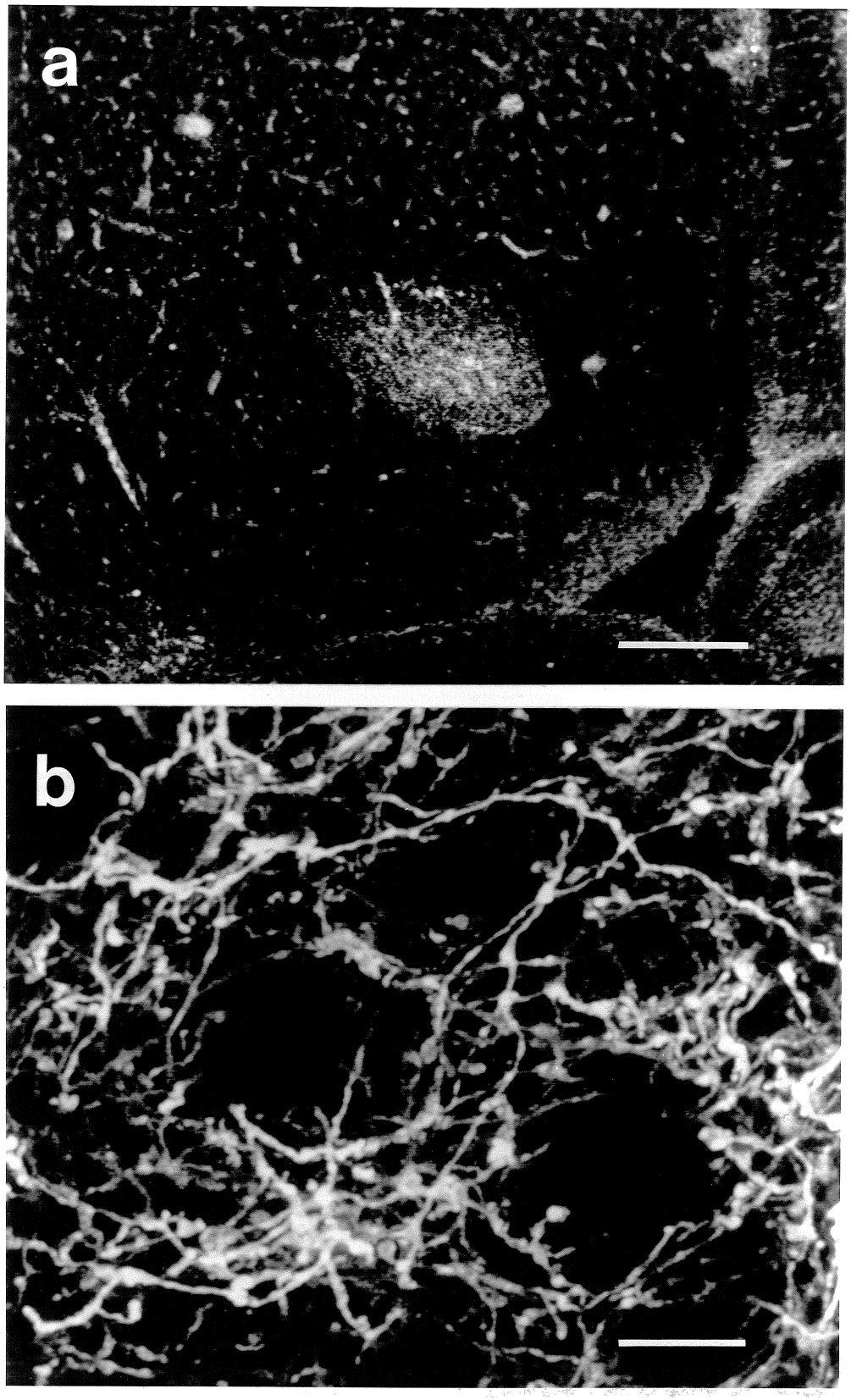
a
b

fluorescent label was confined to the reduced area of the nucleus, and did not appear to extend beyond its borders (data not shown). The two other birds injected were males of thirty and greater than ninety days of age. Although the male RA increased significantly in size over this period, the label continued to fill the entire extent of the nucleus.

Other areas labeled following MAN injections

Regardless of the bird's age or sex, injections of DiI in MAN also resulted in strong retrograde label within the thalamus. Retrogradely labeled cell bodies were confined to a dorsal and posterior part of the thalamus about 1 to 1.5 mm from the midline, thought to be DLM (data not shown).

HVc axonal projections to RA before day 25

Previous studies have revealed that HVc axon terminals actually wait at the border dorsal to RA before entering the nucleus. Tritiated-proline injections made into the HVc of male zebra finches at different ages revealed that although HVc axons reach RA's dorsal border as early as day fifteen, they do not enter the nucleus until ten to fifteen days later (Konishi and Akutagawa 1985). Although proline is a sensitive anterograde tracer, it does not permit high-resolution imaging of the labeled axon terminals, nor does it label cells retrogradely. Therefore, other anterograde and retrograde tracers were used to generate higher-resolution images of the HVc axons during the waiting period.

In six zebra finches less than twenty-five days of age, HVc was injected with either DiI or WGA-HRP. In all cases, regardless of sex, the bulk of the transported label was concentrated just outside RA, and especially along its dorsal edge. Figure 3a typifies the anterograde labeling found outside RA,

following injections of DiI into HVc. We will refer to this region abutting the dorsal border to RA as the waiting compartment.

Injections of either DiI or WGA-HRP placed into HVc *in vivo* were difficult to confine completely to the target area. To surmount this problem, 500 μm thick, fixed parasagittal brain slices were prepared from a fifteen day old male finch. The slice containing HVc and RA was isolated by visual inspection, and a small injection of DiI (25% w/v) was placed in HVc. The efflux of dye from the pipette tip was monitored with an epifluorescence microscope and the injection site was kept smaller than 50 μm in diameter. The slice was stored in fixative at 37°C, then examined periodically under epifluorescent illumination over the course of the next several weeks to determine the extent of labeling. By the end of the first week, several labeled fibers streamed out of the injection site in the direction of RA. By the end of the second week, a larger number of labeled fibers exited the injection site, and the most extensively labeled of these had reached the dorsal border of RA, where they accumulated in the waiting compartment along the edge of the nucleus. Although the number of labeled fibers increased in the waiting compartment between the second and third week, few fibers appeared to break the plane of the nucleus and cross into RA.

Individual fibers coursing from the injection site to the waiting compartment were reconstructed in more detail on a confocal microscope. Although single fibers followed a straight, dorsoventral trajectory over much of their journey, they turned rostrally after entering the archistriatal region immediately dorsal to RA. In this area, labeled fibers were studded with periodic swellings and sometimes ended in knoblike structures, suggestive of axonal growth cones (see **figure 4**).

The right MAN and the left HVc of a fifteen-day male finch were injected with DiI in order to visualize MAN and HVc fibers in the same animal.

After allowing time for transport, the pattern of labeling was examined under epifluorescence. The RA on the side receiving the MAN injection was completely filled with fluorescent label. In contrast, on the side receiving the HVc injection, the waiting compartment was fluorescently labeled, but RA was devoid of any staining within its boundaries (data not shown).

HVc axonal projections to RA after day 25

HVc axons projecting towards RA were also examined in the adult male finch. HVc terminals were stained with DiI in fixed brain tissue, and then viewed with conventional epifluorescence, or used to photoconvert DAB. HVc fibers were highly fasciculated as they ran in a dorsoventral path to RA. Upon reaching RA, however, the labeled axons defasciculated, and elaborated a dense terminal field (see Figure 3b).

To compare the trajectory of the HVc and MAN fiber pathways in a single bird, DiI crystals were implanted in the left MAN and the right HVc of a fixed adult male brain. After transport was complete, the brain was sectioned in the coronal plane, allowing the location of the two fiber pathways to be compared side by side (see Figure 6). Labeled MAN axons ran caudally in the lamina hyperstriatica (LH) towards HVc. MAN axons composed a broad band of fibers that occupied a more lateral position as they travelled caudally. MAN axons turned and cascaded in the ventral direction upon reaching a rostro-caudal point approximately even with, but slightly lateral to, HVc. After descending ventrally to a level approximately even with RA, MAN axons executed a sharp, right-angle turn in the medial direction, then entered RA along its lateral face. In contrast, HVc axons ran dorsoventrally in highly fasciculated bundles towards RA, and proceeded to enter RA along its dorsal edge. Most labeled HVc axons were situated medial to the MAN fiber pathway.

Other areas labeled by HVc injections before day 25

WGA-HRP injections into the HVc of several finches less than twenty-five days old also generated anterograde label within the waiting compartment. Furthermore, these same injections yielded anterograde label in the anterior forebrain, and retrogradely labeled, distinct clusters of cells within other forebrain regions, as well as in the thalamus (see Figure 5). Counterstaining indicated that the retrogradely labeled cells were within the medial portion of MAN, the nucleus interfacialis (NIf), and the thalamic nucleus Uva, while the anterograde label was confined to area X of the lobus parolfactorius.

Figure 3. HVc axons innervate RA late in development.

a) DiI crystals implanted in the paraformaldehyde-fixed brain of a twenty-three day old finch produced a ringlike pattern of anterograde label outside RA. Note the presence of several retrogradely labeled cell bodies dorsal to RA. Section is oriented parasagittally, with dorsal to the top and rostral to the right. Scale bar in b) equals 200 μm in a).

b) DiI crystals implanted in the fixed brain of an adult male finch produced heavy anterograde label within RA. No retrogradely labeled cells were detected along RA's dorsal border. Section is oriented as in a). Scale bar equals approximately 290 μm.

In Figures a) and b), fluorescent excitation of DiI-labeled material was used to photooxidize DAB.

a

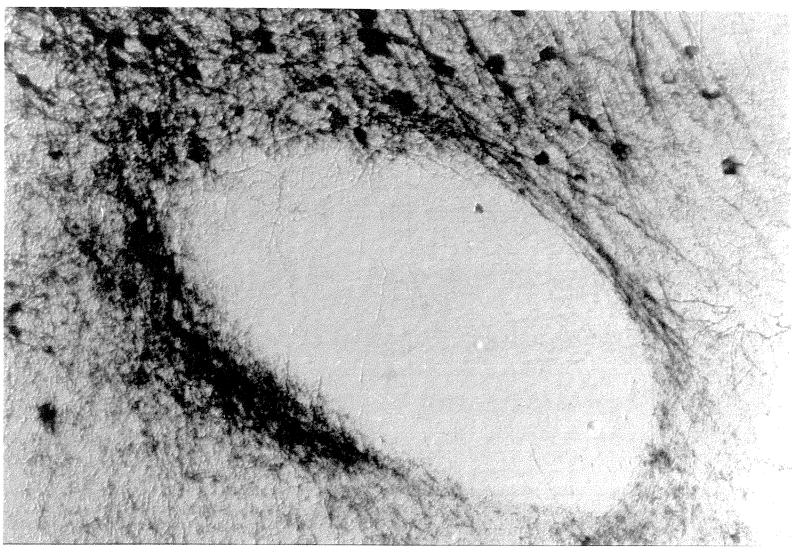

b

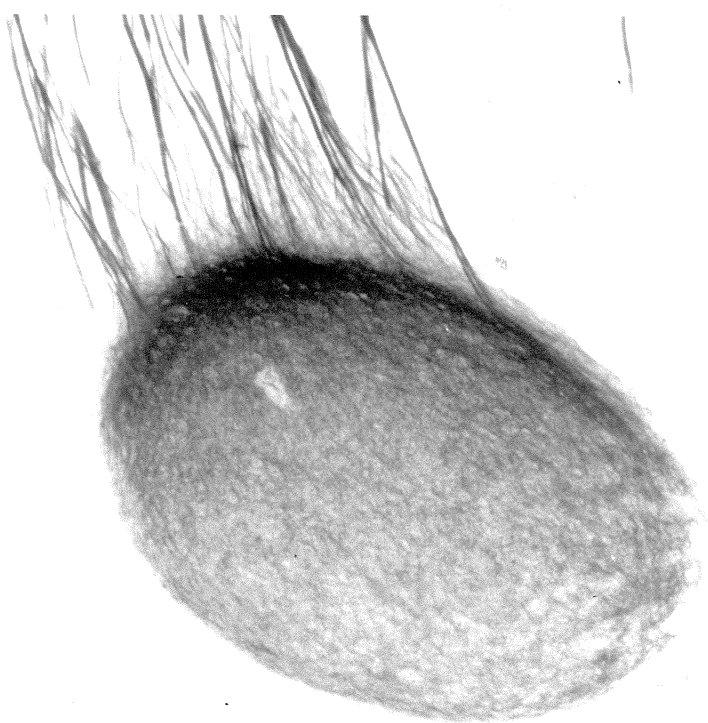

Figure 4. Confocal images of individual HVc axons in the waiting compartment. Individual HVc axons were labeled by placing very restricted DiI injections into HVc in a parasagittal slice of fixed forebrain from a seventeen day male finch. This image is a confocal reconstruction of a 30 μm thick section of the archistriatum immediately dorsal to RA. Filled arrowhead points to a possible growth cone structure. Open arrowhead marks swellings along the length of a single HVc axon that resemble presynaptic terminals. Scale bar equals 50 μm.

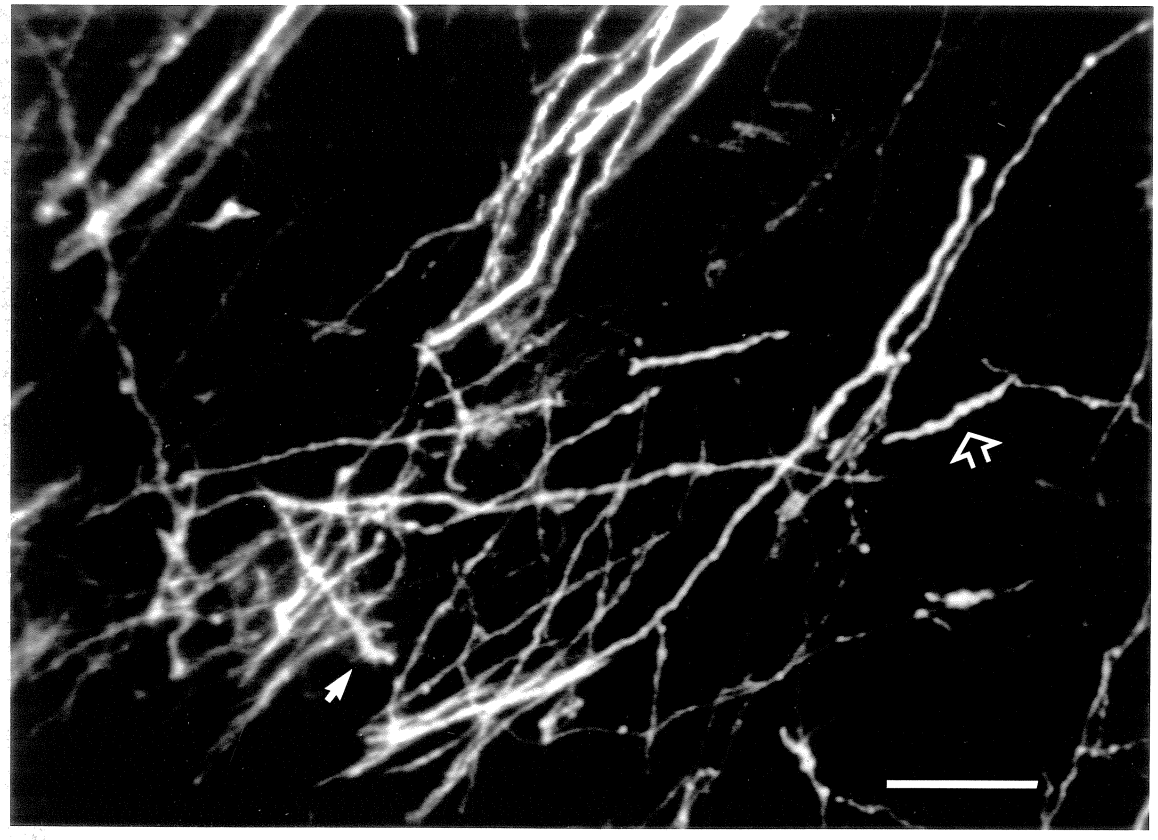

Figure 5. Several areas were labeled by injection of WGA-HRP into HVc before day twenty-five.

Line drawings: WGA-HRP was ionophoresed into a region including HVc (solid black area in Figures, Sections 1-5) in an eighteen day old male finch. Hatched areas represent anterograde label; dots signify the locations of retrogradely labeled cell bodies. Note anterograde label *outside* RA's dorsal border in Sections 1-3, and *within* area X in Sections 4-8. Retrograde label in NIf is depicted in Sections 4-8, while retrograde label in MAN only becomes apparent in Sections 9 and 10. Line drawings of parasagittal brain sections were made with the aid of a camera lucida. Section 1 is approximately 2.6 mm from the midline, and each section represents an advance of 0.15 mm in the medial direction.

Darkfield photomicrographs:

a) retrograde label in medial MAN (taken from Section 9).

b) retrograde label within NIf (taken from Section 5).

c) anterograde label within area X (from Section 6).

d) retrograde label in the thalamic nucleus Uva (from Section 7).

All sections are oriented with rostral to the left, and dorsal upwards. The scale bar equals 200 μm in a-d.

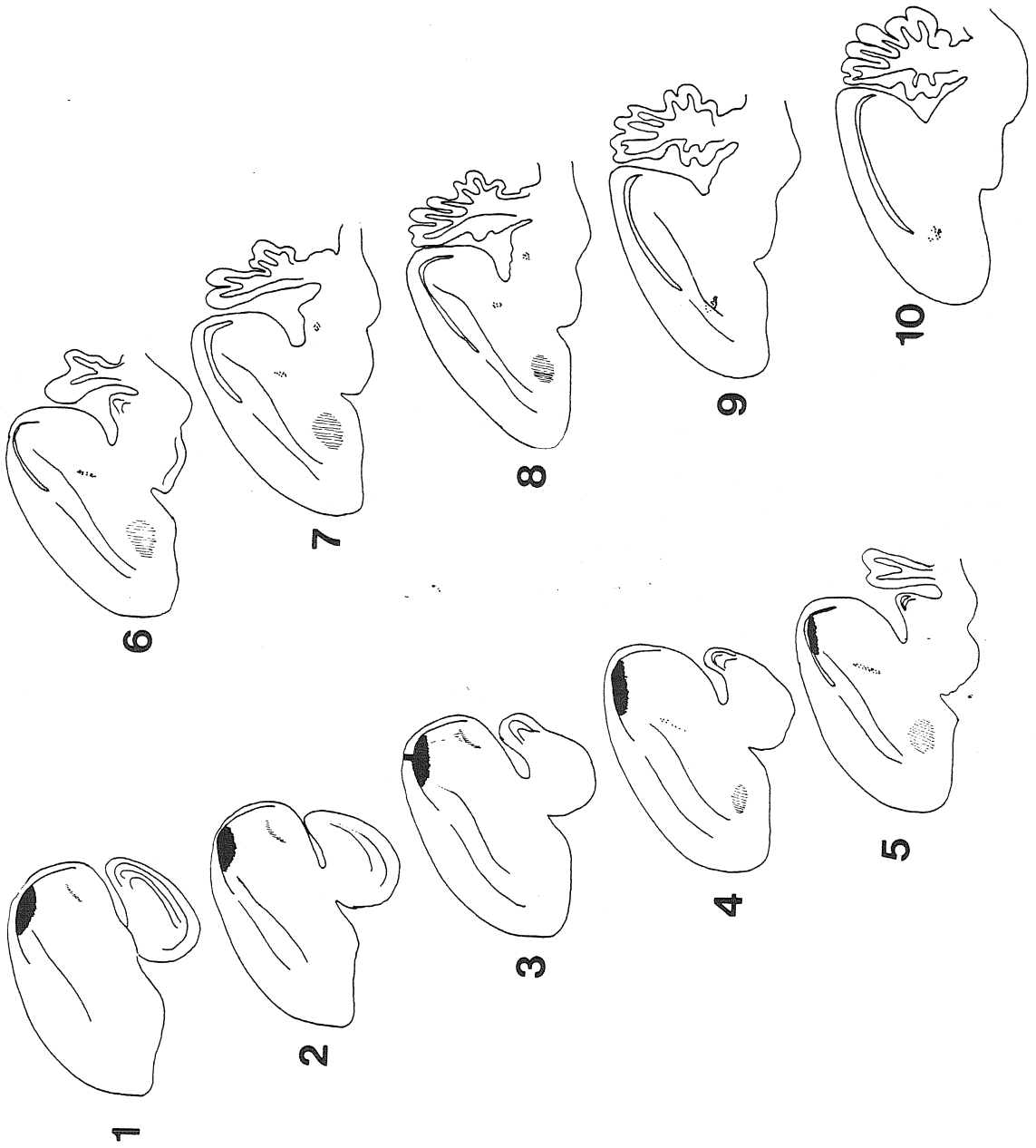
1
2
3
4
5
6
7
8
9
10

a
b
c
d

Figure 6. MAN and HVc axons enter RA from different angles.

A coronal section through the whole brain of an adult male finch at the level of RA. The left MAN and right HVc were implanted with DiI crystals, and DAB was subsequently photooxidized by fluorescently exciting the DiI-labeled axon terminals within RA. In the left hemisphere, axons course down towards RA from their origin in MAN (rostral to this plane of section). Note that MAN axons enter RA primarily along the lateral edge of the nucleus. In the right hemisphere, HVc axons run in a tract displaced medially to the MAN axon tract, and enter RA along its dorsal edge. Scale bar equals 1mm.

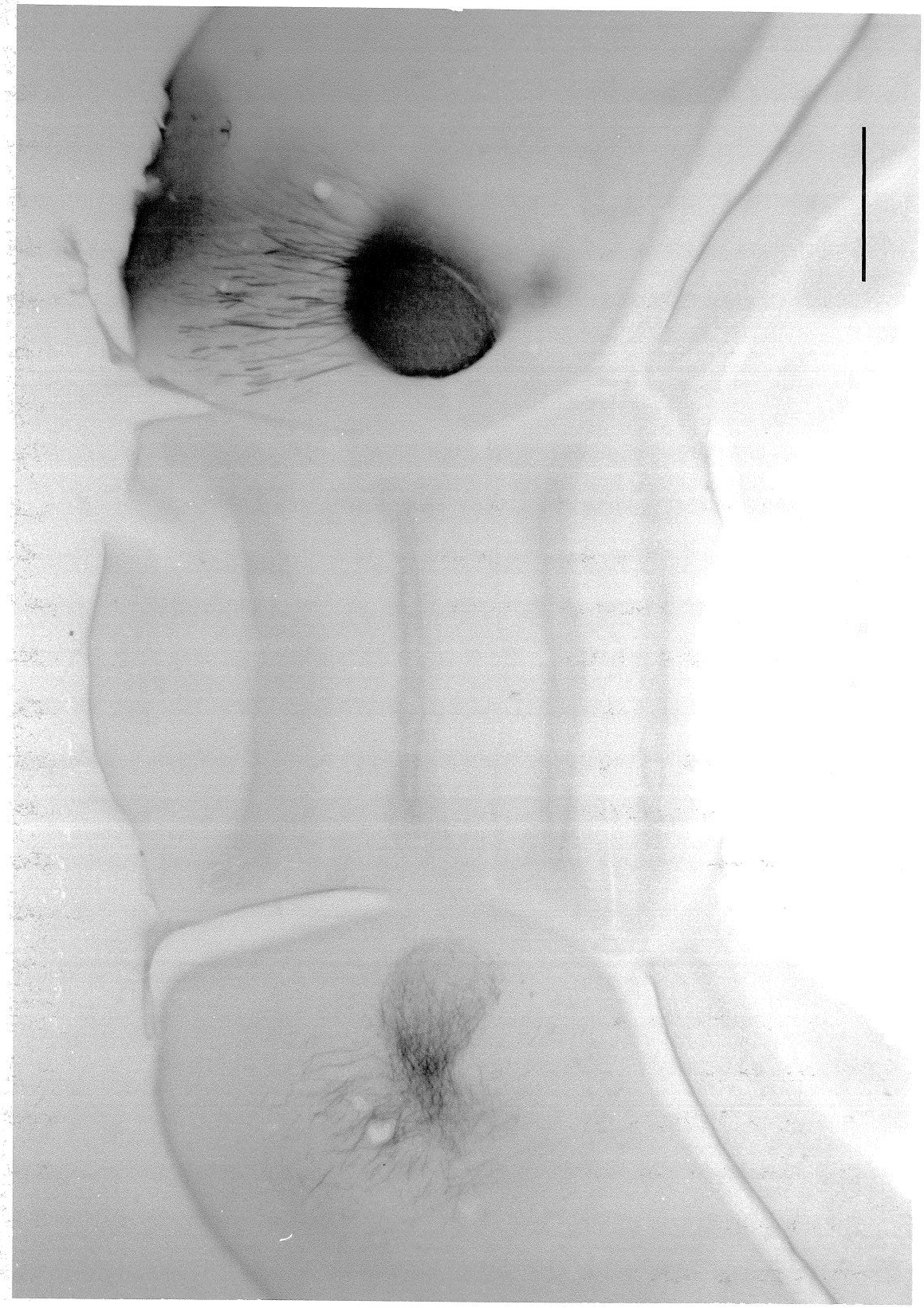

Cells within the waiting compartment before day 25

Multipolar cells abutting the dorsal border of RA were also labeled following DiI and WGA-HRP injections placed into HVc before day twenty-five (see Figure 3a). These cells were enmeshed in the dense plexus of fibers labeled by the HVc injections. In order to determine whether cells within the waiting compartment actually projected back to the vicinity of HVc, intracellular recordings were obtained from them *in vitro*, and the morphology of individual cells was revealed with intracellular staining.

Morphology of waiting compartment neurons

A distinct morphological cell type, closely apposed to the dorsal border of RA, was discovered by dye-filling neurons within the waiting compartment, as seen in Figure 7. Their dendrites were dorsoventrally flattened, and spanned the dorsal edge of RA. Their dendrites did not enter RA, although they extended freely in the waiting compartment. These neurons also supported a network of axon collaterals local to the parent cell, and on several occasions, collaterals were detected heading dorsally towards HVc. Other axon collaterals of these neurons did not appear to enter RA, although they coursed about the region outside the nucleus.

Physiology of waiting compartment neurons

Neurons within the waiting compartment might be innervated by the waiting HVc axons. In order to test this possibility, a total of twenty-two cells situated in the archistriatum immediately dorsal to RA were examined electrophysiologically. Cells impaled within the waiting compartment were classified as neurons because of their propensity to fire rapid action potentials in response to depolarizing currents. Five hundred millisecond long,

suprathreshold currents were used to assess each cell's spiking behavior. Twenty of twenty two cells examined within the waiting compartment responded to such currents by initially firing two or three higher frequency action potentials, followed by a lower frequency train of action potentials (see Figure 8a). In some cases, spike frequency adaptation was quite pronounced, and the cell would cease firing altogether after several action potentials. In two cases, only very slight adaptation was detected.

Electrical stimulation within HVc, or the region immediately ventral to it, where HVc axons travel *en route* to RA, evoked synaptic potentials from all of the waiting compartment neurons encountered in the present study (22/22 cells) (see Figure 8b). These responses could be of variable or long latency (>5msec). The synaptic potentials often drove waiting compartment neurons above spike threshold, and therefore were classified as excitatory.

Figure 7. A neuron within the waiting compartment.

A neuron located within the waiting compartment immediately dorsal to RA. The cell was filled with biocytin in a parasagittal brain slice prepared from an eighteen day old finch. Note the lone collateral traveling dorsally towards HVc. Dorsal is towards the left, and rostral towards the top of the page.

Figure 8. Physiology of a waiting compartment neuron. Intracellular recordings, obtained from the cell illustrated in Figure 7, were typical of neurons impaled within the waiting compartment.

a) Depolarizing the neuron with a 500 millisecond long, +0.46 nA current generated a train of action potentials. Note the decrease in firing rate over the duration of the injected current. Calibration bars at the bottom of the figure equal 150 milliseconds (horizontal), and 40 millivolts (vertical), respectively. Resting potential was -61 mV.

b) Electrical stimulation within HVc evoked a depolarizing synaptic response from the cell in a). At higher stimulus intensities, the PSP elicited an action potential (not shown). Calibration bars equal 60 milliseconds (horizontal), 10 millivolts (vertical). The negative-going deflection preceding the synaptic potential marks the stimulus artifact.

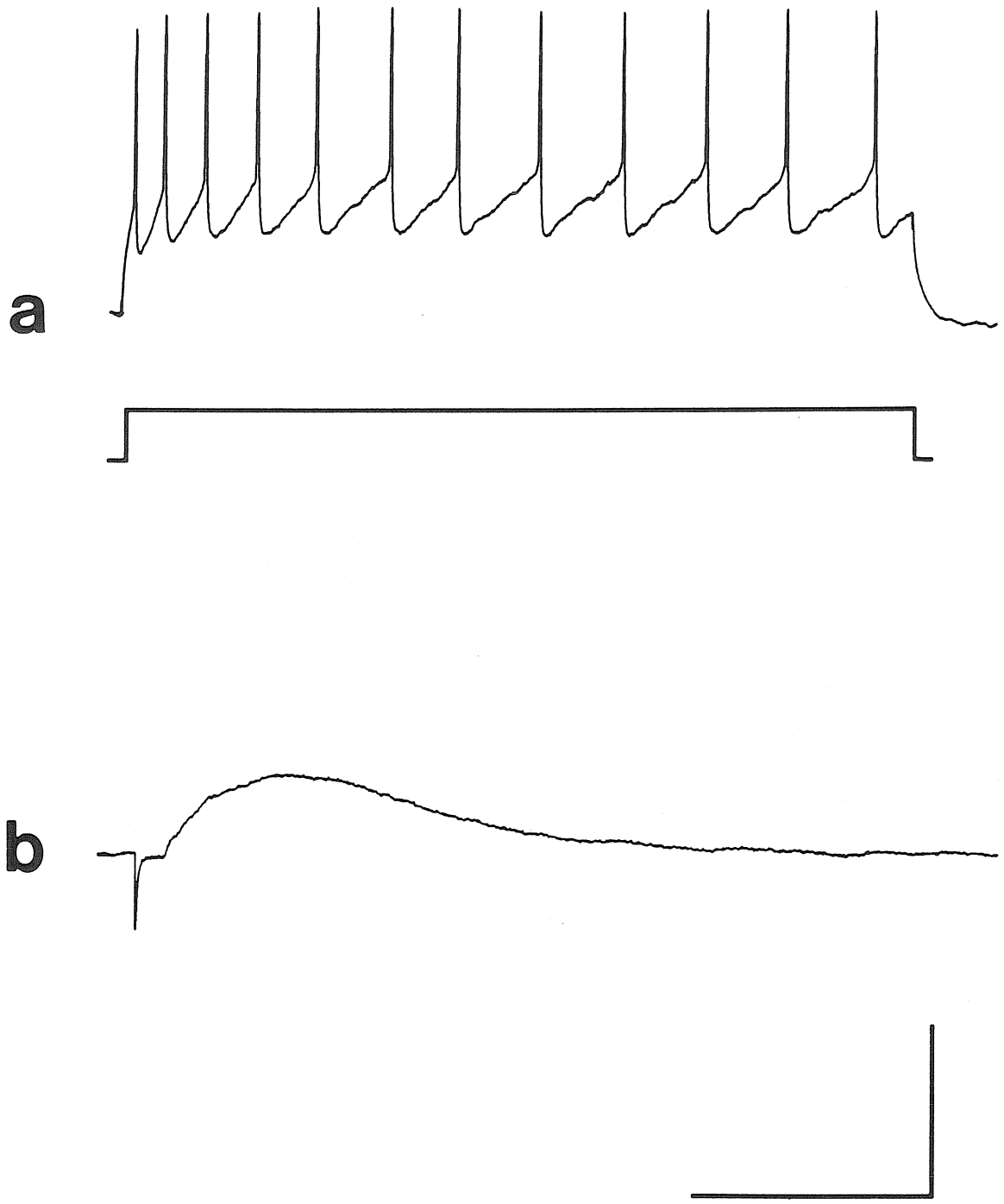
a
b

RA neuronal morphology between 15 and 65 days

In the male zebra finch, the massive ingrowth of HVc axons into RA after day twenty-five is accompanied by a large increase in the volume of the nucleus, presumably because of the addition of large numbers of new synapses (Konishi and Akutagawa 1985). In order to characterize the postsynaptic changes that occur within RA with the ingrowth of HVc axons, individual RA neurons were intracellularly stained in brain slices prepared from birds of fifteen to sixty-five days of age. The present section affords a morphological description of a specific type of RA neuron that fired action potentials in a repetitive and highly regular fashion, without accommodation, in response to depolarizing currents (see the next chapter for details of its intrinsic properties).

Although the recording electrode was usually positioned towards the center of RA, repetitive-spiking RA neurons were distributed throughout RA, and were often located just within its border. Their morphology was studied with both biocytin and Lucifer Yellow staining.

Eleven of fourteen RA neurons filled before day twenty-five possessed spinous dendrites. The remaining three neurons were inadequately filled to resolve whether or not spines were present. Ten out of eleven RA neurons filled in slices after day thirty-five also had spinous dendrites; the eleventh cell was too poorly filled to detect if spines were present.

Confocal images were generated of Lucifer Yellow-filled RA neurons in brain slices from birds less than twenty-five days of age. When located towards the center of RA, repetitive-spiking RA neurons had spinous dendrites oriented about the cell body in a radially symmetric manner (see Figure 9a). In contrast, when their cell bodies were closer to the edge of the nucleus, their dendrites, although spinous, were not radially symmetric. Such border neurons had a flattened appearance because their dendrites did not

extend outside RA, but projected back towards the center of the nucleus (see Figure 9b). Several cells were filled just within RA's dorsal border in slices prepared from birds less than twenty-five days old. Again, their dendrites did not cross out of RA, but extended inwards, towards the center of the nucleus.

A single RA neuron, filled with Lucifer Yellow in a slice prepared from a twenty-four day male, had pronounced, clublike endings at the tips of many of its dendrites (see Figure 9c). In other respects, it had the basic features associated with other spinous RA neurons encountered in this study. A confocal reconstruction of this cell illustrated the clear elaboration of dendritic spines, and several collaterals could be observed branching from the main axon in close vicinity of the parent cell body. The dendritic endings, when viewed in greater detail (see Figure 9d), were enlarged relative to the more proximal dendritic shaft, and then terminated in a very fine distal process.

RA neurons at a variety of ages were also stained with biocytin and reconstructed with the aid of a camera lucida (see Figure 10). The dendritic arbors of RA neurons in brain slices prepared before day 25 were already quite extensive. As was seen with the confocal images, spines were present along most dendrites. In several cases, the axon could be followed as it exited RA. The main axon gave rise to several collaterals in close vicinity to the parent cell body, and then exited RA in the rostro-ventral direction. The axon collaterals, with numerous varicosities visible along their length, were restricted to the volume close to the cell body (see Figure 10). The main axon did not appear to branch after exiting RA.

RA neurons stained with biocytin after day 40 were much like their younger counterparts, but appeared to be more complex in several different ways (see Figure 10). First, distal dendrites were more highly branched in older animals, and individual dendrites were more heavily covered with spines. The

main axon also gave rise to a more substantial network of collaterals, although they still occupied a volume similar to that of the dendritic arbor.

Figure 9. RA neurons filled with Lucifer Yellow in slices prepared from finches less than twenty-five days of age, imaged with a confocal microscope.

a) An RA neuron located near the center of RA. Note radially symmetric dendrites, with spines visible along some portions (upper right quadrant, e.g.). Slice prepared from a seventeen day male finch. Scale bar equals 25 μm.

b) An RA neuron located towards the caudal border of RA (marked by empty arrows). Dendrites were oriented predominantly away from the boundary of the nucleus. Note dendritic spines. From seventeen day old male finch. Same scale as in a).

c) An RA neuron from a twenty-four day male finch. Note the clublike endings on most dendrites. Axon extends from the soma at nine o'clock, and gives rise to several collateral branches. Same scale as in a).

d) Higher magnification of upper-right quadrant of neuron in c). Note the swollen dendritic tips, in some cases with very thin distal termini. Also note the numerous dendritic spines. Scale bar equals 10 μm.

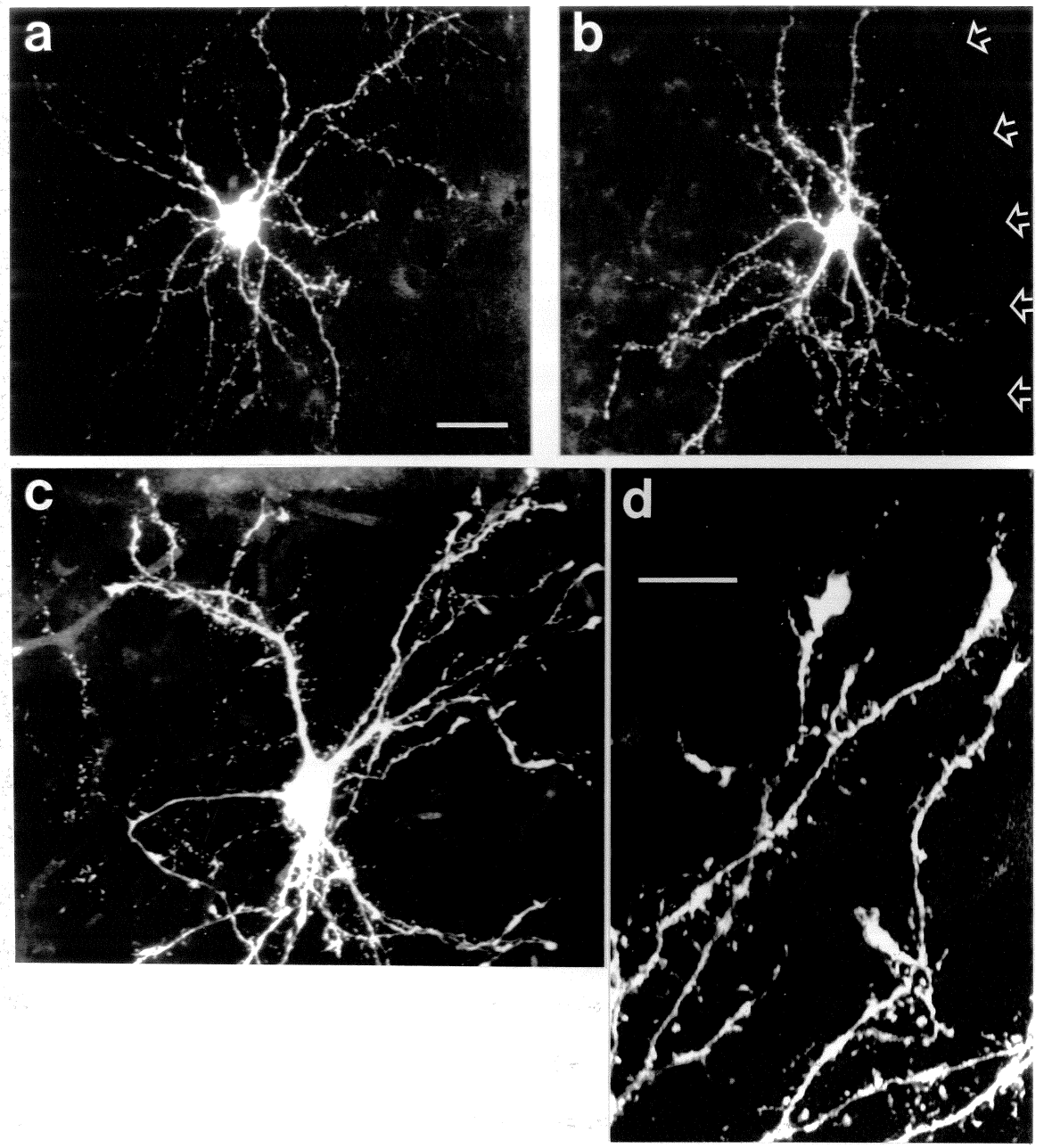
a
b
c
d

Figure 10. RA neurons filled with biocytin in slices prepared from younger and older finches, reconstructed with the aid of a camera lucida. The neuron on the left was filled in a brain slice from a twenty day male finch. The neuron on the right was filled in slice from a sixty day male finch; its position within RA is indicated in the lower magnification image (scale bar equals 100 μm) to the lower left of the cell body. The position of the RA neuron from the twenty day finch was in a similar location, but is not shown. In both cases, orientation is coronal, with dorsal to the top of the figure, and medial to the right. Scale bar equals 20 μm in both cases.

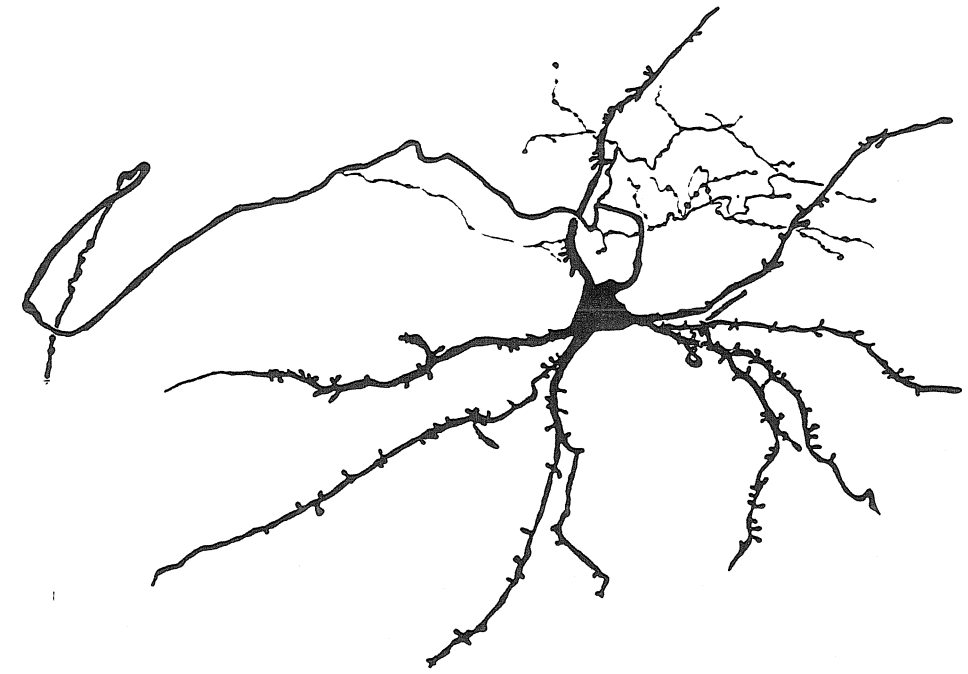

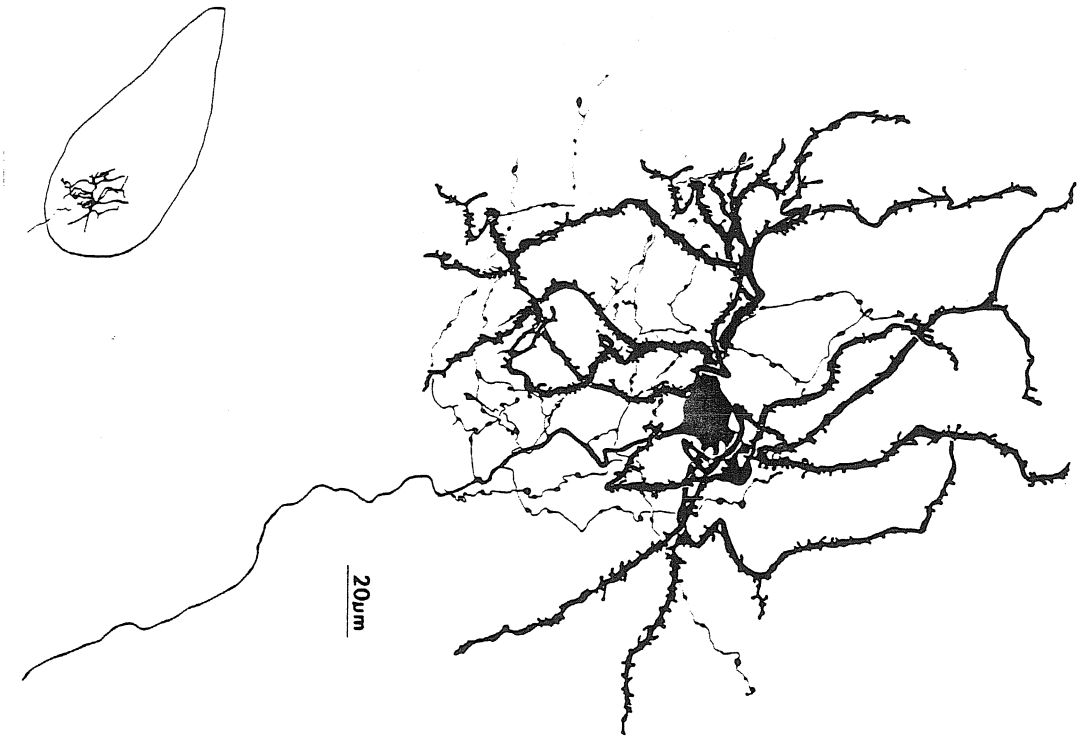
20µm

DISCUSSION

These experiments illustrate that MAN and HVc axons innervate RA at different stages during development. MAN terminals are present within RA by fifteen days after hatching, whereas HVc axons are not detected within RA until ten to fifteen days later. During the period from fifteen to twenty-five days after hatching, HVc terminals ramify extensively in a region immediately dorsal to RA, and certain neurons within this region have features that suggest that they may function as transient targets for developing HVc axons. The delayed ingrowth of HVc axons may have important consequences for the development of RA neurons. Additionally, developmental distinctions between the MAN and HVc axonal projections to RA might relate to the different roles that these two pathways play during song development.

Previous experiments have demonstrated that HVc terminals wait at RA's dorsal border for prolonged periods before entering the nucleus (Konishi and Akutagawa 1985). In the male zebra finch, HVc axon terminals first enter RA in large numbers between day twenty-five and thirty-five. At the same time in the female, however, HVc terminals remain largely excluded from RA, and the nucleus starts to collapse because of neuronal atrophy and death. In fifteen day old male zebra finches, severing the tract between HVc and RA causes RA to atrophy (Konishi and Akutagawa 1987). One hypothesis consistent with these observations is that extrinsic innervation, as supplied by HVc axons, might regulate cell number within RA.

The discovery that MAN terminals are present within the female RA throughout the period of cell atrophy and death renders a simple innervation-dependent mechanism less plausible. In both male and female zebra finches, the projection from MAN to RA forms as early as twelve to fifteen days after hatching, preceding the period of cell death in the female RA by

several weeks. By itself, the afferent input from MAN apparently cannot prevent RA cell death. Perhaps HVc terminals possess neurotrophic properties that are essential to RA neuronal survival. Another possibility is that MAN and HVc axons might interact to prevent cell death within the male RA.

Since HVc and MAN axons run adjacent to one another in the tractus archistriatalis, knife cuts made in this region may have disrupted both sets of afferents. This complication makes it difficult to distinguish between the effects of total deafferentation (i.e., cutting both MAN and HVc axons), as opposed to prevention of late innervation (i.e., the destruction of HVc axons). At the very least, though, tract-cutting experiments do indicate that RA neuronal survival is not controlled merely by the early posthatch hormonal milieu. Chemical lesions of HVc, as well as MAN, neurons might yield a more unequivocal picture.

The mechanisms responsible for the prolonged arrest of HVc axons at RA's dorsal border are not well understood. Tritiated-thymidine birthdating, coupled with retrograde labeling, have revealed that many of the HVc neurons ultimately projecting to RA are not born until after day 20 in the zebra finch (Nordeen and Nordeen 1988). Delayed neurogenesis can explain why some HVc terminals arrive and enter RA at late stages of development. It does not explain why the axon terminals of earlier-generated HVc neurons, having reached the dorsal border of RA as early as day 15, do not enter RA immediately, but ramify in the region bordering the nucleus. Other factors may contribute to this delay. One suggestion is that HVc axons are delayed from entering RA because they recognize cells immediately dorsal to RA as suitable, albeit temporary, synaptic targets.

Neurons within the waiting compartment displayed properties that suggest that they might function as synaptic targets of HVc axons. *In vitro*,

electrical stimulation of HVc evoked synaptic potentials from many neurons in the waiting compartment. Intracellular staining revealed that a subset of these cells, closely apposed to the dorsal border of RA, had dendrites that spanned the edge of the nucleus in an orientation similar to the HVc axon terminals. These features might be expected of cells that receive transient synaptic input from HVc axons during early stages of posthatch development.

Neurons within the waiting compartment also have axon collaterals that project towards HVc. The final target of these axon collaterals is unknown, although retrogradely labeled cell bodies are found within the dorsal cap following injections of DiI or WGA-HRP into HVc and adjacent areas. One possibility is that waiting compartment neurons form reciprocal connections either with HVc, or with regions adjacent to it.

Developing geniculocortical projections in the mammalian visual system also are characterized by a prolonged "waiting period," in which presynaptic axon terminals are arrested transiently in a zone adjacent to the mature target (Lund and Mustari 1977; Shatz and Luskin 1986). Geniculocortical development is further characterized by reciprocal connections between neurons in the waiting zone and the lateral geniculate nucleus (McConnell et al., 1989). Despite parallels between the development of the mammalian visual pathway and the development of the avian song system, important differences should be noted. First, only one of the two afferents supplying RA appears to wait before entering the nucleus. MAN axons already have innervated RA successfully during the time that HVc axons are still restricted from the nucleus. We cannot rule out the possibility that MAN axons are also delayed in entering RA, only at a much earlier stage of development, but a more likely scenario is that the cues retarding HVc axon entry into RA are specific to this pathway.

Another difference is that geniculate neurons are born much earlier than their target cell population in layer IV of visual cortex (Luskin and Shatz 1985; Shatz 1983). Therefore, LGN axons may wait simply because the neurons that ultimately constitute layer IV have not yet migrated from the ventricular zone and have not acquired mature characteristics necessary to support extrinsic innervation (Shatz et al., 1988). In contrast, many RA neurons are born between embryonic day 6 (E6) and E8 (Konishi and Akutagawa 1990), long before the HVc neurons that will eventually innervate them (Kirn and DeVoogd 1989; Nordeen and Nordeen 1988). In addition, RA affords a suitable environment for MAN axons as early as day fifteen. Therefore, HVc axons probably do not wait before entering RA simply because the target is too immature to support innervation.

Regardless of the actual mechanisms regulating the waiting behavior of HVc axons, their eventual entry into RA is accompanied by several postsynaptic changes. In the male, there are dramatic increases in RA volume, as well as decreases in RA neuronal density, coincident with HVc axonal ingrowth (Konishi and Akutagawa 1985; Konishi and Akutagawa 1987). These changes probably reflect the establishment of new synaptic connections between HVc and RA, and part of this process appears to involve RA dendritic expansion (our results; see also DeVoogd et al., 1986). The growth-cone like structures that I observed on the tips of individual RA dendrites may be evidence of such expansion. One of the most striking differences observed in RA neuronal morphology between day twenty and day sixty is the apparent increase in the density of dendritic spines. Perhaps many of the new HVc synapses that are added to RA over this period are being made onto these spines. This interpretation is reinforced by EM data in both the canary and the

zebra finch, suggesting that the majority of HVc axons terminate on the dendritic spines of RA neurons (Canady et al., 1988; Herrmann and Arnold 1989).

The present study also reveals that many nuclei of the accessory pathway are linked together before certain key connections are established in the primary pathway. Before day 20, HVc terminals are present within area X, and MAN terminals are present within RA. At the same time, cells within DLM are retrogradely labeled following tracer injections into MAN. Taken together, these results imply that much of the accessory loop may be connected by day 20. In contrast, HVc axons do not form substantial connections with RA until days 25 to 35. The mechanisms regulating the differences in developmental timing in these two pathways are not totally clear, although thymidine birthdating suggests that HVc neurons projecting to area X are born well before those projecting to RA (Alvarez-Buylla et al., 1988; Kirn and DeVoogd 1989; Nordeen and Nordeen 1988). The heterochronic neurogenesis of HVc's two efferent subpopulations may provide an initial bias that favors the early development of the accessory pathway.

The developmental differences between these two pathways may have important behavioral implications. Lesion studies support the division of the song control circuit into both a primary pathway, which must be intact for normal song production in the adult, and an accessory pathway, which appears to play an essential role only in the early stages of song development (Bottjer et al., 1984; Nottebohm et al., 1976; Sohrabji et al., 1990). Recently, song-selective auditory responses have been detected in both MAN and area X in the adult zebra finch (Doupe and Konishi 1991). X-projecting HVc neurons, also known to respond selectively to song (Margoliash 1983), may provide auditory input to the accessory pathway (Katz and Gurney 1981). Therefore, neuronal populations exhibiting highly specific auditory response properties in the adult

are connected as early as fifteen to twenty days after hatching, coincident with the onset of sensory acquisition, when young zebra finches first begin to listen to and memorize an external song model. In contrast, connections between two vocal premotor areas, HVc and RA, are not established until ten to fifteen days later, coinciding quite closely with the onset of subsong (Immelmann 1969). Staggering the development of the primary and accessory pathways might permit song nuclei involved in sensory acquisition to be connected first, where they then might guide the later-developing connections of the vocal motor control pathway.

CHAPTER 3. THE PHYSIOLOGY OF SYNAPTIC TRANSMISSION IN NUCLEUS RA

ABSTRACT

This chapter examines the physiological properties of synapses that MAN and HVc axon terminals make on RA neurons. The previous chapter utilized anatomical techniques to illustrate that MAN and HVc axons innervate RA at different stages during development. MAN, but not HVc, terminals are present within RA before day twenty-five. By day forty, however, both MAN and HVc axons innervate RA. An *in vitro* brain slice preparation was developed, and intracellular recordings obtained from RA neurons were used to describe the development of MAN and HVc axonal synapses within RA. Electrical stimulation of MAN, but not HVc, fibers evoked excitatory synaptic potentials from virtually all RA neurons in brain slices prepared from birds less than twenty-five days of age. "MAN" EPSPs were blocked by kynurenic acid (1mM) and were substantially reduced by the NMDA receptor antagonist, D-APV (50 to 100 μM), or hyperpolarization of the postsynaptic membrane. In contrast, electrical stimulation of the MAN *and* the HVc fiber tracts evoked synaptic responses from over 70% of the same RA neurons when slices were prepared from male birds of forty to seventy days of age. Although the MAN EPSPs were still blocked by D-APV or postsynaptic hyperpolarization, the "HVc" EPSPs were relatively insensitive to D-APV, but almost completely abolished by CNQX, a non-NMDA glutamate receptor antagonist. Polysynaptic excitation and inhibition could also be evoked within RA by stimulating either afferent at higher intensity. Our experiments indicate that MAN and HVc axons make pharmacologically distinct synapses on the same RA neurons, and that these synapses are first formed at different stages during development.

INTRODUCTION

The neurophysiological mechanisms underlying song learning are unknown, despite extensive information about the plasticity of the song behavior itself. Presumably, synapses within the song system are modified during the course of song learning, but the physiological basis of such modification is unclear. Because of an absence of detailed intracellular electrophysiological analyses in the song system, the physiological nature of synaptic transmission between song system neurons is largely unknown. Although the cholinergic activity within the song system has been mapped (Ryan and Arnold 1981; Watson, Adkins-Regan et al. 1988; Zuschratter and Scheich 1990), and the acetylcholine and catecholamine contents of several song control nuclei have been assayed with HPLC (Sakaguchi and Saito 1989), the synaptic physiology of the song system is still poorly understood. The present study uses intracellular recording techniques to examine synaptic transmission between several forebrain song control nuclei, and to assess whether their synaptic properties change during development.

The robust nucleus of the archistriatum (RA) occupies a pivotal position in the vocal motor control pathway. RA neurons project axons directly onto the tracheosyringeal portion of the hypoglossal nucleus (nXIIts; see Figure 1) (Gurney 1981; Nottebohm et al., 1982), which in turn innervates the syringeal muscles involved in song (Gurney 1981; Manogue and Nottebohm 1982; Vicario and Nottebohm 1988). Afferents supplying RA originate in two other forebrain song nuclei, the caudal part of the nucleus of the ventral hyperstriatum (HVc), and the lateral part of the magnocellular nucleus of the anterior neostriatum (MAN; unless it is specifically stated, I will use MAN to refer to the lateral portion of MAN) (Bottjer et al., 1989; Gurney 1981; Nottebohm et al., 1982).

In the previous chapter, I used anatomical techniques to show that MAN terminals enter RA by fifteen days after hatching, even though HVc terminals do not enter RA until ten to fifteen days later. Four related problems are pursued in the present chapter. The first is to elucidate the synaptic physiology of MAN terminals found within RA before day twenty-five. The second is to establish whether MAN and HVc synapses present in RA at later stages of development possess similar or different physiological properties. The third is to determine whether these two afferents innervate the same, or different, RA neurons, and the fourth is to identify the morphology and intrinsic properties of these postsynaptic cells. In the present experiments, an *in vitro* brain slice preparation was developed in which intracellular recordings could be obtained from RA neurons, and the MAN and HVc fiber pathways could be electrically stimulated independent of one another. This approach was used to examine the physiological properties of MAN and HVc synapses, and to assess their changes between days fifteen and seventy, when vocal plasticity is greatest. Brain slices were prepared from finches less than twenty-five days old, when MAN, but not HVc, terminals were known to be present within RA, or from male finches more than forty days old, when both types of terminals were present within RA. These studies indicate that MAN axons form electrophysiologically detectable synapses within RA substantially earlier than do HVc axons. Ultimately, MAN and HVc axons innervate many of the same RA neurons, but evoke synaptic potentials with distinctly different pharmacological properties. The possible implications for song development and production are discussed.

METHODS

Slice preparation and intracellular recording

Brain slices were prepared from fifteen to ninety day old zebra finches (*Taeniopygia guttata*) or Bengalese finches (*Lonchura striata*) obtained from our breeding colony (all dates refer to posthatch age: the hatch day is p0). Birds were anesthetized with ketamine hydrochloride (0.03 to 0.06 ml), followed by 5 to 10 minutes of Metofane™ (Pitman-Moore, Inc.) inhalation, which was discontinued when the respiratory rate decreased markedly and breathing became more relaxed. A second, larger injection of ketamine (0.06 to 0.09 ml) was then administered, followed by decapitation. The brain was rapidly removed and placed in ice-cold artificial cerebrospinal fluid (ACSF) equilibrated with 95% oxygen (O_2) and 5% carbon dioxide (CO_2). (See below for ACSF recipes.) Initially, slices were prepared in the parasagittal orientation by blocking the brain along the sagittal midline, and gluing the medial face of each hemisphere to the stainless steel tray of a vibratome (DSK Microslicer). To prepare coronal slices, a razor blade was used to block the brain transversely about 5 mm rostral of the bifurcation of the midsagittal sinus. The caudal half of the brain was glued (Loc-tite) rostral face down to the stainless steel tray of the vibratome. In either case, the tissue was subsequently immersed in ice-cold ACSF, and slices were cut at 400 μm thickness, then transferred with the blunt end of a Pasteur pipette onto polycarbonate film (Nuclepore; 12 μm pore size) resting on the surface of ACSF in an interface chamber. The ACSF in the interface chamber was supplemented with 0.1% BSA (Sigma), and D,L-APV to a final concentration of 100 μM. The upper surfaces of the slices were exposed to a humidified atmosphere of 95% O_2/5% CO_2.

After a 1 to 2 hour recovery period, individual brain slices were transferred to a semisubmersion type recording chamber maintained at 35°C,

with a perfusion rate of 3 to 5 ml/min. The fluid level was lowered to within less than 500 µm of the upper surface of the slice. ACSF (without BSA or D,L-APV) was warmed to 35°C and gassed with 95% O_2/5% CO_2 before entering the chamber. Humidified 95% O_2/5% CO_2 was also supplied to the recording chamber.

Initial experiments utilized parasagittal slices of forebrain prepared from birds less than twenty-five days old. Slices containing RA were identified under transillumination, and a tungsten stimulating electrode was placed in the region between HVc and RA known as the tractus archistriatalis (TA). In many cases, electrical stimulation in the TA evoked synaptic responses from RA neurons, as long as the slice also contained tissue lateral to RA. Despite the possibility that stimulation in this dorsal region might excite axons arising either from MAN or HVc, previous anatomical studies showed that MAN, but not HVc terminals, were present within RA before day twenty-five (see Chapter 2). Therefore, even though the pharmacological analyses of these synaptic responses were treated separately, they probably reflect the synaptic connections MAN axons make with RA neurons before day twenty-five. Further anatomical reconstruction showed that MAN and HVc axons describe different paths to reach RA (see Chapter 2, and also Bottjer et al., 1989). Although MAN and HVc fibers run roughly parallel to each other, in dorsoventral trajectories towards RA, and thus might be included in the same parasagittal slice, MAN fibers are displaced laterally to those arising from HVc. Ultimately, MAN axons turn and enter RA along its lateral face, whereas HVc axons, being more medially situated, enter RA along its dorsal edge (see Figure 6). Given this anatomical organization, coronal slices containing RA could be prepared that permitted the MAN and HVc fiber tracts to be electrically stimulated independently of one another. Therefore, all subsequent experiments utilized

coronal slices, and bipolar tungsten stimulating electrodes were placed ≤1.0 mm lateral and dorsal to nucleus RA, in areas containing either the MAN or HVc axon tracts entering the nucleus (see Figure 11). Electrical stimulation of each fiber tract was accomplished by applying brief voltages (0.5 to 20 Volts), 100 µsec in duration, at a frequency of 0.1 to 100 Hz (WPI Pulsemaster), across the two poles of either stimulus electrode.

In some experiments, drugs were delivered to the slice by switching between various bathing solutions via a solenoid-operated valve assembly (General Valve). Alternatively, a pressure-driven puffer pipette (WPI PicoPump), prepared from 1mm capillary glass and drawn to a final tip diameter of 10 to 100 µm, was positioned within 300 µm of the recording site. Drugs of choice were dissolved in ACSF at known concentrations and then loaded into the pipette. With this method, drug concentrations refer to the pipette solution. The actual bath concentrations were assumed to be substantially lower than the upper limit set by the pipette concentration. D(-)-2-Amino-5-phosphonopentanoic acid (D-APV) and 6-Cyano-7-nitroquinoxaline-2,3 dione (CNQX) were purchased from Tocris Neuramin. QX-314 (a gift of Dr. Henry Lester) was dissolved in 2 molar-potassium acetate at a final concentration of 75 mM. All other drugs were purchased from Sigma.

Intracellular recordings were obtained by impaling RA neurons with 50 to 150 MΩ electrodes fabricated on a Brown-Flaming microelectrode puller from 1mm borosilicate glass (WPI 1B1001F). Electrodes were filled with 3 molar-potassium acetate. The postsynaptic membrane potential was monitored with an intracellular amplifier (NeuroData IR-283, bridge circuit) and individual events stored on videotape (Sony SLO-1800) in a pulse code format (Neuro-Corder DR-484). DC hyperpolarization of the postsynaptic membrane potential was accomplished by tonically passing negative currents through the

recording electrode. Signals were low pass filtered at five kHz, digitized at ten kHz, signal averaged, and analyzed with the aid of digital oscilloscope software written by Larry Proctor for a MASSCOMP graphics workstation. Software for performing Fast Fourier Transforms (FFTs) was supplied by James Mazer. Synaptic potentials are the averages of 6 to 16 individual traces, unless otherwise specified. Measurements of the EPSP slope were calculated over the first millisecond of the EPSP, starting from the EPSP onset. Onset latencies were measured from the initial deflection of the stimulus artifact to the initial deflection of the EPSP above baseline. EPSP amplitudes were calculated as the maximum positive deflection from baseline. Quantification of the EPSP amplitude reflects the mean, as normalized to the control value preceding drug treatment, ± S.E.M. Average values of an EPSP's peak latency and onset slope were not normalized. Statistical significance was determined with an unpaired *t*-test (two-tailed) for comparing means, and the Mann-Whitney *U* test, for populations. The *t*-test values in each case are reported as p<significance level; the Mann-Whitney *U* test values, when given, are reported as p=significance level. The firing frequency (in Hz) was calculated as twice the total number of spikes observed over the duration of the 500 millisecond current pulse, as the firing rate exhibited little or no adaptation below within the test range. Resting potential was calculated as the difference between the observed potential immediately before and after withdrawal of the recording electrode from the cell.

Intracellular staining

Lucifer Yellow CH (Aldrich) (Stewart 1978), or biocytin (Sigma) (Horikawa and Armstrong 1988), was used to stain individual RA neurons. Details of the both procedures were outlined in the previous chapter.

ACSF Recipes

Normal ACSF: NaCl, 134.0; $NaHCO_3$, 25.7; NaH_2PO_4, 1.3; KCl, 3.0; $MgSO_4(7H_2O)$, 1.3; $CaCl_2(2H_2O)$, 2.4; glucose, 12.0; urea, 1.0.

Low Temperature ACSF: NaCl, 112.6; $NaHCO_3$, 47.6; NaH_2PO_4, 1.3; KCl, 3.0; $MgSO_4(7H_2O)$, 1.3; $CaCl_2(2H_2O)$, 2.4; glucose, 12.0; urea, 1.0.

High Divalent ACSF: NaCl, 134.0; $NaHCO_3$, 25.7; NaH_2PO_4, 1.3; KCl, 3.0; $MgSO_4(7H_2O)$, 3.9; $CaCl_2(2H_2O)$, 4.0; glucose, 12.0; urea, 1.0.

Very High Divalent ACSF: NaCl, 134.0; $NaHCO_3$, 25.7; NaH_2PO_4, 1.3; KCl, 3.0; $MgSO_4(7H_2O)$, 7.8; $CaCl_2(2H_2O)$, 8.0; glucose, 12.0; urea, 1.0.

All concentrations are in millimolar (mM).

Figure 11. Schematic of the brain slice preparation. Coronal slices of the telencephalon were made at the level of RA. By superimposing the labeled MAN and HVc axons shown earlier (see Figure 6) with the aid of a camera lucida, the relative anatomical separation of these two pathways innervating RA is illustrated. Arrows identify MAN and HVc axon tracts, respectively, and also indicate the approximate placement of the two bipolar stimulating electrodes. Individual neurons within RA were impaled with intracellular electrodes, and electrical stimulation was applied to either MAN (lateral), or HVc (dorsal), fiber tracts. Slices were made either from birds less than twenty-five days of age, when only MAN terminals were present within RA, or after day forty, when terminals from both afferents were present within the nucleus. Scale bar equals 1 mm.

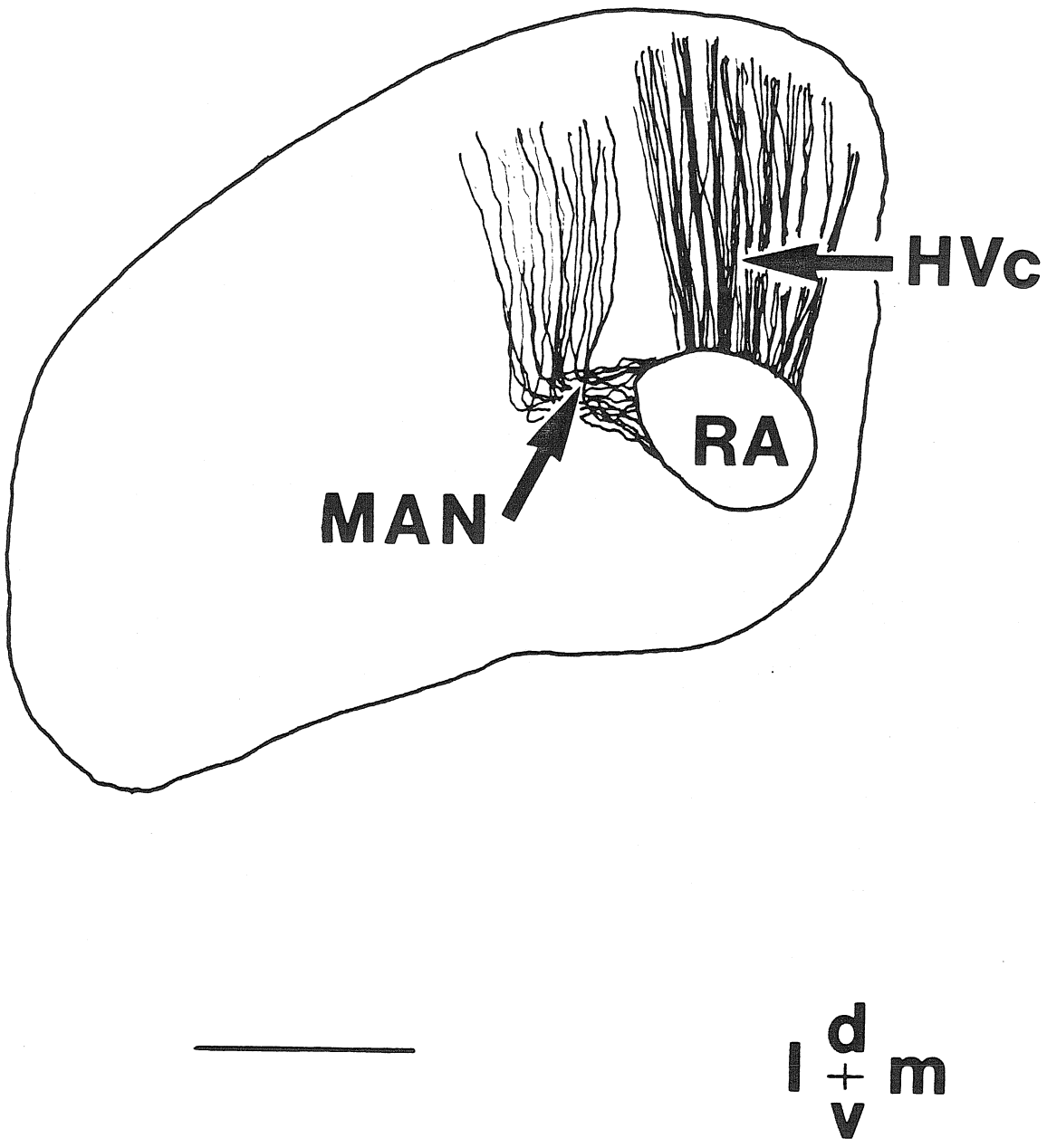
HVc
RA
MAN
l
d
v
m

RESULTS

INTRINSIC PROPERTIES OF RA NEURONS

RA neurons were characterized by high levels of spontaneous activity *in vitro*. RA neurons in slices prepared from finches of all ages exhibited spontaneous subthreshold oscillations of the membrane potential, as well as highly regular and tonic genesis of action potentials. Because these intrinsic properties were quite similar from cell to cell, even across different ages, RA neurons are treated as a single class in the following section.

Subthreshold properties

Subthreshold oscillations of the membrane potential were a conspicuous feature of most RA neurons encountered *in vitro*. Subthreshold oscillations often occurred spontaneously, as seen in Figure 12a_1, but could also be elicited by steady depolarizing current injection (see Figures 12b_1 and c_1, as well as Figure 14). Fast Fourier Transforms (FFTs) of the subthreshold oscillations revealed a dominant oscillatory component that increased in both frequency and amplitude when the cell was depolarized by tonic current injection (Figure 12 a_2-c_2). When tonic currents displaced the membrane potential just above spike threshold, a continuous, regular train of action potentials was generated (Figure 12d_1). The action potential frequency was markedly lower than the dominant frequency of the subthreshold oscillation observed in the same cell when just below spike threshold (compare Figures 12c_2 and 12d_2).

Input resistance

The input resistances of RA neurons were measured by passing small (50 to 300 pA), hyperpolarizing current pulses through the recording electrode, and measuring the resultant changes in membrane potential (see Figure 13a). The membrane potential often exhibited a slight "sag" back towards baseline within the first 50 milliseconds of the current pulse. Therefore, the pulse length was varied between 100 and 500 milliseconds to insure that the membrane potential had achieved a steady value, and the change in membrane potential relative to the baseline was made at the end of the current pulse. Input resistances of RA neurons ranged between 40 and 120 MΩ (Figure 13b).

Suprathreshold properties

RA neurons fired highly regular action potential trains in response to suprathreshold, depolarizing currents, as shown in Figure 14a-c. When current pulses just exceeded spike threshold (Figure 14a), a prolonged "subthreshold" oscillation preceded the onset of the spike train. As increased depolarizing current was injected into the cell, threshold was reached progressively earlier, and the duration of the subthreshold oscillations diminished. With very large currents, these oscillations disappeared altogether (see Figure 14b,c).

The firing frequency of RA neurons approximated a linear function of the amplitude of the injected current pulse (see Figure 15a). The slope of the firing frequency/injected current (f-I) relationship averaged 63.1±11.4 Hz/nA (mean ±SD; N=12). Although most RA neurons were injected with maximum currents less than or equal to +1 nA, several cells tested above this range failed to show any pronounced saturation in firing rate, even at +3nA.

The highly periodic action potentials of RA neurons exhibited little acceleration or frequency adaptation when subjected to depolarizing currents several hundred milliseconds in duration. With current pulse amplitudes less than +1.0 nA, the interspike interval remained nearly constant over the duration of a 500 millisecond stimulus, as illustrated in Figure 15b. The interspike interval also remained extremely constant when the cell was tonically depolarized slightly above threshold, and did not vary even over several seconds of continuous firing (see Figure 12d, e.g.).

Figure 12. Subthreshold membrane potential oscillations recorded from an RA neuron. a_1-c_1 illustrate the fluctuations in membrane potential common to RA neurons *in vitro*. a_1 was recorded at the cell's actual resting potential at -49 mV. b_1 through d_1 were obtained at increasingly more positive potentials by injecting positive currents through the recording electrode. In d_1, the membrane potential was depolarized above spike threshold, resulting in a highly regular train of action potentials (note that the scale for both the raw data and the FFT in **d** differs from **a-c**; spikes also are truncated in d_1). a_2-d_2 are the respective Fast Fourier Transforms (FFTs) of the raw data; the abscissa corresponds to frequency plotted in 10 Hz intervals; the ordinate specifies power in arbitrary units.

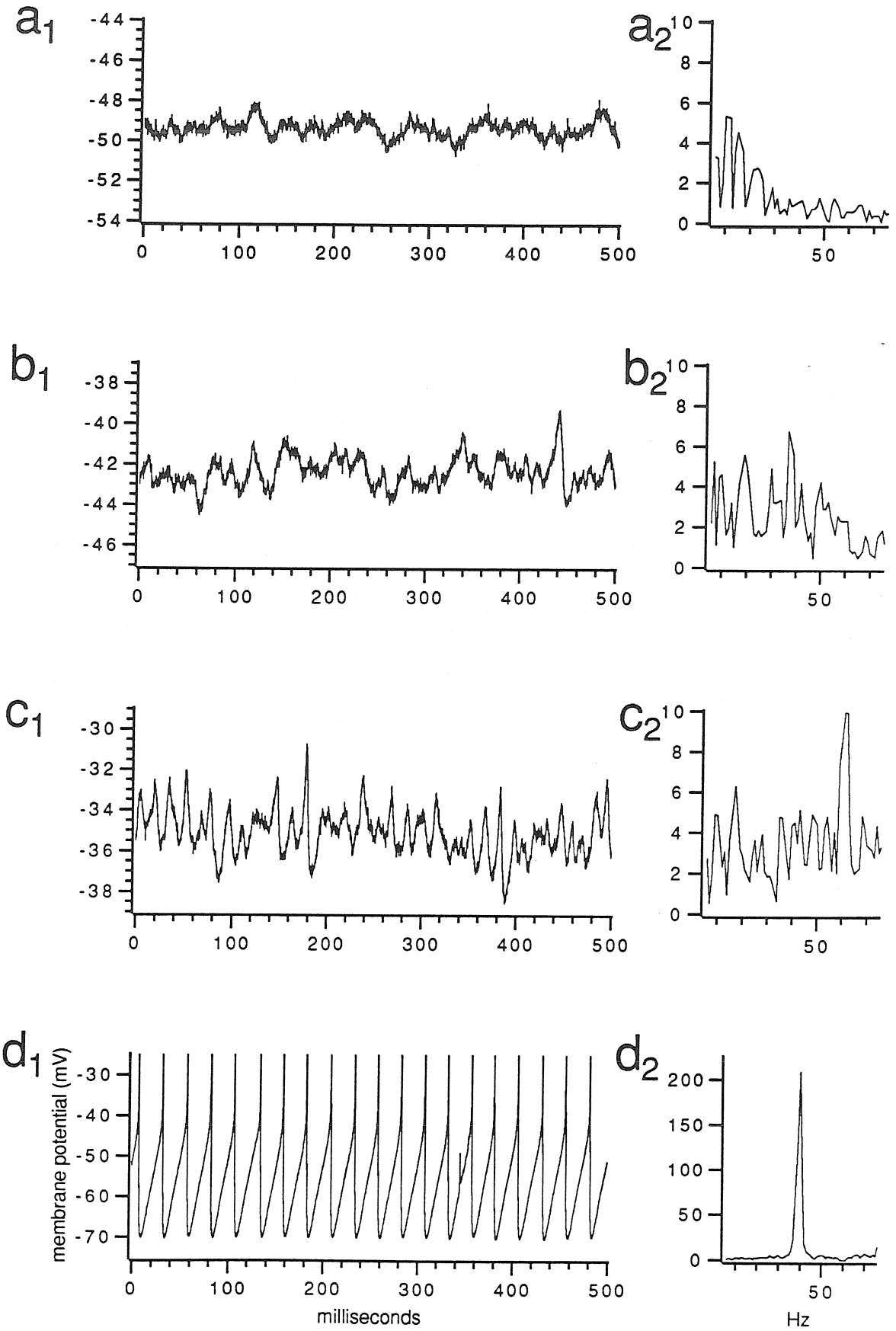
a1
-44
-46
-48
-50
-52
-54
0
100
200
300
400
500
a2
10
8
6
4
2
0
50
b1
-38
-40
-42
-44
-46
0
100
200
300
400
500
b2
10
8
6
4
2
0
50
c1
-30
-32
-34
-36
-38
0
100
200
300
400
500
c2
10
8
6
4
2
0
50
d1
membrane potential (mV)
-30
-40
-50
-60
-70
0
100
200
300
400
500
milliseconds
d2
200
150
100
50
0
50
Hz

Figure 13. Estimates of input resistance of RA neurons.

a) The input resistance of RA neurons was calculated by passing hyperpolarizing currents through the recording electrode (represented by the square traces in lower part of the figure), and measuring the change in membrane potential (rounded traces in upper portion of figure), relative to the resting potential before current application. The vertical calibration bar equals 10 mV in the upper trace, and 75 pA in the lower trace; the horizontal scale bar equals 40 milliseconds in both cases. Resting potential was -52 mV.

b) Plots depict the change in membrane potential as a function of the injected current for five "typical" RA neurons. Straight-line fits of the data were used to calculate the input resistance. Cell in a) is plotted as open circles; straight line fit yielded a value of 137 MΩ. Note that straight-line fit limited to the 0 to -100 pA range for the same cell yielded an estimate of input resistance of approximately 75 MΩ. This is the range that most cells were tested over.

a

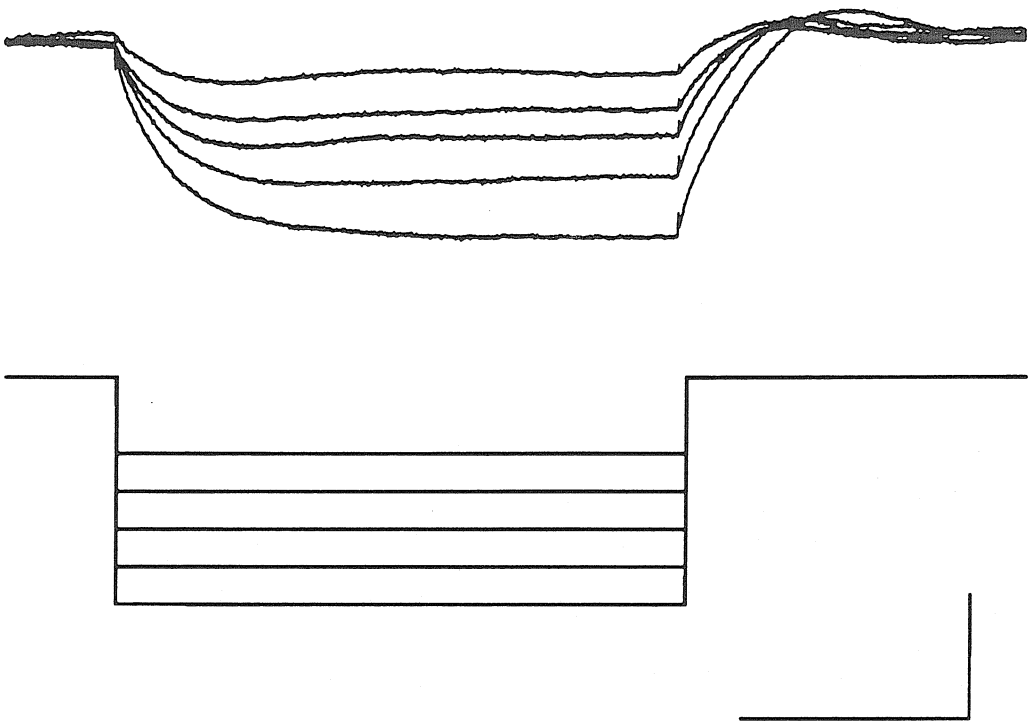

b

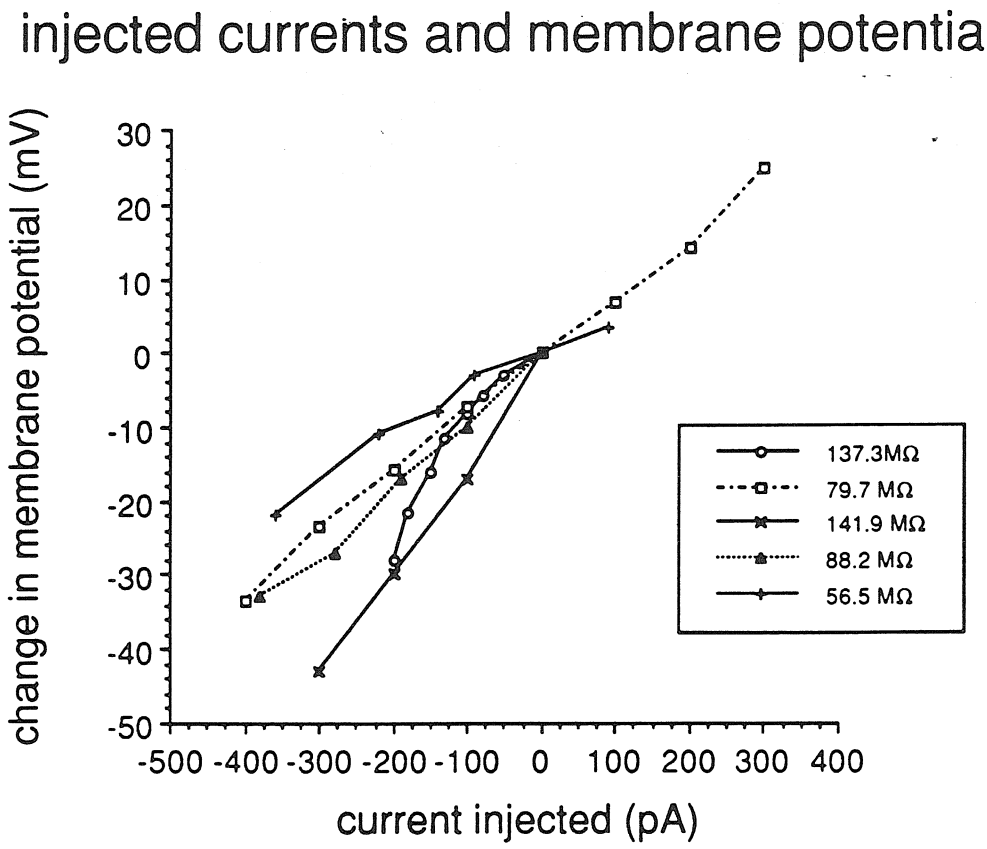
injected currents and membrane potential
change in membrane potential (mV)
30
20
10
0
-10
-20
-30
-40
-50
-500 -400 -300 -200 -100 0 100 200 300 400
current injected (pA)
137.3MΩ
79.7 MΩ
141.9 MΩ
88.2 MΩ
56.5 MΩ

Figure 14. RA neurons fired repetitive and highly regular action potentials when injected with suprathreshold depolarizing currents.

a) A +240 pA current just exceeded spike threshold. A prolonged subthreshold membrane potential oscillation preceded action potential onset. Also note the relatively high spike rate at threshold.

b) Response to a +375 pA current.

c) Response to a +550 pA current.

RA neuron recorded *in vitro* from a slice prepared from a forty-five day old male finch. Calibration bars for a-c equal 40 mV (vertical), 150 milliseconds (horizontal). Square trace at the bottom of the figure represents the timing of the injected current pulse. Resting potential was -55 mV.

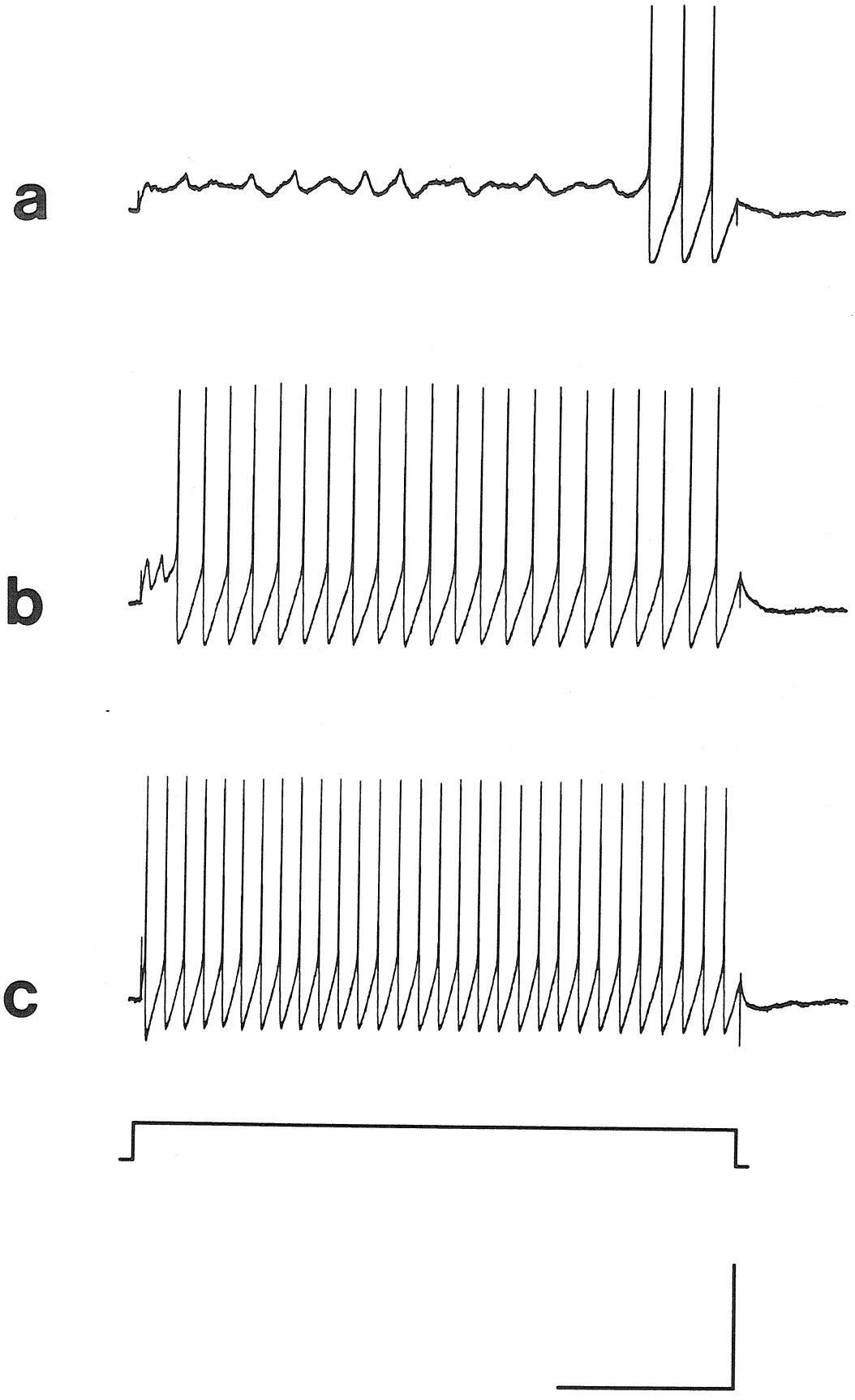
a
b
c

Figure 15. Firing frequency and interspike interval.

a) The firing frequency (in spikes per second) plotted as a function of the amplitude of the depolarizing current pulse. These curves typify the frequency/current (f-I) relationships exhibited by RA neurons.

b) A plot of interspike interval versus the interval number demonstrates the highly regular nature of the spiking behavior recorded from RA neurons. Measurements were made over the duration of a 500 millisecond long depolarization, at +180, +550, and +920 pA, respectively. No pronounced accommodation was exhibited.

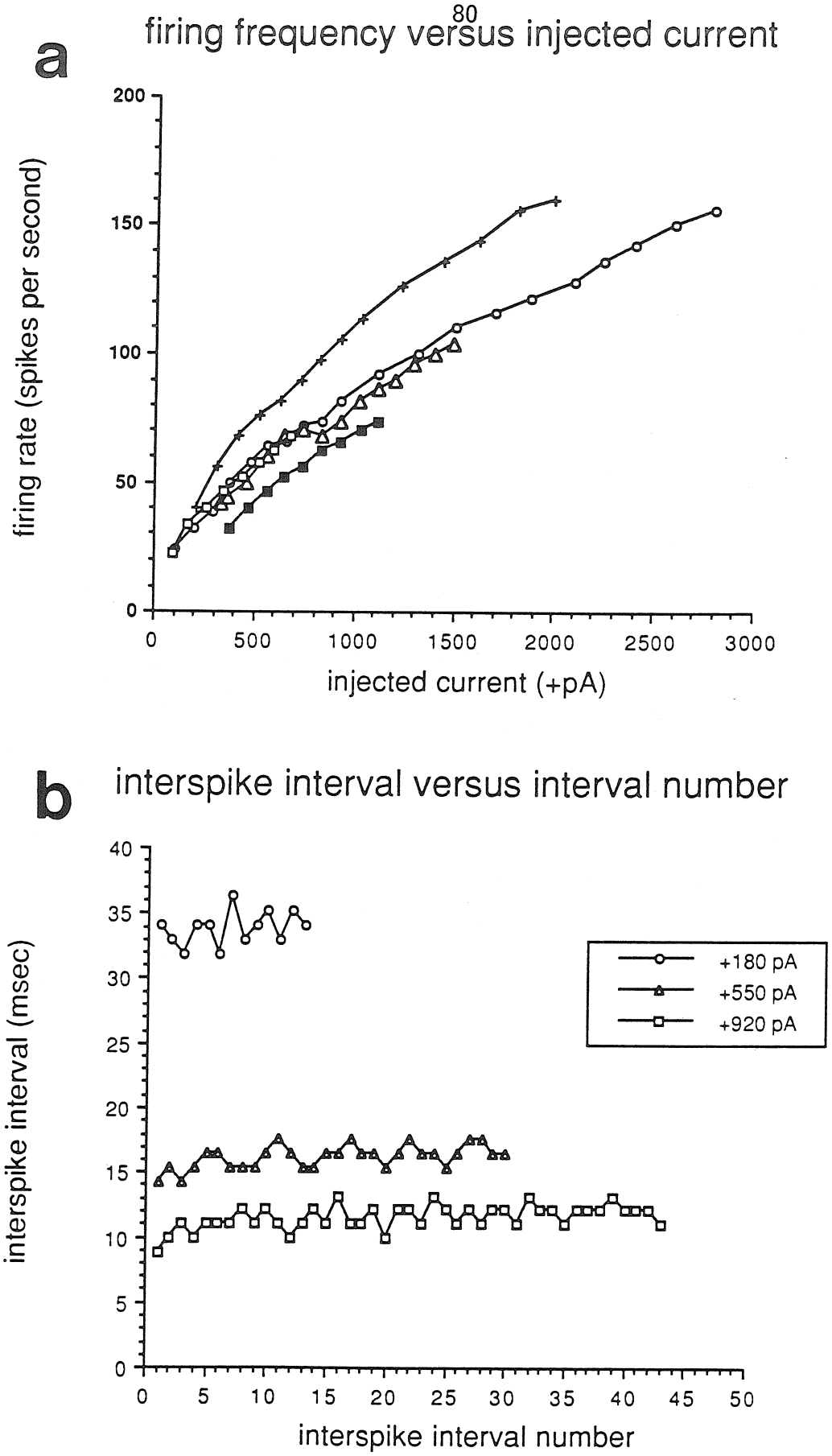
a
firing frequency versus injected current
firing rate (spikes per second)
200
150
100
50
0
0
500
1000
1500
2000
2500
3000
injected current (+pA)
b
interspike interval versus interval number
interspike interval (msec)
40
35
30
25
20
15
10
5
0
0
5
10
15
20
25
30
35
40
45
50
interspike interval number
+180 pA
+550 pA
+920 pA

Pharmacological analyses of intrinsic properties: QX-314

Eight repetitive-spiking RA neurons were impaled with recording electrodes loaded with 75 mM QX-314 in 2 molar-potassium acetate. In the presence of QX-314, the regular trains of fast action potentials elicited by depolarizing currents rapidly disappeared, presumably because of the blockade of voltage-dependent sodium conductances (Strichartz 1973). Despite removal of the sodium spike, depolarizing currents (> +0.5 nA) still evoked broad, rhythmic oscillatory potentials in QX-314 treated cells, as seen in Figure 16. The frequency of the oscillatory potentials increased when the amplitude of the injected current pulse was raised. Noticeable damping of the potentials occurred over the duration of the current pulse (see Figure $16a_1$-c_1). FFTs indicated that the frequency of the oscillation's major component increased as a function of the injected current pulse amplitude (see Figure $16a_2$-c_2).

Low calcium ACSF

The repetitive action potential discharge exhibited by RA neurons in response to depolarizing currents persisted in calcium-free ACSF, although with some minor differences, when recording with 3 molar-potassium acetate electrodes. In both the control and low-calcium conditions, a +100 pA, 500 millisecond long current pulse depolarized the cell above spike threshold, resulting in regular action potential trains (Figure 17a). However, in the absence of external calcium, the spike rate was higher, and the interspike hyperpolarizing phase noticeably shallower, relative to the control response. The divalent cation concentration was kept constant throughout the experiment by elevating the magnesium-ion concentration in the calcium-free ACSF. Therefore, these differences probably do not reflect the removal of divalent

cations from sites on the extracellular surface of the membrane, which in other instances can increase excitability by altering the effective transmembrane potential experienced by voltage-sensing gating elements (Frankenhaeuser and Hodgkin 1957).

The QX-314-insensitive oscillations also depended on the external calcium-ion concentration. Two QX-314-treated RA neurons that had displayed pronounced oscillations in response to depolarizing currents in normal ACSF were subsequently examined in the absence of external calcium (magnesium was supplemented to maintain the divalent concentration at a constant level throughout). The QX-314-insensitive oscillations disappeared when the normal ACSF (2.4 mM calcium) was replaced with nominally calcium-free ACSF, but returned when the normal ACSF was reintroduced into the recording chamber (see Figure 17b).

Cesium chloride

Cesium ions block a number of different voltage-activated potassium channels (Hille 1984). Four RA neurons impaled with recording electrodes containing 3 molar-cesium chloride exhibited distinct spike-broadening when depolarized above threshold (see Figure 18a). The first spike could exceed 50 msec in duration, and although the durations of subsequent spikes decreased, they were still quite broad. Subthreshold oscillations preceding the first action potential were distinctly absent from cesium-dialyzed cells. The firing rate observed in the presence of cesium increased as a linear function of the injected current (Figure 18b). Constant suprathreshold depolarizing currents were accompanied by a distinct acceleration of the spike rate, as can be seen by the decrease in the interspike interval over time (Figure 18c).

Figure 16. The membrane potential of RA neurons treated with QX-314 oscillated in response to depolarizing currents. In a_1-c_1, positive currents were injected into the cell for 500 milliseconds, beginning at t=100 milliseconds. The actual current amplitude applied in each case is listed in the box at top center. In a_2-c_2, FFTs of the raw data are shown. The ordinate is power in arbitrary units; note that a_2-c_2 are scaled differently from each other. The peak of the FFT shifts to the right with increasing depolarization. Also note damping of the oscillation over time, especially prominent in c_1.

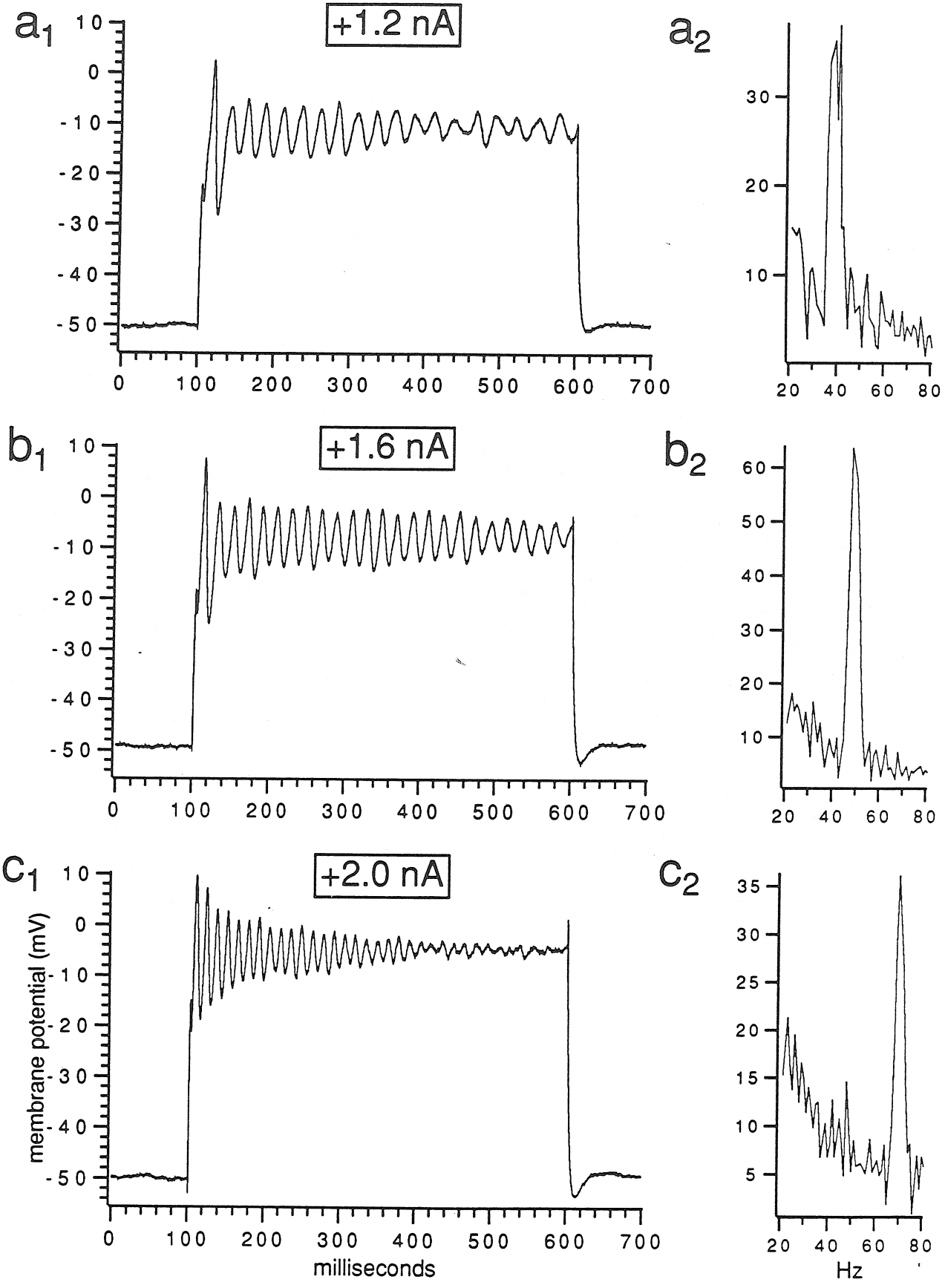
a1
+1.2 nA
a2
b1
+1.6 nA
b2
c1
+2.0 nA
c2
membrane potential (mV)
milliseconds
Hz

Figure 17. Lowering the external calcium ion concentration altered the excitability of RA neurons *in vitro*.

a) A typical RA neuron, impaled with a standard 3 molar-potassium acetate electrode, and bathed in control ACSF (2.4 mM external calcium, 2 mM magnesium; *solid trace*), fired a regular train of action potentials at ~10 Hz when depolarized with a 500 millisecond long, +100 pA current. When bathed in "calcium-free" ACSF (0 mM calcium, 4.4 mM magnesium; *open circles*), the spike rate of the same cell was nearly 20 Hz when depolarized with the same, +100 pA current as in the control conditions. Note that in the absence of external calcium, the interspike hyperpolarization was much less pronounced.

b) An RA neuron impaled with a QX-314-loaded pipette exhibited an oscillating membrane potential when depolarized with a 100 millisecond long, +800 pA current. After bathing the slice in "calcium-free" ACSF (as in a)), the same depolarizing currents evoked an essentially flat response.

a

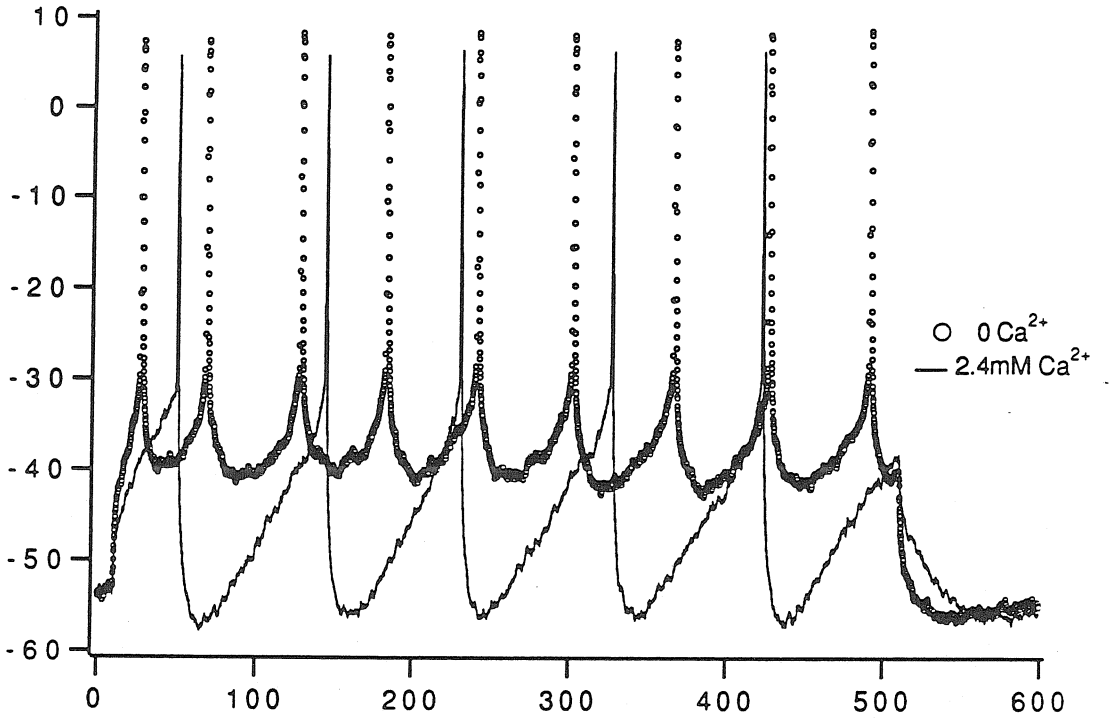
10
0
-10
-20
-30
-40
-50
-60
0
100
200
300
400
500
600
O 0 Ca2+
— 2.4mM Ca2+

b

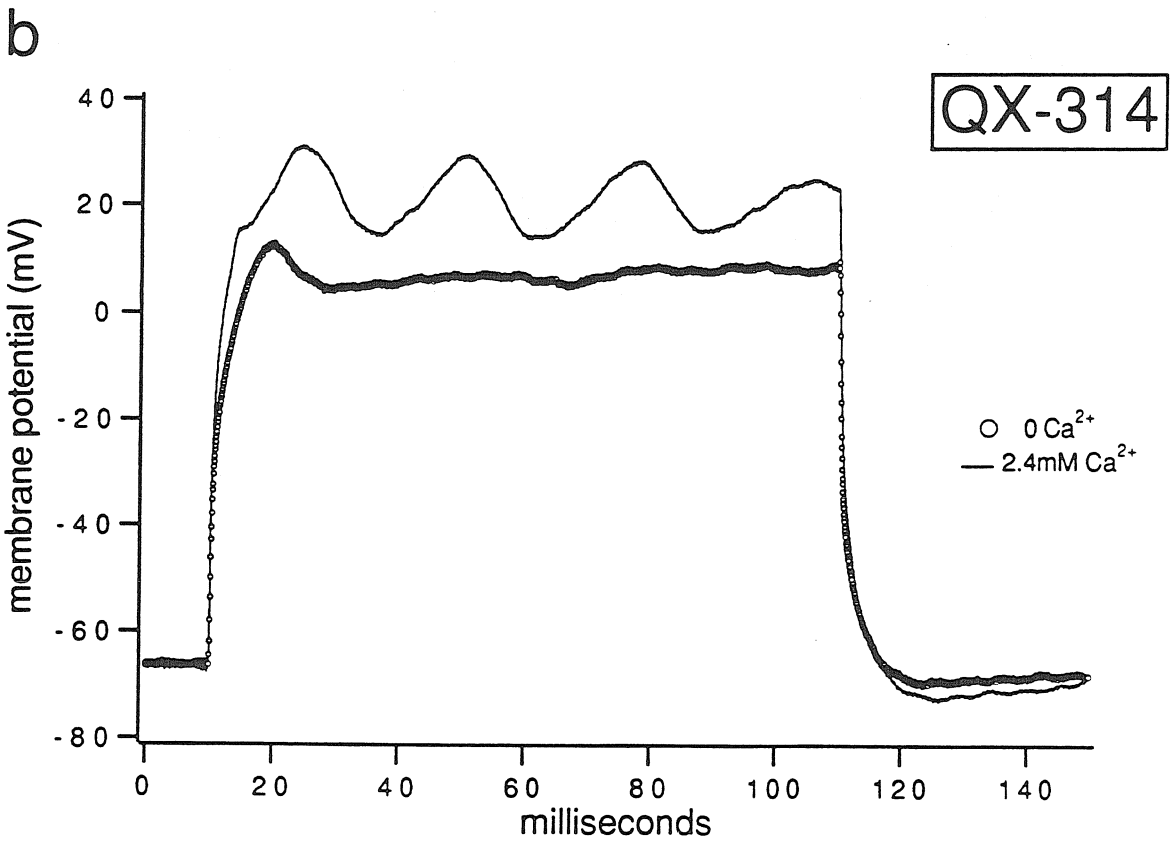
QX-314
40
20
0
-20
-40
-60
-80
membrane potential (mV)
0
20
40
60
80
100
120
140
milliseconds
O 0 Ca2+
— 2.4mM Ca2+

Figure 18. Cesium ions broaden the action potentials of RA neurons.

a) Response of an RA neuron dialyzed with cesium chloride to a 500 millisecond long, +180 pA depolarizing current. Scale bars equal 50 mV (vertical), and 140 msec (horizontal). Resting potential was -76 mV.

b) Firing rate of a cesium-treated cell plotted as a function of the injected current.

c) In the presence of cesium, the interspike interval decreased dramatically from the first interval, and then more gradually over subsequent intervals. Cell was injected with a one second long, +1.0 nA current.


a

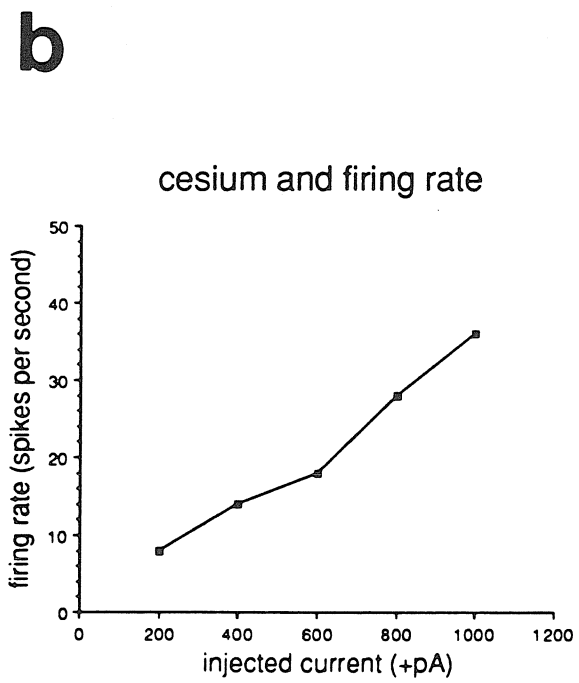
b
cesium and firing rate
firing rate (spikes per second)
0
10
20
30
40
50
0
200
400
600
800
1000
1200
injected current (+pA)

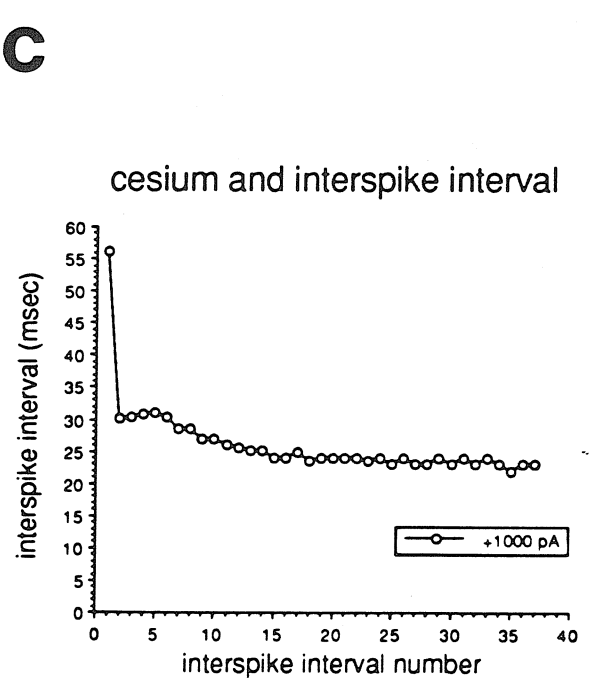
c
cesium and interspike interval
interspike interval (msec)
0
5
10
15
20
25
30
35
40
45
50
55
60
0
5
10
15
20
25
30
35
40
interspike interval number
+1000 pA

SYNAPTIC RESPONSES WITHIN RA BEFORE DAY 25

Parasagittal slices

Preliminary experiments used parasagittal slices of forebrain and demonstrated that before day twenty-five, depolarizing potentials could be evoked from RA neurons by stimulating the region dorsal to the nucleus (see Methods). These potentials often reached spike threshold, and were therefore classified as excitatory (EPSPs). A preliminary pharmacological profile of the EPSPs was obtained by the bath application of various neurotransmitter antagonists to the slice. A total of seventeen RA neurons that had responded to stimulation dorsal to the nucleus were studied in this fashion. Six cells were examined in normal ACSF, and eleven others in zero-magnesium ACSF.

Parasagittal slices: normal ACSF

Kynurenic acid, a glutamate receptor antagonist, exerted a specific blocking effect on EPSPs recorded within RA before day twenty-five. All of the cells studied in normal ACSF were treated with kynurenic acid (EPSPs not shown). In 1 mM kynurenic acid, the EPSP amplitude decreased sharply, declining to 0.20±0.06 of the control value ($p<.0001$, $p=.002$, $N=6$; the EPSP amplitude was normalized to the amplitude measured before drug application). In all six cases, washout of the kynurenic acid with the control ACSF restored the EPSP amplitude to the control value. Five of these same cells were also treated with the nicotinic receptor antagonist, hexamethonium bromide (500 μM), but this drug did not exert a significant effect on the EPSP amplitude (1.02±0.05 relative to the control EPSP amplitude, $p<.67$, $p=1$, $N=5$). Finally, one cell was also treated with the NMDA receptor antagonist D,L (-)-2-Amino-5-phosphonopentanoic acid (D,L-APV) (Davies, Francis et al. 1981) at 250 μM,

which resulted in a marked reduction of the EPSP amplitude (0.25 of the control level). However, since no washout was obtained in this case, it only suggested that NMDA receptors might contribute to the EPSP.

Parasagittal slices: zero-magnesium ACSF

The possibility that NMDA receptors might mediate a portion of the EPSP prompted a second series of experiments in which slices were bathed in zero-magnesium ACSF. Since NMDA receptor-mediated currents can be enhanced by lowering the external magnesium-ion concentration (Thomson 1986), any contribution they might make to the EPSP would be more obvious in these conditions. In fact, switching from normal ACSF to zero-magnesium ACSF always resulted in large increases in the EPSP amplitude (5.42±1.70-fold of the control amplitude, $p<.026$, $p=.002$, $N=6$). Subsequent bath application of D,L-APV (50 to 100 μM) always sharply diminished the EPSP amplitude evoked in zero-magnesium ACSF (0.26±0.04 of the control amplitude in zero-magnesium ACSF, $p<.0001$, $p=.0001$, $N=12$). Successful washout of the APV was accomplished in eleven of these cases, and restored the EPSP amplitude to the control value (0.997±0.11, $p<.98$, $p=1$, $N=11$). Finally, in four of these same cells, bath application of kynurenic acid (1 mM) reduced the EPSP amplitude to an even greater degree than had treatment with D-APV, to 0.04±0.03 of the control value that was recorded in zero-magnesium ACSF. Washout was obtained in three of these cases, with a return to control levels.

These results suggest that RA neurons receive extrinsic innervation as early as day fifteen, well before HVc axons actually enter RA. My pharmacological analyses suggested that this early, excitatory input to RA was glutamatergic, and acted at least in part through NMDA receptors. The actual

source of this excitatory input was difficult to determine from these experiments, however, because it was not clear which fiber pathway (MAN or HVc) was being stimulated in parasagittal slices (see Methods). Furthermore, the recording conditions (i.e., zero-magnesium ACSF) tended to enhance polysynaptic transmission. These factors obscured the true source of the early excitatory input to RA.

Coronal slices: RA before day 25

Coronal slices were used to clarify the identity of the axons supplying the excitatory input to RA before day twenty-five (see Methods). Stable intracellular recordings were obtained from a total of eighty-eight RA neurons in coronal slices prepared from fifteen to twenty-five day old finches. Direct currents were injected into each cell to ascertain its spiking behavior and input resistance, and dye-filling was used in some cases to determine the neuron's morphology. The RA neurons encountered in coronal slices fired repetitive action potentials without accommodation in response to depolarizing currents (see previous section on intrinsic properties), and had spinous dendrites (see Figure 10a). Tonic hyperpolarizing currents were used in some cells to silence spontaneous spiking or to suppress subthreshold membrane potential oscillations, thereby permitting examination of the subthreshold EPSP. In these instances, the term "holding potential" was used in place of resting potential.

MAN versus HVc fiber stimulation before day 25

Almost all RA neurons responded to MAN fiber stimulation, whereas very few responded to stimulation of the HVc fiber pathway. Stimulation of the MAN fiber tract, via the laterally positioned stimulus electrode,

evoked depolarizing potentials from virtually all of the RA neurons encountered in coronal slices (86 of 88 cells). These responses were classified as excitatory (EPSPs) because they could trigger action potentials. Stimulation of the HVc fiber tract, via the dorsal stimulus electrode, only evoked synaptic potentials from twelve cells, ten of which had also responded to MAN fiber stimulation (10 of 88 cells), and in two cells that had not responded to MAN fiber stimulation (2 of 88 cells).

Time course of the MAN EPSP

The potentials evoked by MAN fiber stimulation were abolished by bathing the slice in very low calcium ACSF, consistent with calcium-dependent synaptic transmission (data not shown). In normal ACSF, subthreshold EPSPs evoked by MAN fiber stimulation had both shallow onset slopes and long rise times, but were of a fixed and relatively short latency to onset (<4 msec) (see Figure 19, e.g.). In twelve RA neurons that responded only to MAN fiber stimulation, the MAN EPSPs exhibited an average onset slope of 0.89±0.13 mV/msec, and attained their peak amplitude at an average of 17.93±2.13 msec after onset.

Voltage dependence of the MAN EPSP

The postsynaptic membrane potential exerted a strong effect on the MAN EPSP amplitude. Hyperpolarization of the postsynaptic membrane strongly attenuated the MAN EPSP amplitude (Figure 19a). Twelve RA neurons that responded to MAN fiber stimulation were examined: six in normal ACSF, five in high divalent ACSF (4 mM calcium, 4 mM magnesium), and one in very high divalent ACSF (8 mM calcium, 8 mM magnesium). In every condition, hyperpolarization decreased the MAN EPSP amplitude to between 0.36 and

0.77 of the control value (median=0.55, N=12; for each cell, the EPSP amplitude at any given membrane potential was normalized to the amplitude at the most positive membrane potential examined). In ten of these twelve cells, hyperpolarization also reduced the EPSP's time to peak (range 0.23 to 1.36 ms, median=0.65, N=12; normalized as above). The effects of membrane hyperpolarization on EPSP amplitude and time to peak were plotted against the range of membrane potentials actually observed in each case (see Figure 20). Note that the initial membrane potential did not reliably predict the degree to which subsequent membrane hyperpolarization actually reduced the EPSP amplitude.

In contrast, membrane depolarization augmented the MAN EPSP amplitude. Since the EPSP triggered an action potential when the membrane was extensively depolarized, several cells were impaled with electrodes containing QX-314 in order to block voltage-dependent sodium channels (Strichartz 1973). Consequently, the MAN EPSP could be observed at more positive potentials without sodium-spike contamination. The EPSP continued to increase in amplitude until ca. -40 mV, at which point a broad, biphasic potential was occasionally triggered (Figure 19b). Because of its all or none behavior, pronounced afterhyperpolarization, and persistence in the presence of QX-314, the biphasic component was tentatively identified as a calcium-mediated action potential (see previous section on intrinsic properties).

NMDA receptor antagonists block the MAN EPSP

The voltage dependence exhibited by the MAN EPSP suggested that an NMDA receptor-mediated component contributed to the synaptic response. To clarify the role of putative NMDA receptors in the genesis of the MAN EPSP, the NMDA receptor antagonist D(-)-2-Amino-5-

phosphonopentanoic acid (D-APV) (Davies et al., 1981), was applied to seven RA neurons. Three were examined in zero-magnesium ACSF, one in normal ACSF, and three in high divalent ACSF. In each case, applying APV significantly reduced the amplitude of the MAN EPSP (see Figure 19c).

In normal and high divalent ACSF, bath application of 60 to 75 μM D,L-APV was accompanied by a decline in the MAN EPSP amplitude to 0.42±0.06 of the control amplitude ($p<.0001$, $p=.0139$, $N=4$). One cell was also treated with 1 mM kynurenic acid, which reduced the EPSP amplitude even more extensively, to 0.11 of the control. In zero-magnesium ACSF, 30 μM D-APV or 50 μM D,L-APV also markedly reduced the MAN EPSP, to 0.27±0.08 of the control value measured in zero-magnesium ACSF ($p<.001$, $p=.0369$, $N=3$). In six of these seven cases, recordings were maintained long enough to obtain successful washouts, in which the EPSP amplitude recovered to the control value.

In three of the cases recorded in normal or high divalent ACSF, the effects of membrane hyperpolarization and APV on the MAN EPSP were directly compared. At more positive membrane potentials, the APV-treated EPSP was greatly diminished relative to its control counterpart. As the membrane potential was made more negative, however, the differences between the control and APV-treated EPSP diminished, and at the most negative potentials examined, they were almost indistinguishable from each other (data not shown).

Figure 19. In slices prepared from birds less than 25 days of age, EPSPs evoked from RA neurons by electrically stimulating the MAN fiber tract were sensitive to both the postsynaptic membrane potential, and the application of APV.

a) An MAN EPSP evoked from an RA neuron at the actual resting potential of -63 mV, and after negative current injection had hyperpolarized the cell to -75 mV. The negative-going artifact preceding the onset of the EPSP marks the application of a brief (100 μsec) electrical stimulus to the MAN fiber tract. Scale bars are shown in Figure b).

b) An MAN EPSP evoked from an RA neuron that had been dialyzed with QX-314. Positive current was used to bring the resting membrane potential to -40 mV. Stimulation of the MAN fiber tract evoked an EPSP that was often accompanied by an all-or-none, biphasic potential.

c) The bath application of 75 μM D,L-APV reversibly reduced the amplitude of the MAN EPSP. Resting potential was -65 mV. Recorded in high divalent ACSF (4 mM calcium, 4 mM magnesium).

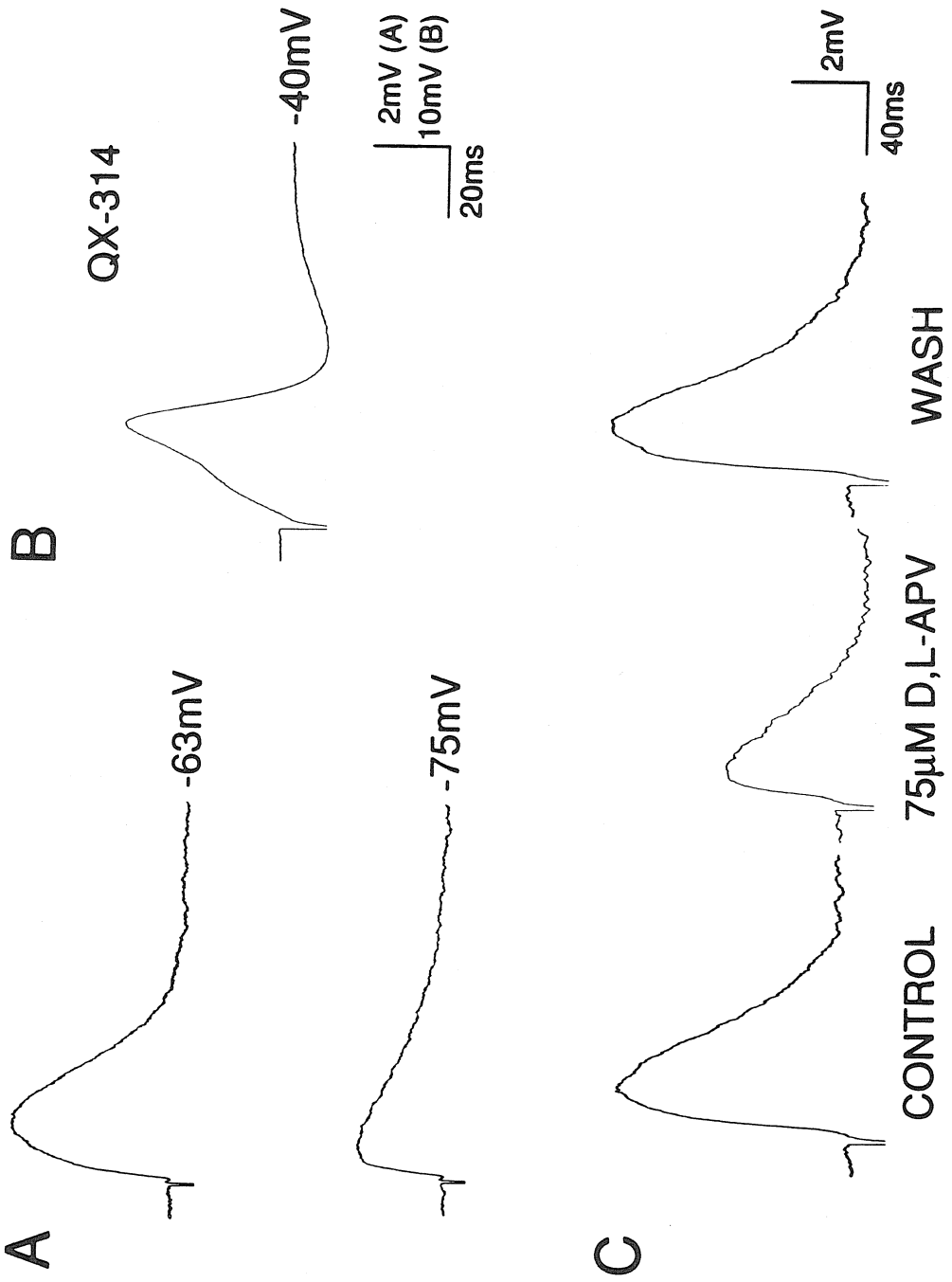
A
-63mV
-75mV
B
QX-314
-40mV
2mV (A)
10mV (B)
20ms
C
CONTROL
75µM D,L-APV
WASH
2mV
40ms

Figure 20. The postsynaptic membrane potential affected the amplitude and the time course of the MAN EPSP.

a) The normalized EPSP amplitude plotted as a function of the membrane potential for twelve different RA neurons in slices prepared before day 25. Each EPSP was measured close to the resting potential, then again at more negative "holding" potentials, which were obtained by passing tonic, hyperpolarizing currents through the recording electrode. EPSP amplitude was then normalized to the maximum observed value (which was always observed at the most positive membrane potential, in these cases).

b) The time between the onset and the peak amplitude of the EPSP is plotted as a function of the postsynaptic membrane potential. Normalization was to the value obtained at the most positive membrane potential. Ten of the twelve EPSPs exhibited a decrease in the time to reach peak amplitude as the postynaptic membrane was made more negative.

a

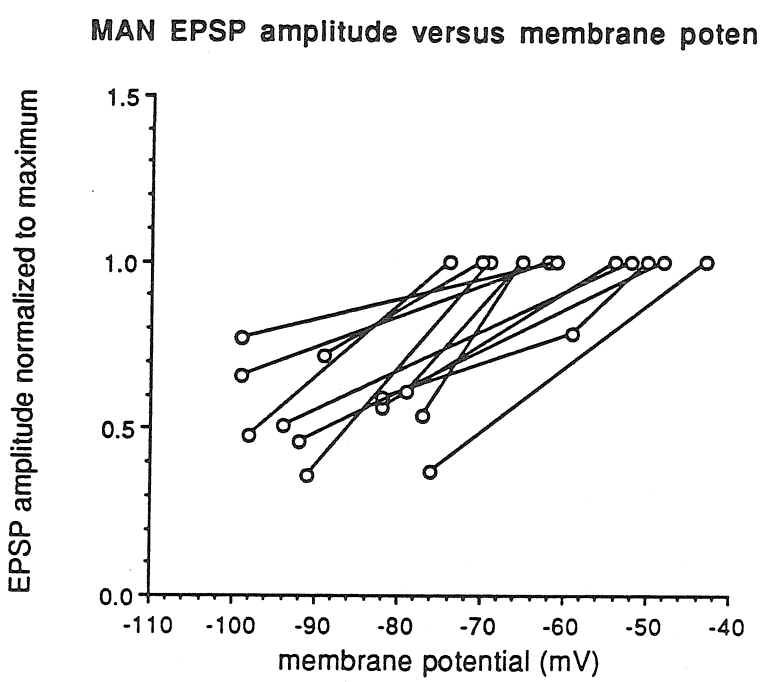
MAN EPSP amplitude versus membrane potential
EPSP amplitude normalized to maximum
1.5
1.0
0.5
0.0
-110
-100
-90
-80
-70
-60
-50
-40
membrane potential (mV)

b

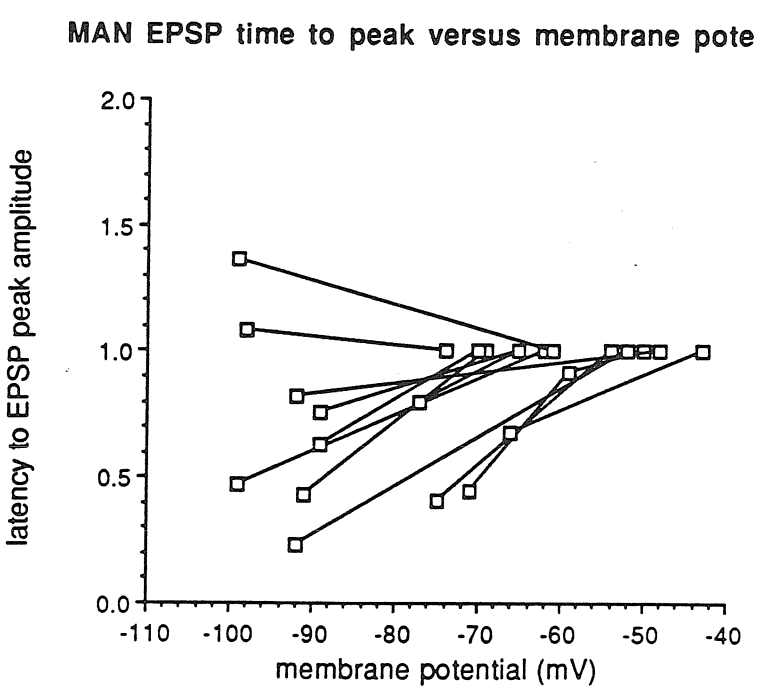
MAN EPSP time to peak versus membrane potential
latency to EPSP peak amplitude
2.0
1.5
1.0
0.5
0.0
-110
-100
-90
-80
-70
-60
-50
-40
membrane potential (mV)

SYNAPTIC RESPONSES WITHIN RA AFTER DAY 40

MAN versus HVc fiber stimulation after day 40

One hundred and ten RA neurons were examined in brain slices prepared from male finches of 40 to 70 days posthatch age. These RA neurons responded to steady depolarizing current injection by firing repetitive trains of action potentials, as described in the section on intrinsic properties (see Figure 14). Their morphological features included a radially symmetric, spinous dendritic arbor, local axon collaterals, and a main axon that exited the nucleus (see Figure 10b, Chapter 1). In these respects, the RA neurons impaled in brain slices made from older birds resembled those encountered in slices from birds less than twenty-five days of age.

Unlike their counterparts in younger animals, however, the majority of RA neurons in older animals responded both to MAN and HVc fiber stimulation (72 of 99 cells in 30 experiments). Electrical stimulation in both the MAN and HVc fiber tracts could evoke depolarizing potentials from such "dually innervated" RA neurons (two lower amplitude traces in Figure 21). Of the remaining RA neurons encountered, slightly more than 20% (21 of 99 cells) responded only to HVc fiber tract stimulation, and approximately 6% (6 of 99 cells) responded only to MAN fiber tract stimulation.

Thirty-five RA neurons that had responded to stimulation of either one or both inputs were analyzed in greater detail. Twenty-seven of these cells responded to both MAN and HVc fiber stimulation. Fifteen of these dually innervated cells were treated with D-APV, eight with CNQX, two with kynurenic acid, and two by varying the membrane potential. Of the eight remaining cells, four responded to MAN fiber stimulation only and were tested with D-APV, and

four responded to HVc fiber stimulation only, three of which were tested with D-APV, and one that was tested with kynurenic acid.

Time courses of the MAN and HVc EPSPs

The EPSPs plotted in Figure 21 typify recordings obtained from RA neurons that responded to MAN and HVc fiber stimulation. Since the depolarizing potentials evoked by stimulating either input by itself could exceed spike threshold, they were classified as excitatory (EPSPs). A consistent feature of the MAN and HVc EPSPs was that their time courses differed from each other, as shown in Figure 21. These differences were apparent when the MAN and HVc EPSPs were compared directly to one another in dually innervated RA neurons, or when the comparisons were made between cells responding to only one of the two inputs. The MAN EPSPs displayed a shallow onset slope and took a long time to attain peak amplitude, similar to the MAN EPSPs evoked in slices prepared from birds less than twenty five days old. In contrast, HVc EPSPs exhibited a steeper onset slope and a substantially shorter time to peak. In twenty-nine cells, the MAN EPSP onset slope averaged 1.05±0.12 mV/msec, significantly less than the value of 1.54±0.12 mV/msec obtained for the HVc EPSP ($p<.007$, N=29). In the same RA neurons, the time to peak of the MAN response, at 12.2±0.81 msec, was significantly longer than the value of 7.06±0.68 msec measured for the HVc EPSP ($p<.0001$, N=29).

Summation of the MAN and HVc EPSPs

The interactions between the MAN and HVc EPSPs observed in dually innervated RA neurons were explored by stimulating the two fiber pathways simultaneously. Simultaneous stimulation of the MAN and HVc fiber pathways often drove the cell past spike threshold, even though the EPSPs

evoked by driving either input alone remained subthreshold. In these cases, the individual stimulus intensities were lowered until the simultaneous stimulation of the two inputs produced a subthreshold response. The *linear sum* of the MAN and HVc EPSPs, computed by digitally adding the EPSPs evoked by stimulating either input alone, was compared to the EPSP evoked by stimulating the two inputs simultaneously (the *observed sum*). The results of such a comparison can be seen in Figure 21. In five cases analyzed in this manner, the observed sum closely approximated the linear sum, although in four of these cases, the observed sum actually exceeded the linear sum of the MAN and HVc EPSPs by a slight amount.

Effects of D-APV on the MAN and HVc EPSPs

The pharmacological properties of the MAN and HVc EPSPs were tested by applying the NMDA receptor antagonist, D-APV, to fifteen dually innervated RA neurons. Two of these cells were examined in normal ACSF, twelve in high divalent ACSF (4 mM calcium, 4 mM magnesium), and one in very high divalent ACSF (8 mM calcium, 8 mM magnesium) supplemented with 10 μM bicuculline methiodide. Regardless of the ionic conditions, D-APV significantly reduced the MAN EPSP amplitude, without exerting a significant effect on the HVc EPSP amplitude (see Figure 22). D-APV reduced the MAN EPSP amplitude to 0.43±0.03 of the control value ($p<.0001$ with respect to the control, N=15; EPSP amplitudes in each condition were normalized to the amplitude preceding drug application). In these same RA neurons, the HVc EPSP amplitude measured in D-APV was 0.98±0.06 of the control value ($p<.81$, N=15). In thirteen cells, where a successful washout of the D-APV was obtained, the MAN EPSP amplitude recovered to the control value (1.08±0.08 of the control EPSP amplitude, $p<.322$, N=13). The HVc EPSP sometimes

exhibited an unusual washout effect, occasionally "recovering" to an amplitude greater than either the control or D-APV values (1.31±0.10; $p<0.005$ with respect to the control value, $p<0.01$ with respect to the D-APV value; N=13). Since the same "excess" recovery of the HVc EPSP also occurred in the presence of 10 μM bicuculline methiodide, it is unlikely that this effect can be explained by an D-APV-sensitive, $GABA_a$-mediated inhibitory pathway.

In several cases, negative current injection was used to prevent the cell from firing spontaneously. To control for the possibility that the recordings were obtained at the very negative end of the current-voltage relationship of the NMDA component, the magnitude of the D-APV effect on MAN and HVc EPSP amplitude was plotted against the observed membrane potential. The degree of the D-APV effect on the MAN or HVc EPSP amplitudes was not correlated with the postsynaptic membrane potential (see Figure 23). Therefore, it is less likely that the membrane potential contributed to the differential effects D-APV exerted on these two types of EPSPs.

In those RA neurons that responded to stimulation of only the MAN or HVc fiber tract, D-APV always reduced the amplitude of the MAN, but not HVc, EPSP. D-APV reduced the MAN EPSP amplitude to 0.47±0.05 of the control value in four RA neurons that had responded only to stimulation of the MAN fiber pathway. In contrast, in three RA neurons that responded only to stimulation of the HVc fiber pathway, the HVc EPSP amplitude in D-APV was 0.98±0.02 of the control value. When grouped with the values obtained for dually innervated cells, D-APV reduced the MAN EPSP amplitude to 0.44±0.03 of the control ($p<.0001$, N=19), without significantly affecting the HVc EPSP amplitude (0.98±0.05, $p<.75$, N=18).

Besides depressing the MAN EPSP amplitude, D-APV consistently reduced the actual onset slope and the time to peak of the MAN

EPSP. In D-APV, the onset slope of the MAN EPSP decreased from the control value of 1.05±0.12 mV/msec (N=28), to 0.67±0.11 mV/msec (N=19) ($p<.03$). The time to peak of the MAN EPSP also decreased from 12.2±0.81 msec (N=29), to 6.58±0.7 msec, in the presence of D-APV ($p<.0001$). D-APV did not significantly reduce either of these parameters of the HVc EPSP. Note that the time to peak of the MAN EPSP measured in the presence of D-APV approximated the control values obtained for the HVc EPSP. Blocking NMDA receptor-mediated components of the MAN EPSP unmasked a faster component with a time course similar to the D-APV-resistant HVc EPSP.

Figure 21. Electrical stimulation of both the MAN and HVc fiber tracts evoked EPSPs from the majority of RA neurons when slices were prepared from 40 day and older male finches. The EPSPs shown here, recorded from a typical "dually innervated" RA neuron *in vitro*, were obtained in a brain slice made from a fifty day old finch. The MAN EPSP (*heavier solid trace*) exhibited a shallower onset slope and longer time to peak than did the HVc EPSP (*lighter solid trace*). The MAN and HVc EPSPs summed in a nearly linear fashion when the two fiber tracts were stimulated simultaneously. The actual EPSP observed when driving the two inputs together (*dotted trace*) slightly exceeded the linear sum (*open circles*) of the two EPSPs obtained when driving each input separately. Cell shown at actual resting potential; recorded in high divalent ACSF (4 mM calcium, 4 mM magnesium). In all cases, electrical stimuli were applied at t=10 milliseconds.

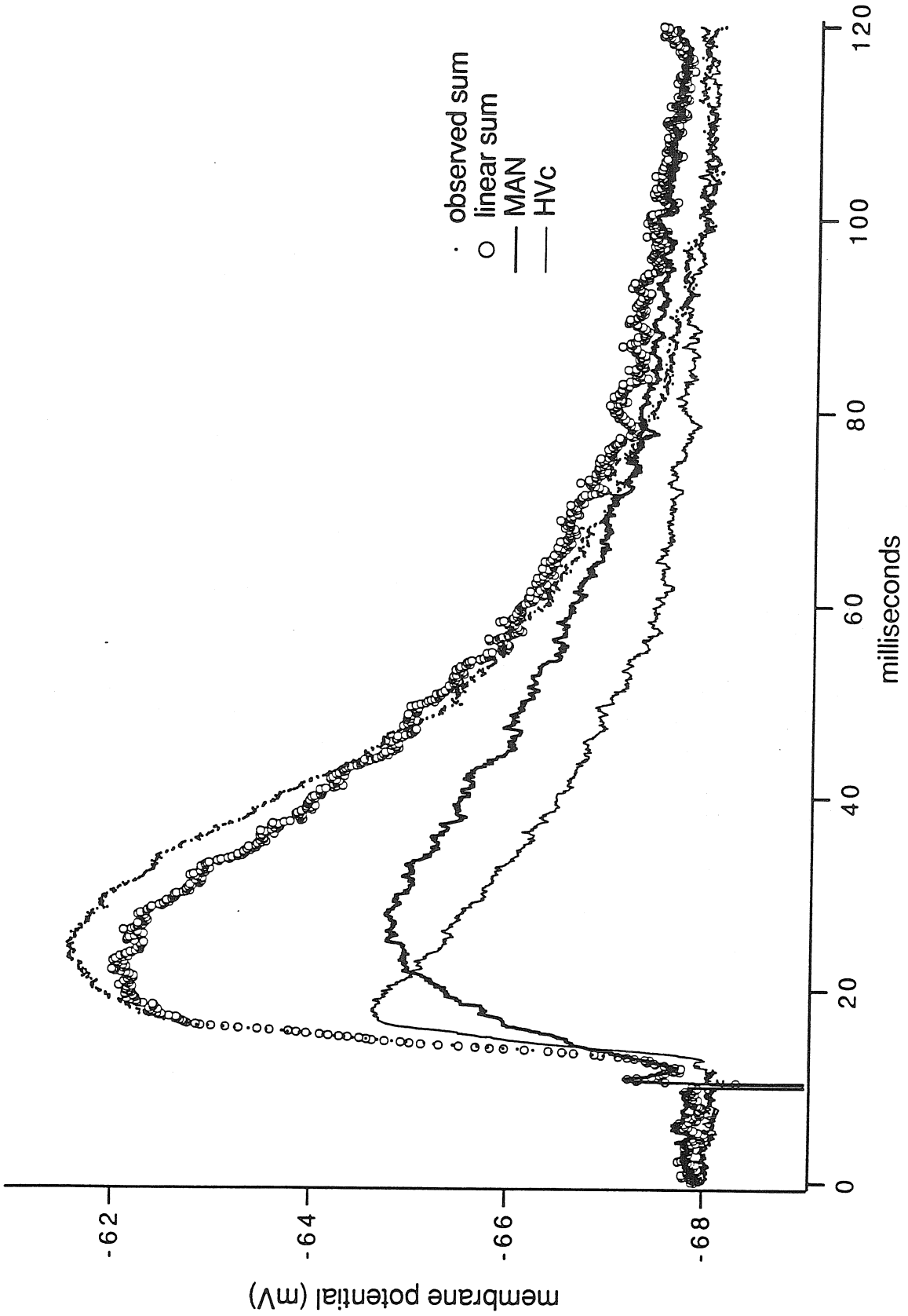
membrane potential (mV)
-62
-64
-66
-68
0
20
40
60
80
100
120
milliseconds
observed sum
linear sum
MAN
HVc

Figure 22. D-APV lowered the MAN EPSP amplitude, without depressing the amplitude of the HVc EPSP. These EPSPs were recorded from an RA neuron that responded to electrical stimulation of both the MAN and HVc fiber tracts. After obtaining baseline averages (*control*), 100 μM D-APV was applied near the recording site with a puffer pipette (see Methods), and the EPSPs were again evoked by stimulating the MAN and HVc fiber tracts (*APV*). Fifteen minutes after drug application was discontinued, recovery was complete (*washout*). Recordings were made in high divalent ACSF (4 mM calcium, 4 mM magnesium). Slice prepared from a 40 day old male finch.

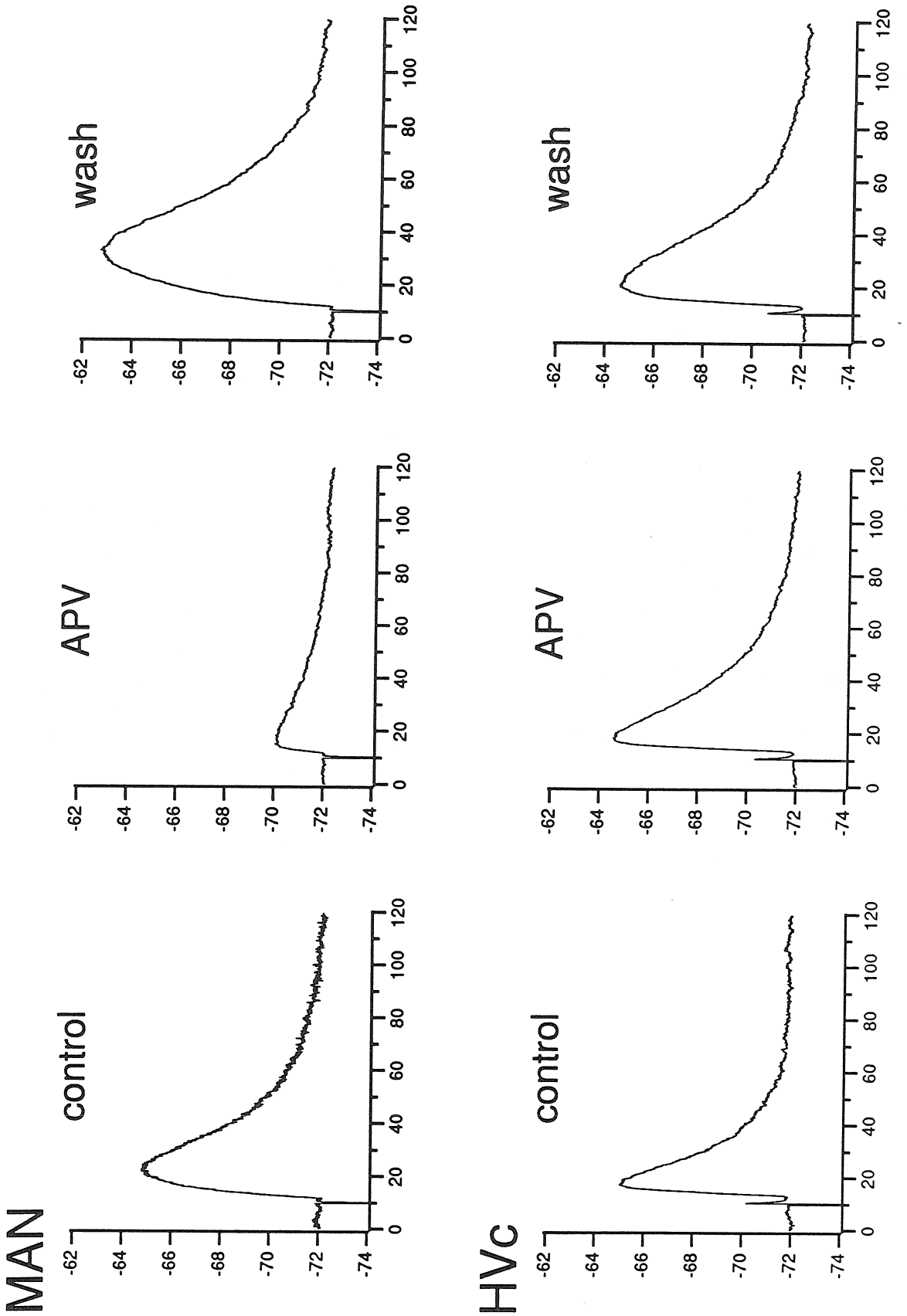
MAN
control
APV
wash
HVc
control
APV
wash
-62
-64
-66
-68
-70
-72
-74
0
20
40
60
80
100
120

Figure 23. No correlation was observed between the postsynaptic membrane potential of an RA neuron, and the degree to which D-APV altered the amplitude of either the MAN (*circles*) or the HVc (*crosses*) EPSPs.

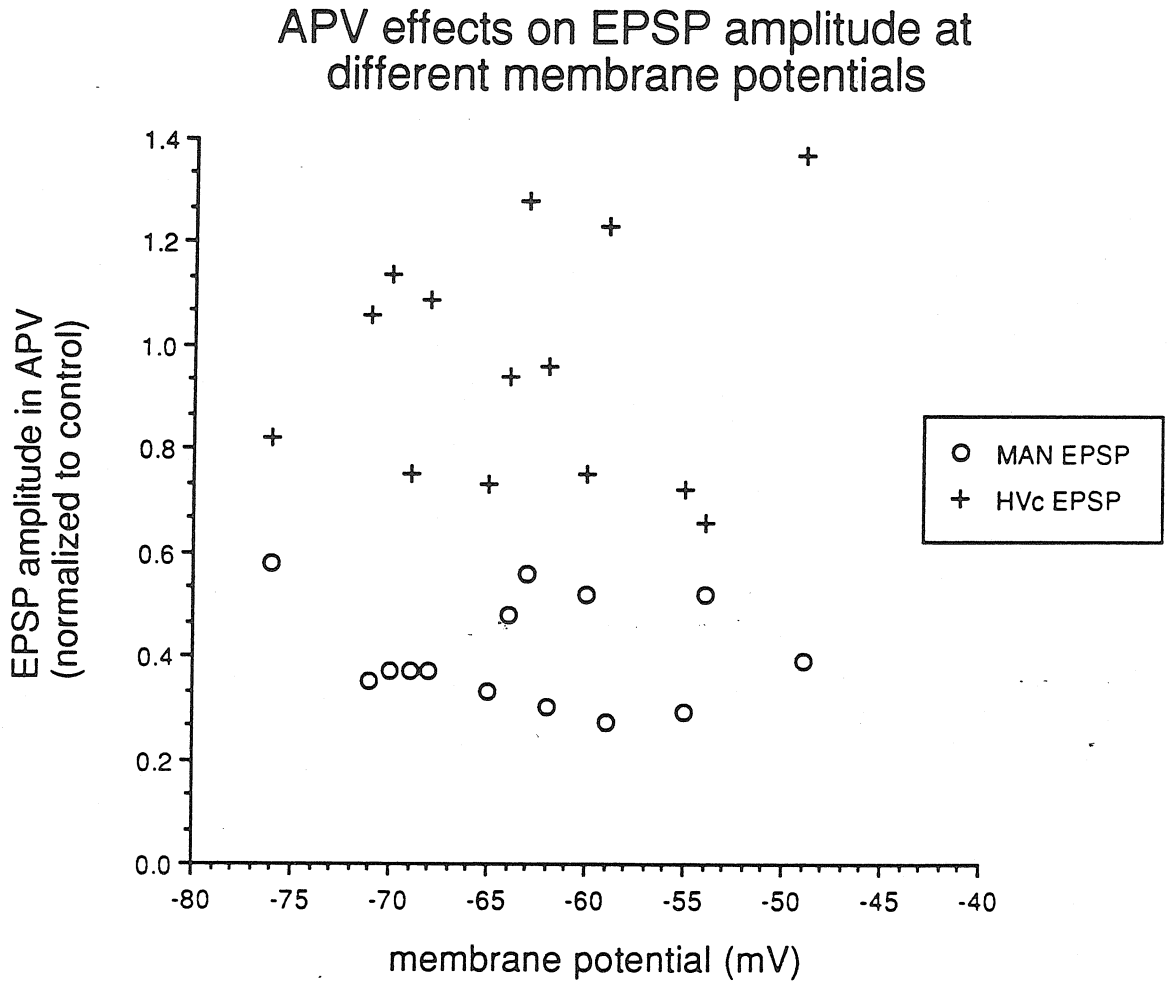
APV effects on EPSP amplitude at different membrane potentials
EPSP amplitude in APV (normalized to control)
1.4
1.2
1.0
0.8
0.6
0.4
0.2
0.0
-80
-75
-70
-65
-60
-55
-50
-45
-40
membrane potential (mV)
MAN EPSP
HVc EPSP

CNQX application

Although the HVc EPSP was insensitive to the effects of D-APV, it was strongly blocked by the non-NMDA glutamate receptor antagonist, 6-Cyano-7-nitroquinoxaline-2,3 dione (CNQX) (Honore, Davies et al. 1988). Eight dually innervated RA neurons were treated with CNQX. In all experiments, 10 μM CNQX was applied in the immediate vicinity (< 500μm) of the recording site with a puffer pipette (see Methods). All experiments were performed in conditions designed to suppress polysynaptic transmission. Five cells were tested in high divalent ACSF (4 mM calcium, 4 mM magnesium), two in very high divalent ACSF (8 mM calcium, 8 mM magnesium), and one in very high divalent ACSF with 10 μM bicuculline methiodide. Regardless of the ionic conditions, CNQX always exerted a strong blocking effect on the HVc EPSP, while reducing the MAN EPSP only slightly or not at all (see Figure 24). In these eight neurons, CNQX treatment reduced the HVc EPSP amplitude to 0.27±0.03 of the control value ($p<.0001$, N=8; normalized as above). For the same RA neurons, the MAN EPSP amplitude measured in the presence of CNQX was 0.93±0.11 of the control value ($p<.55$, N=8). A partial or complete washout was accomplished in six of the eight cells treated with CNQX. The HVc EPSP amplitude recovered, on average, to a level 0.72±0.09 of the control value. The washout amplitude was significantly greater than the amplitude in CNQX ($p<.0002$, N=6), but was still lower than the control value ($p<.003$, N=6). Upon washout, the average MAN EPSP amplitude was slightly larger (1.34±0.20) than the control value, but the two populations were not different ($p=.25$, Mann-Whitney U test, N=6).

The onset slope of the HVc EPSP was also significantly reduced by CNQX treatment. The slope decreased from the control rate of 1.54±0.12 mV/msec (N=29) to 0.44±0.04 mV/msec (N=8) in the presence of CNQX

($p<.0001$). The time to reach peak amplitude increased slightly, from 7.06 msec to 8.77 msec, but this difference was not significant. The MAN EPSP onset slope and time to peak did not change in a significant fashion when treated with CNQX.

CNQX and APV application

One dually innervated RA neuron was treated in rapid succession with 10 μM CNQX, followed by 100 μM D-APV, both applied from a puffer pipette (see Figure 24b). The onset slope, but not the peak amplitude, of the MAN EPSP was depressed following CNQX application. The subsequent application of D-APV almost completely abolished the response, reducing the peak EPSP amplitude from 4.96 mV to 0.82 mV, or 0.16 of the control value. These results suggest that CNQX- and D-APV-sensitive components may account for virtually all of the MAN EPSP. The HVc EPSP amplitude recorded from the same cell decreased from 3.12 mV to 0.74 mV, or 0.24 of the control, following CNQX application. However, the subsequent application of D-APV was not accompanied by any further reduction in the HVc EPSP amplitude (data not shown).

Figure 24. CNQX exerted a strong blocking effect on the HVc EPSP, without significantly affecting the MAN EPSP.

a) In an RA neuron responding to stimulation of both the MAN and HVc fiber pathways, application of 10 μM CNQX through a puffer pipette almost completely blocked the HVc EPSP, while exerting a negligible effect on the MAN EPSP. Holding potential was -65 mV. Scale bars equal 4 mV (horizontal), and 20 milliseconds (vertical).

b) Rapid, sequential application of 10 μM CNQX and 100 μM D-APV (through a puffer pipette), almost completely blocked the MAN EPSP in a dually innervated RA neuron. The HVc EPSP, which was almost completely abolished by CNQX, was not further reduced by D-APV (not shown). Scale bars in a) equal 2 mV and 20 milliseconds, respectively, in b).

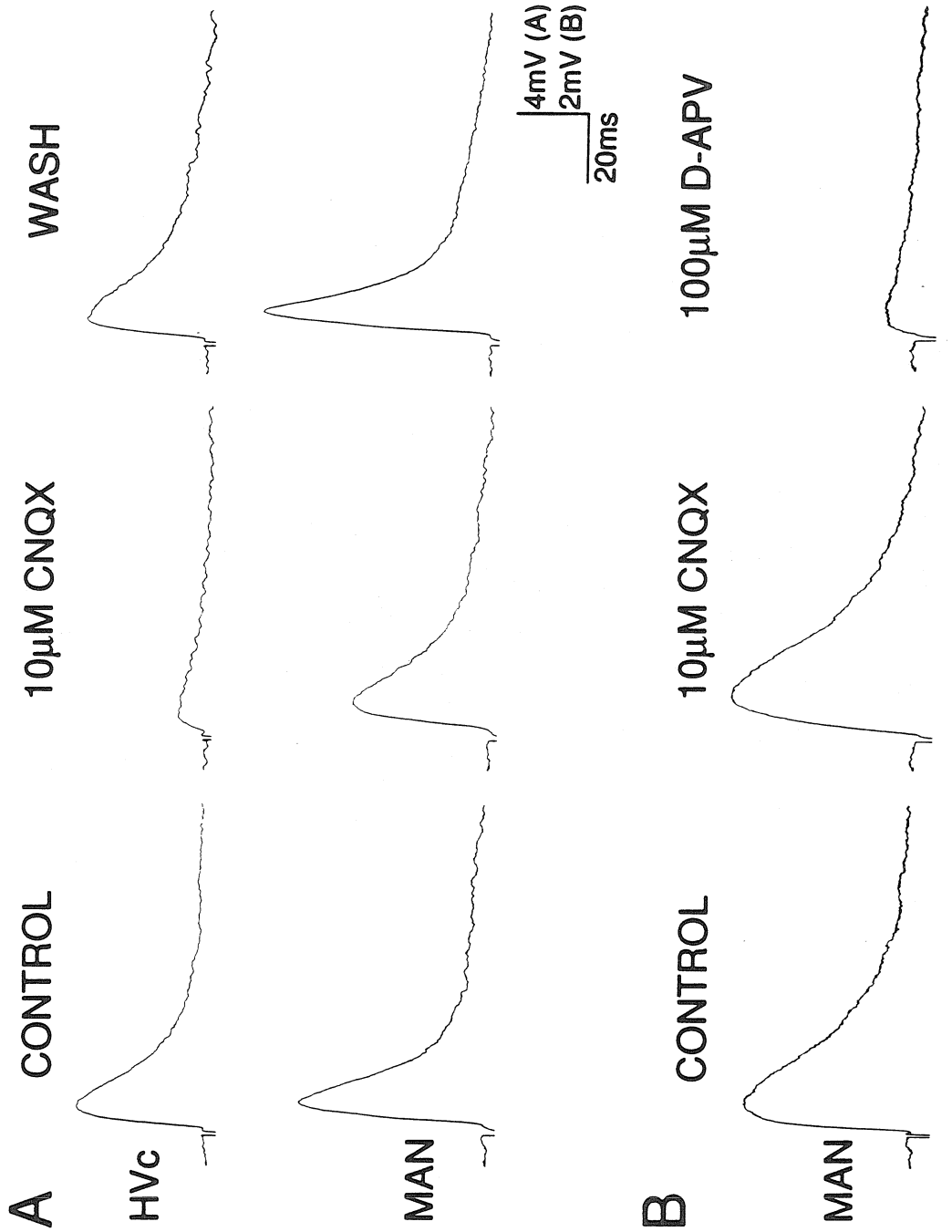
A
CONTROL
10μM CNQX
WASH
HVc
MAN
4mV (A)
2mV (B)
20ms
B
CONTROL
10μM CNQX
100μM D-APV
MAN

Subtracted waveforms

A feature detected in four of the eight dually innervated RA neurons treated with CNQX was that the MAN EPSP amplitude actually increased slightly upon drug application (1.19±0.07 of the control value). In the remaining four cases, CNQX treatment caused a slight decrease in the MAN EPSP amplitude (0.68±0.06 of the control level). In order to examine more clearly the component(s) blocked by CNQX treatment in each case, the EPSP recorded in the presence of CNQX was digitally subtracted from the control EPSP. In those cases where the CNQX treatment had reduced the MAN EPSP, the difference waveform was fast-rising and positive-going, with a simple monotonic decay (see Figure 25a). This would be the predicted difference if CNQX had blocked a fast, non-NMDA component of the EPSP. In contrast, in those cases where CNQX treatment slightly increased the MAN EPSP, the difference waveform was more complex, and was composed of two different elements: an initial one that was brief and positive-going, followed by a slower one that was negative-going (see Figure 25b). These difference waveforms were quite similar to a superimposed EPSP and IPSP actually observed in other RA neurons (see below). Although not directly conclusive, this similarity suggests that the four MAN EPSPs augmented by CNQX treatment may have been partially shunted by IPSPs in the control conditions. Two further observations were consistent with this interpretation. First, in one RA neuron that was studied in the presence of 10 μM bicuculline, CNQX actually reduced the MAN EPSP amplitude to 0.52 of the control. Second, the IPSPs observed within RA were blocked not only by bicuculline, but also by CNQX (see below). Therefore, CNQX treatment could block fast components of the monosynaptic EPSP, and in certain cases, could eliminate shunting polysynaptic IPSPs, as well.

Figure 25. Subtraction of the MAN EPSP recorded in the presence of CNQX (*heavier solid trace*) from the control EPSP (*lighter solid trace*) produced two types of difference waveforms (*open circles*).

a) For an MAN EPSP moderately reduced by CNQX (10 μM applied through a puffer pipette), the difference waveform was fast-rising, then underwent essentially monotonic decay.

b) For an MAN EPSP that increased slightly in amplitude in the presence of CNQX (10 μM applied through a puffer pipette), the difference waveform was more complex, and bore some resemblance to a fast EPSP superimposed on an IPSP (see Results Section addressing polysynaptic inhibition).

Both MAN EPSPs were recorded from dually innervated RA neurons in which the HVc EPSP was almost completely blocked by CNQX. Slice was prepared from a forty-five day old male finch. In both cases, the holding potential was -70 mV; slices were bathed in high divalent ACSF.

a

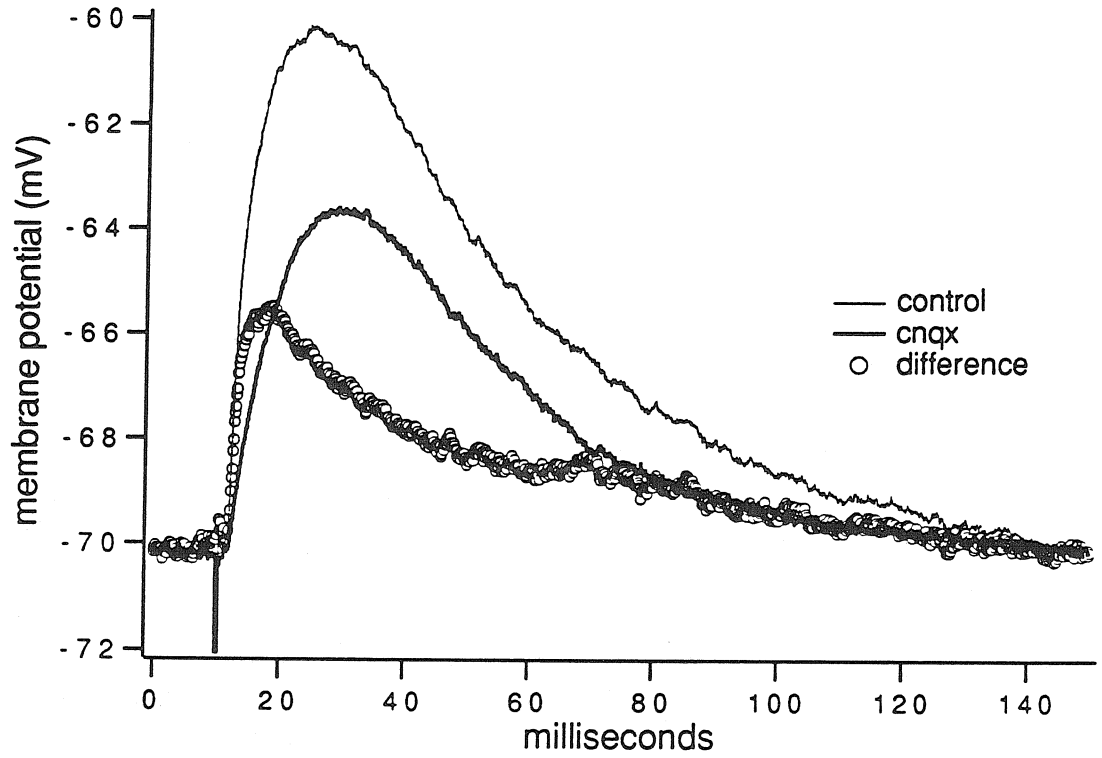
-60
-62
-64
-66
-68
-70
-72
membrane potential (mV)
0
20
40
60
80
100
120
140
milliseconds
control
cnqx
difference

b

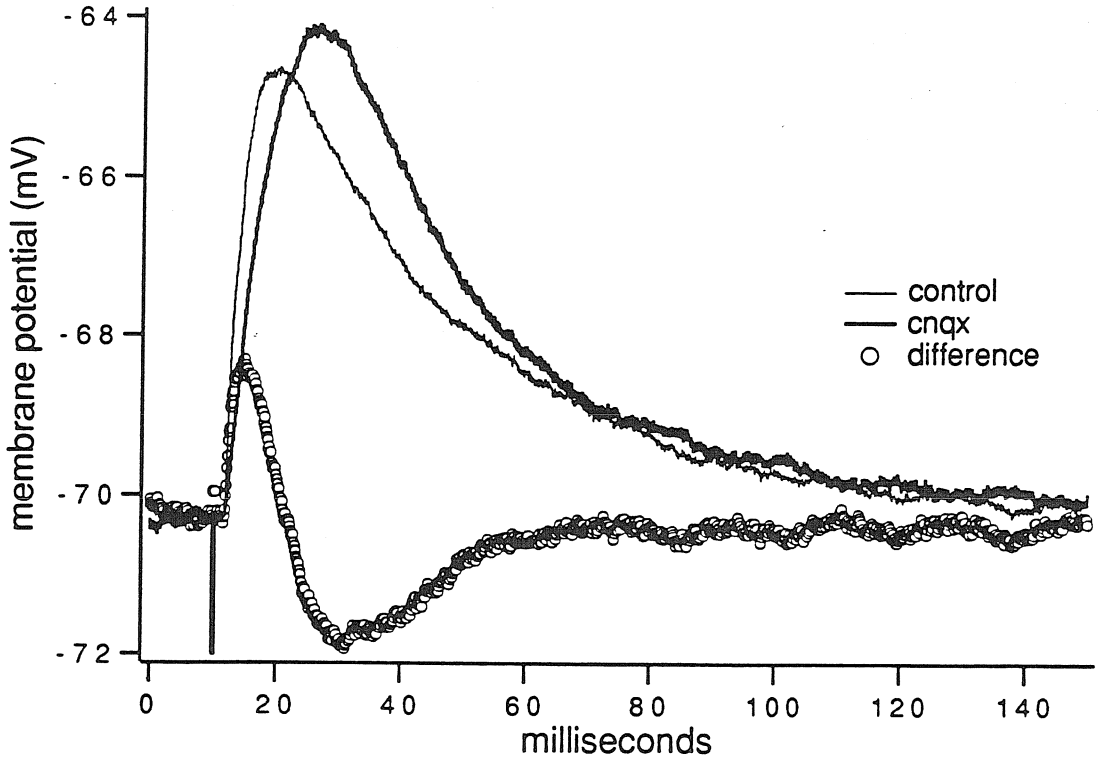
-64
-66
-68
-70
-72
membrane potential (mV)
0
20
40
60
80
100
120
140
milliseconds
control
cnqx
difference

Kynurenic acid application

Despite the selective effects of D-APV and CNQX on the MAN and HVc EPSPs, kynurenic acid strongly blocked both types of input. Two dually innervated RA neurons, as well as a single RA neuron that responded only to HVc fiber stimulation, were treated with kynurenic acid (1 mM, bath application or puffer pipette). In these two dually innervated cells, application of kynurenic acid was accompanied by a pronounced decrease in both the MAN and HVc EPSP amplitudes (data not shown). In the presence of kynurenic acid, the MAN EPSP amplitude measured 0.30±0.06, and the HVc EPSP amplitude measured 0.28±0.06, normalized to the EPSP amplitude preceding treatment. Washout of the drug was accompanied by recovery of the HVc EPSP amplitude to 0.98±0.22 of the control value, and of the MAN EPSP amplitude to 1.26±0.02 of the control value. In the case of the single cell that had responded only to the HVc input, kynurenic acid reduced the HVc EPSP amplitude to 0.25 of the control level. These results suggest that MAN and HVc axons provide glutamatergic input onto the same RA neurons, but activate different subtypes of postsynaptic glutamate receptors.

Voltage dependence of the MAN and HVc EPSPs

Besides their different pharmacological sensitivities to D-APV and CNQX, NMDA and non-NMDA receptor mediated EPSPs can be affected in opposite ways by changes in the postsynaptic membrane potential. NMDA receptor-mediated EPSPs diminish with increasing postsynaptic hyperpolarization, since the cation-selective channel opened by the NMDA receptor is blocked in a voltage-dependent fashion by extracellular magnesium ions (Ascher and Nowak 1988). In contrast, non-NMDA glutamate receptors gate cation-selective ion channels that do not exhibit a voltage-dependent

magnesium blockade, and therefore the EPSPs that they mediate are actually augmented by hyperpolarization of the postsynaptic membrane (Hestrin, Nicoll et al. 1990). These contrasting responses to postsynaptic membrane potential afforded another means, independent of drug application, by which the NMDA and non-NMDA components of the MAN and HVc EPSPs could be dissected. Therefore, MAN and HVc EPSPs were examined at or near the actual resting membrane potential, as well as at more hyperpolarized potentials, which were attained by injection of steady hyperpolarizing current into the postsynaptic cell. In two dually innervated RA neurons tested in this manner, hyperpolarization of the postsynaptic cell diminished the MAN EPSP, but augmented the HVc EPSP.

One cell was impaled with a pipette containing QX-314 to block sodium spikes, permitting the cell to be depolarized extensively as well. As the membrane potential was manipulated from -40 to -95 mV, the MAN EPSP decreased in amplitude, while the HVc EPSP amplitude simultaneously increased (see Figure 26). Similar results were obtained in very high divalent ACSF (8 mM calcium, 8 mM magnesium) with 10 μM bicuculline methiodide, suggesting that the voltage dependence of the HVc EPSP did not reflect contamination by reversed GABAergic IPSPs. However, it should be added that in certain cases, the HVc EPSP could be mildly attenuated by membrane hyperpolarization (data not shown). Therefore, NMDA receptors might mediate a small portion of the HVc EPSP, at least in certain individual cells, or if postsynaptic depolarization was more extensive than in the present experiments.

Figure 26. The membrane potential of the postsynaptic RA neuron could exert contrasting effects on the MAN and HVc EPSPs.

$a_{1\text{-}2}$) An MAN EPSP recorded from a dually innervated RA neuron was strongly attenuated as the membrane potential was hyperpolarized from -41 to -97 mV.

$b_{1\text{-}2}$) The HVc EPSP recorded from the same cell increased substantially as the membrane potential was hyperpolarized from -46 to -95 mV. Note that the MAN and HVc EPSPs are plotted with different vertical scaling.

Neuron was impaled with a QX-314-loaded pipette, and the slice was bathed in high divalent ACSF. Slice prepared from a 35 day old male finch.

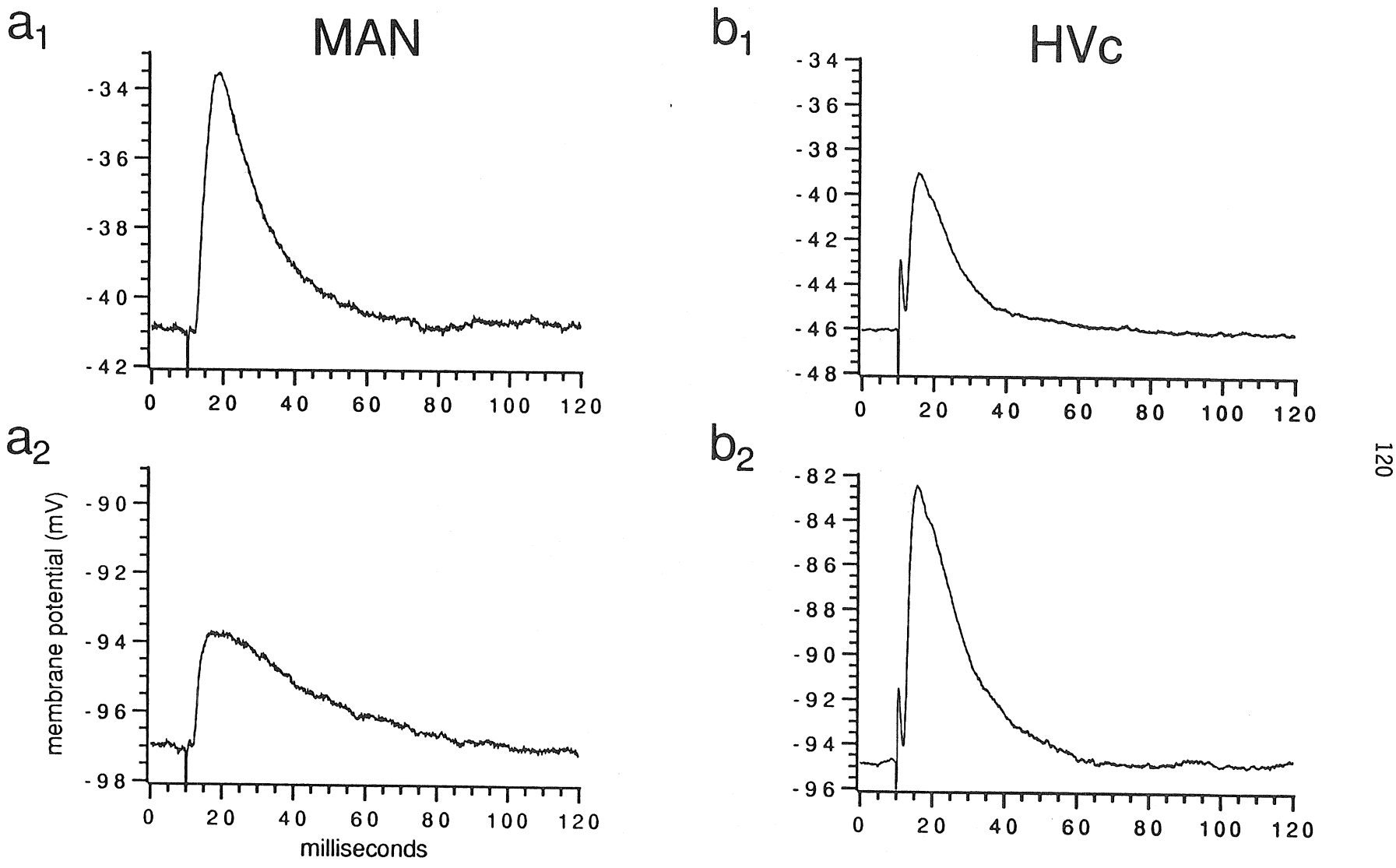
a1
MAN
-34
-36
-38
-40
-42
0
20
40
60
80
100
120
b1
HVc
-34
-36
-38
-40
-42
-44
-46
-48
0
20
40
60
80
100
120
a2
membrane potential (mV)
-90
-92
-94
-96
-98
0
20
40
60
80
100
120
milliseconds
b2
-82
-84
-86
-88
-90
-92
-94
-96
0
20
40
60
80
100
120

Synaptic inhibition within nucleus RA

High-intensity MAN fiber stimulation could also evoke more complex synaptic potentials from RA neurons at all ages studied. When the cell's resting potential was more positive than -60 mV, these complex potentials were characterized by a brief, short-latency, depolarizing potential that was immediately followed by a hyperpolarizing component (see Figure $27a_1$). The negative-going component reversed and became positive-going as the postsynaptic membrane was hyperpolarized to potentials more negative than -60 mV (see Figure $27a_2$).

Higher-intensity stimulation of the HVc fiber tract could also evoke similar complex potentials in brain slices prepared from male birds older than 40 days. At resting potentials more positive than -60 mV, high-intensity HVc fiber stimulation often generated a brief, depolarizing potential followed by a slower, hyperpolarizing potential. The negative-going portion reversed between -60 and -70 mV (see Figure $27b_{1-2}$).

Bicuculline methiodide (10 μM in a puffer pipette) was applied to slices in order to characterize the complex synaptic potentials. In three RA neurons tested, bicuculline blocked the hyperpolarizing component in a reversible fashion (see Figure 28a). In the presence of bicuculline, the initial depolarizing potential was augmented, and unless the stimulus intensity was reduced, usually exceeded spike threshold. The IPSP was also abolished by treatment with either kynurenic acid, or in the case of the HVc fiber response, CNQX. Unlike bicuculline, however, treatment with CNQX blocked the early, depolarizing component as well (see Figure 28b).

Afferent fiber stimulation in the presence of bicuculline or picrotoxin produced short-latency EPSPs as before, as well as longer-latency, very large amplitude EPSPs (data not shown). Typically, the latency to onset of

these "polysynaptic" EPSPs declined with increasing stimulus intensity. A very long-lasting afterhyperpolarization, several hundred milliseconds in duration, always followed these massive EPSPs. Spontaneous synaptic activity also increased in the presence of $GABA_a$ blockers. In either bicuculline (10 μM) or picrotoxin (1-5 μM), RA neurons displayed episodes of spontaneous, high-frequency action potential discharge, often followed by prolonged periods of sustained depolarization. In general, GABA receptor antagonists greatly increased the excitability of RA neurons *in vitro*.

Figure 27. High-intensity electrical stimulation of the MAN and HVc fiber pathways could evoke polysynaptic IPSPs within RA.

a_1) Low-intensity stimulation of the MAN fiber pathway evoked an EPSP from an RA neuron (*lighter trace*). This response typified EPSPs evoked by MAN fiber stimulation, as it was attenuated by postsynaptic hyperpolarization (not shown). As the intensity of the stimulus to the MAN fiber pathway was increased, a complex potential was evoked from the same cell (*heavier trace*).

a_2) Hyperpolarizing the membrane potential of the impaled RA neuron reversed the negative-going component of the complex potential. The negative-going component inverted and became positive-going near -60 mV. Note that after reversal, the complex potential actually increased in amplitude as the membrane potential was made increasingly negative, unlike the MAN EPSP elicited at low intensity.

b_1) A similar complex potential could also be evoked by high-intensity stimulation of the HVc fiber pathway (*heavier trace*). Low-intensity stimulation in the same cell evoked an EPSP (*lighter trace*).

b_2) Hyperpolarization of the postsynaptic membrane reversed the negative-going component of the complex potential near -65 mV. After reversal, the PSP was augmented with increasing postsynaptic hyperpolarization.

All stimuli applied at t=10 milliseconds.

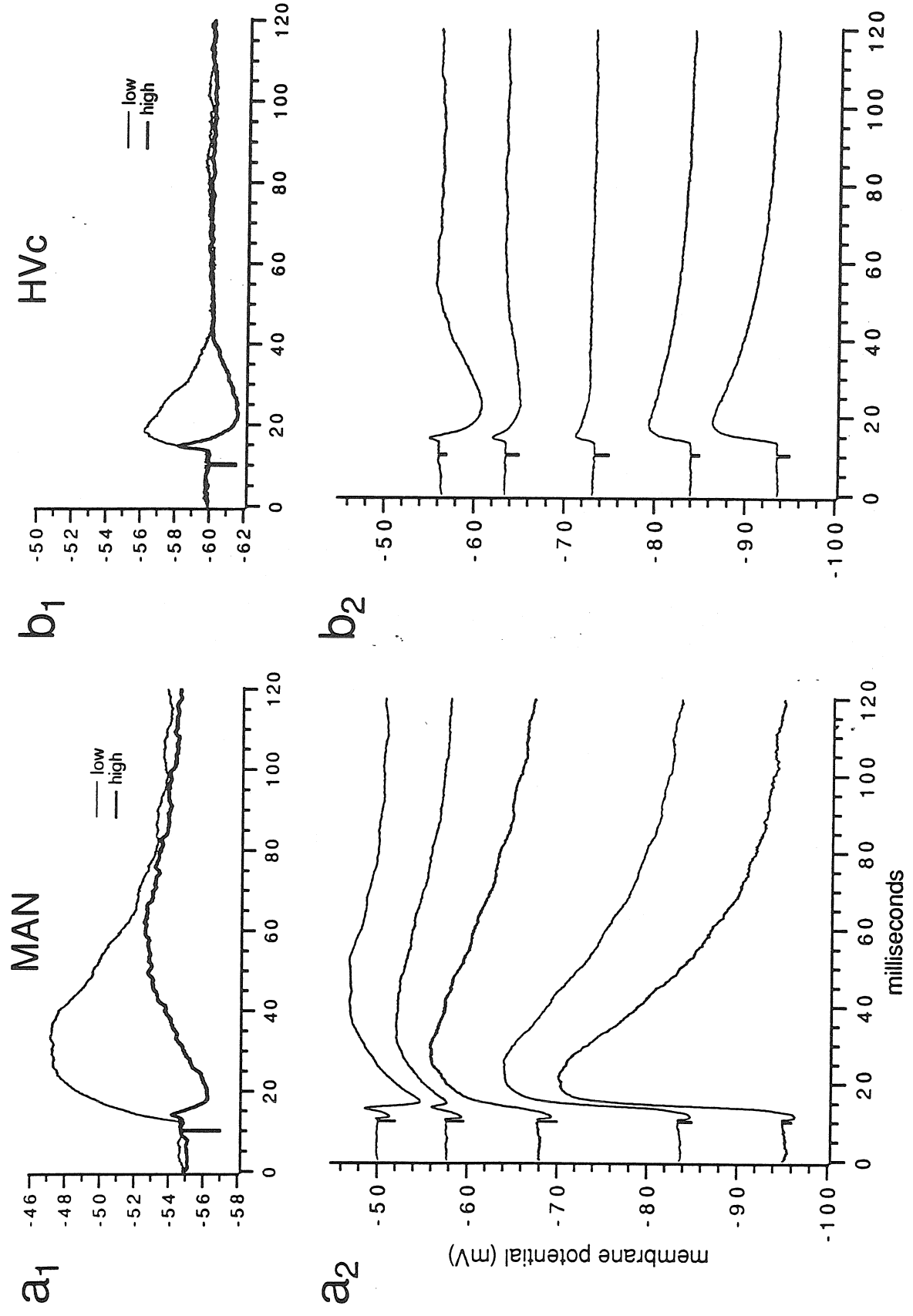
a1
MAN
low
high
b1
HVc
low
high
a2
b2
membrane potential (mV)
milliseconds

Figure 28. Pharmacology of the complex potential was consistent with a polysynaptic, $GABA_a$-mediated IPSP.

a) The negative-going component of a complex potential evoked by HVc fiber stimulation (*control trace*) was almost completely blocked when 10 μM bicuculline methiodide was applied through a puffer pipette close to the recording electrode (*bicuculline trace*). Note that the positive-going component remained, however. A ten-minute washout with very high divalent ACSF (8 mM calcium, 8 mM magnesium), restored the complex potential to its control state.

b) In a different cell, CNQX application (10 μM applied through a puffer pipette) blocked both parts of a complex potential.

Both cells were recorded from RA neurons in a slice prepared from a forty-five day old male finch. Cells shown at actual resting potentials. Electrical stimulation at t=10 milliseconds in all cases.

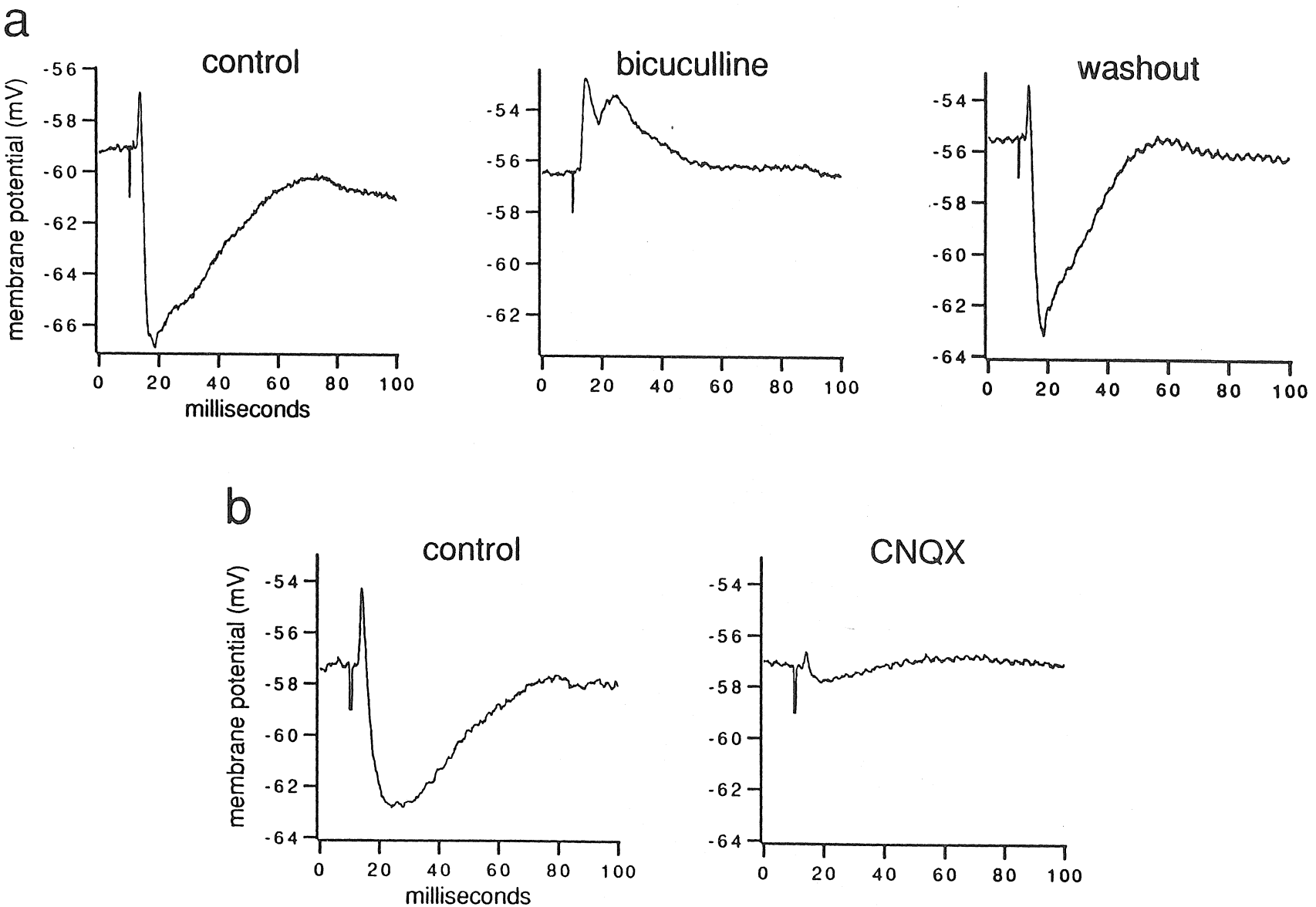
a
control
bicuculline
washout
membrane potential (mV)
-56
-58
-60
-62
-64
-66
-54
0
20
40
60
80
100
milliseconds
b
control
CNQX

DISCUSSION

In this study, an intracellular analysis of RA neurons yielded information about their intrinsic membrane properties, and supplied the first detailed picture of synaptic transmission within a song control nucleus. The anatomically discrete nature of the various song control nuclei makes them especially tractable to *in vitro* brain slice techniques. Ultimately, as this approach is applied to other song nuclei, a more detailed understanding will emerge of how cellular properties contribute to vocal plasticity and song production.

Nearly 90% of the RA neurons in slices prepared from fifteen to twenty-five day old birds responded only to stimulation of the MAN fiber tract. The EPSPs produced by MAN fiber stimulation were blocked by kynurenic acid, D-APV, and hyperpolarization of the postsynaptic membrane. At this age , HVc fiber stimulation elicited a response in only about ten percent of the cells I examined. In slices prepared from birds forty to seventy days of age, however, over seventy percent of the RA neurons recorded from responded to both MAN and HVc fiber stimulation. Although the EPSPs generated by MAN fiber stimulation resembled those observed before day 25, the EPSPs evoked by HVc fiber stimulation were not affected significantly by D-APV, but were blocked by the non-NMDA receptor antagonist, CNQX. Although MAN and HVc ultimately innervate many of the same neurons within RA, their synapses are detectable at different stages of development, and exhibit pharmacologically distinct properties.

RA neuronal types: intrinsic physiology

In vitro, RA neurons behaved as a single homogeneous class on the basis of their intrinsic electrophysiological properties. Intracellular staining

of these RA neurons always revealed one morphological class of neuron, with radially symmetric, spinous dendrites, a main projection axon exiting the nucleus, and a local network of axon collaterals (see Chapter 2). The homogeneity encountered *in vitro* contrasts with Golgi-impregnation studies that have identified two distinct RA neuron types in the zebra finch (Gurney 1981), and perhaps four types in the canary (DeVoogd and Nottebohm 1981). RA neurons I dye-filled *in vitro* were most reminiscent of Gurney's spinous RA neuron of the zebra finch, and DeVoogd's type IV RA neuron in the canary. In the zebra finch, Golgi staining impregnated another class of RA neuron, with aspinous dendrites, but these were not encountered in the present study. The homogeneity of neurons recorded from *in vitro* may have reflected an inherent bias in intracellular techniques, as aspinous RA neurons have smaller soma diameters than spinous ones (Gurney 1981).

RA neurons exhibited a repetitive, and highly regular, firing pattern when injected with suprathreshold, depolarizing currents, regardless of the age of the animal from which the slices were prepared. These trains of action potentials exhibited little or no frequency adaptation over the duration of the injected current pulse, and displayed a nearly linear increment in firing rate as the depolarizing currents were increased.

The repetitive spiking behavior displayed *in vitro* appeared to be the product of the intrinsic membrane properties of RA neurons, and not of a local synaptic circuit. Repetitive spiking persisted in the presence of both glutamate and GABA receptor antagonists, as well as in the absence of external calcium, suggesting that it was not dependent on synaptic transmission.

Several ionic conductances contributed to the highly regular spiking patterns of RA neurons. When treated with QX-314, a compound known to block voltage-gated sodium conductances (Strichartz 1973), RA

neurons lost their ability to generate fast action potentials. Depolarization still elicited slower, large-amplitude membrane potential oscillations in RA neurons treated with QX-314, however. These QX-314-insensitive oscillations were abolished by bathing slices in zero-calcium ACSF. The frequency of the calcium-dependent, QX-314-insensitive oscillations increased as a function of the depolarization, suggesting a voltage-dependent mechanism. The external calcium concentration also affected the firing rates of RA neurons that were not treated with QX-314. RA neurons injected with suprathreshold currents fired at a much higher frequency in the absence of external calcium, and their interspike hyperpolarizations were much less pronounced, than when calcium was present. Cochlear hair cells in reptiles can generate oscillatory membrane potentials that superficially resemble the QX-314-insensitive oscillations of RA neurons (Crawford and Fettiplace 1981). The electrical resonance displayed by reptilian and amphibian hair cells stems from alternating depolarizing and hyperpolarizing currents produced by voltage-dependent calcium channels, and calcium-dependent potassium channels (Hudspeth and Lewis 1988). In RA, similar conductances might moderate the firing frequency of repetitive-spiking RA neurons by increasing the interspike hyperpolarization, and thus decreasing the overall firing rate near threshold.

Subthreshold oscillations were another distinguishing feature of repetitive-spiking RA neurons. These subthreshold oscillations were probably identical to the QX-314-insensitive oscillations discussed previously, as the frequency of the subthreshold oscillations increased with depolarization, and they were not observed in the absence of external calcium. The subthreshold oscillations appeared to dampen the cell's excitability, and depolarizing currents might have to saturate the oscillator before action potential threshold can be surpassed.

A comparison to other vertebrate CNS neurons

The repetitive firing of RA neurons was reminiscent of several other neuronal types that have been analyzed intracellularly. In the sense that RA neurons fired repetitively even over prolonged periods of depolarization, they resembled a wide variety of mammalian CNS neurons, including regular-spiking neocortical neurons (McCormick et al., 1985), layer V neocortical neurons (Stafstrom et al., 1984), and spinal motoneurons (Jodkowski et al., 1988). The slope of the firing frequency versus injected current (f-I) relationship for RA neurons fell within a range described by neocortical neurons firing in steady state (Mason and Larkman 1990), and was about tenfold higher than the value estimated for some spinal motoneurons (Jodkowski et al., 1988; Kernell 1965). Unlike either of these cell types, however, RA neurons *in vitro* did not exhibit frequency adaptation even when stimuli were several hundred milliseconds in duration.

Layer V pyramidal neurons in some areas of the mammalian neocortex also display subthreshold membrane potential oscillations that resemble those seen within RA (Silva et al., 1991; Stafstrom et al., 1984). Given that previous comparisons between RA and layer V of mammalian motor cortex were made on the basis of their similar descending anatomical projection patterns (Karten 1969; Nottebohm et al., 1976), these electrophysiological similarities may be especially relevant.

The repetitive, clocklike activity of RA neurons has also been recorded intracellularly *in vivo* , suggesting that it was not due to an artefact of the brain slice technique (Larry Katz, personal communication). The high degree of spontaneous activity that characterized extracellular recordings in this nucleus was preserved *in vitro.* Given RA's close proximity to the vocal musculature, one function that such regular, repetitive firing might serve is in the

maintenance and modulation of syringeal muscle tone during vocalization. The steep but linear f-I relationship could make the output of an RA neuron quite sensitive to even a small fraction of its synaptic inputs, which would be desirable in a system where finely graded control of output is essential. The RA neuron's lack of frequency adaptation might then insure constant muscle tension over the duration of the individual vocal elements comprising song syllables.

Synchronization of RA neuronal discharge may also be essential for the fine motor control required during song. Since detailed anatomical studies have shown that the syringeal muscles are topographically mapped within RA, it will be especially useful to determine if coupling occurs within or across these myotopic boundaries (Vicario and Simpson 1988). The network of axon collaterals sustained by spinous RA neurons could provide the means to synchronize the output of functionally related clusters of cells.

Early innervation by MAN activates NMDA receptors

In vitro, MAN axons provided excitatory input to RA as early as fifteen days after hatching. Although stimulating the MAN fiber tract always evoked an EPSP within RA at this age, HVc fiber stimulation rarely evoked EPSPs in RA before day twenty-five. The present physiological investigation indicates that MAN provides the dominant extrinsic input to RA before day 25, and confirms the anatomical observations made in the previous chapter.

EPSPs evoked by MAN fiber stimulation were probably mediated by excitatory amino acid receptors, since the broad-spectrum glutamate receptor antagonist, kynurenic acid, blocked the synaptic response almost completely. Hyperpolarization of the postsynaptic membrane also significantly reduced the EPSP amplitude. EPSPs mediated by the NMDA subtype of

glutamate receptor exhibit similar characteristics (Thomson 1986), apparently because of a voltage-dependent blockade of the receptor-activated channel by extracellular magnesium ions (Ascher and Nowak 1988). The pronounced reduction of the MAN EPSP by postsynaptic hyperpolarization suggests that many of the NMDA receptors mediating the EPSP were located on the impaled RA neuron, not on interneurons of a polysynaptic, excitatory pathway.

NMDA receptor antagonists reduced the MAN EPSP to approximately the same extent as postsynaptic membrane hyperpolarization. D(-)-2-amino-5-phosphonovalerate (D-APV), a selective, competitive antagonist of glutamate at the NMDA receptor (Davies et al., 1981), reversibly blocked the MAN EPSP. The shallow onset slope, and long latency to peak, of the MAN EPSP resembled those of known monosynaptic NMDA receptor-mediated currents (Dale and Roberts 1985; Forsythe and Westbrook 1988; Hestrin et al., 1990). However, the slow kinetics of monosynaptic NMDA receptor-mediated potentials can often make them difficult to distinguish from polysynaptic EPSPs. Therefore, most of the present experiments were conducted in high divalent ACSF designed to suppress polysynaptic transmission. Even in these conditions, D-APV still reduced the MAN EPSP amplitude to less than half of the control value. Therefore, before day twenty-five, MAN terminals mediate glutamatergic excitation within RA, and much of the synaptic current is probably carried by NMDA receptor-activated channels located on spinous RA neurons.

Dual innervation of RA neurons by MAN and HVc terminals

After day forty, electrical stimulation of both the MAN and HVc fiber tracts routinely produced EPSPs within RA. The vast majority of RA neurons responded to both inputs, although some cells responded only to MAN or HVc

fiber stimulation. A simple interpretation is that between days twenty-five and forty, HVc terminals enter RA and synapse on neurons that already are recipients of synaptic input from MAN. This physiological analysis is consistent with anatomical observations of massive HVc axon ingrowth into RA beginning after day 25 (Konishi and Akutagawa 1985). Apparently, spinous RA neurons develop from an early stage in which their sole extrinsic innervation is derived from MAN, to a later stage of dual innervation by axons from MAN and HVc.

In those RA neurons receiving dual innervation, the MAN and HVc EPSPs summated in an approximately linear fashion, as long as the combined response remained below spike threshold. The summation of MAN and HVc EPSPs suggests that the two stimulating electrodes activated different synapses on the same neuron. Assuming a passive dendritic membrane, then the linear summation of these two EPSPs implies that MAN and HVc synapses could be electrically isolated from each other (Rall et al., 1967). In the canary, however, serial EM reconstructions have shown that although both MAN and HVc axons terminate on spinous type IV RA neurons, these two different synaptic populations are randomly intermixed along the dendrite (Canady et al., 1988). If the same is true for the zebra finch, then the linear interaction of the MAN and HVc EPSPs might reflect a more subtle compartmentalization of the dendrite, or of more complex processes that are due to an active dendritic membrane. Non-linear interactions could be expected to occur if HVc EPSPs depolarized the dendrite sufficiently to relieve the voltage-dependent blockade of NMDA receptors, thus bringing the MAN EPSP into its non-linear range.

MAN and HVc provide pharmacologically distinct input

The MAN EPSPs recorded from dually innervated RA neurons after day forty were blocked substantially by both D-APV and postsynaptic

hyperpolarization, and had shallow onset slopes and relatively long rise times. In contrast, HVc EPSPs in the same cells had steeper onset slopes and shorter times to peak, and in some cases were augmented by postsynaptic hyperpolarization. Finally, although both EPSPs were reduced to the same extent by kynurenic acid, they had contrasting sensitivities to NMDA and non-NMDA receptor antagonists. Even after D-APV had curtailed much of the MAN EPSP, the HVc EPSP recorded from the same cell was largely unaffected. On the other hand, treatment with CNQX, an antagonist acting at the AMPA and kainate subtypes of glutamate receptors (Honore et al., 1988), strongly blocked the HVc EPSP, but exerted no consistent effect on the MAN EPSP. Therefore, HVc and MAN appear to activate EPSPs in RA primarily through different subtypes of glutamate receptors.

The postsynaptic receptors activated within RA by either MAN or HVc fiber stimulation were not purely homogeneous populations. Although APV blocked much of the MAN EPSP, some faster components remained unaffected, and may have reflected contributions made by non-NMDA receptors. Similarly, in CNQX, stimulation of the HVc EPSP sometimes evoked a slower, small-amplitude, NMDA-like component. Such dual component EPSPs, characterized by both fast (non-NMDA) and slow (NMDA) components, typify monosynaptic transmission in many vertebrate systems (Dale and Roberts 1985; Thomson et al., 1989). In RA, both afferents may activate mixed populations of NMDA and non-NMDA receptors, but these populations have markedly different compositions. On a given RA neuron, it thus appears that MAN terminals primarily activate NMDA receptors, while HVc terminals predominantly activate non-NMDA receptors.

NMDA and Vocal Plasticity

The pharmacological heterogeneity of the MAN and HVc synaptic pathways may have special functional significance for song development and production. Lesion experiments have shown that MAN is of critical importance during plastic stages of song (Bottjer et al., 1984). Since RA is the only known efferent target of MAN, and RA is the last forebrain node in the descending motor-control pathway, it is an obvious site where MAN could exert an influence on vocal output. It is quite striking that two functionally distinct streams of the song control circuit, arising respectively from MAN and HVc, converge to form synapses on the same spinous RA neurons. Since RA neurons are only one synapse removed from the hypoglossal motoneuron pool, MAN and HVc may be critically positioned to influence vocal motor control.

Behaviorally, the sensorimotor phase of song learning depends on auditory feedback to provide error correction to the motor system. Recently, auditory units within MAN have been characterized that are highly selective for the bird's own song (Doupe and Konishi 1991). One possibility is that during plastic song, auditory feedback from MAN can alter synaptic connectivity within RA, and consequently restructure the descending motor-control pathway.

A cellular mechanism that might enable MAN axons to reorganize connections within RA could involve the activation of NMDA receptors located on RA neurons. NMDA receptors have the unique capacity to respond selectively to extracellular glutamate based on the local membrane potential. When receptor-binding of glutamate is simultaneous with postsynaptic depolarization, then the receptor-activated channel exhibits a large calcium conductance (Ascher and Nowak 1988). This feature renders the NMDA receptor an exquisite device for sensing coincident presynaptic (i.e., glutamate release) and postsynaptic (depolarization) activity.

In fact, NMDA-receptor activation is fundamental to several forms of synaptic reorganization occurring within the vertebrate CNS. In the developing *Xenopus* optic tectum, the realignment of binocular retinal maps following eye rotation can be blocked by NMDA receptor antagonists (Scherer and Udin 1989). Furthermore, although the capacity for binocular realignment is typically limited to the first three months after metamorphosis, continuous infusion of NMDA allows realignment to occur even after the normal end of the critical period (Udin and Scherer 1990). In the song system, NMDA receptor activation within RA may permit the synaptic respecification necessary for modifying the vocal output. In this regard, it may be especially relevant that MAN cell number declines steeply during the intermediate and latter stages of plastic song (Korsia and Bottjer 1989). If this decline in cell number results in a smaller number of MAN axons innervating RA, activating fewer NMDA receptors on RA neurons, then the overall capacity for synaptic reorganization may be lost.

NMDA receptor activation is also essential to the synaptic modification that characterizes some forms of hippocampal long term potentiation (Bliss and Lomo 1973; Collingridge et al., 1983). When presynaptic terminals depolarize hippocampal CA1 neurons beyond a certain threshold, postsynaptic calcium influx through NMDA receptor-associated channels triggers a long-lasting increase in synaptic strength (Malenka et al., 1988; Regehr and Tank 1990; Wigstrom et al., 1986). The associative nature of this process results in selective strengthening of all synaptic inputs to the cell that were active when threshold was exceeded (Barrionuevo and Brown 1983). In the developing song system, as HVc terminals establish their first synaptic contacts with RA neurons, preexisting synapses from MAN may interact with them in an associative fashion. Perhaps synaptic connections between HVc

and RA that generate vocalizations matching the tutor song could be selectively reinforced, if song-selective MAN neurons then activated NMDA receptors in close proximity to the "correct" HVc synapses.

NMDA and Neuronal Oscillators (Lamprey)

Several neural circuits utilize NMDA receptors in the generation of patterned, rhythmic discharge (Brodin and Grillner 1985; Brodin et al., 1985; Dale and Roberts 1984). In the lamprey spinal cord, NMDA induces oscillatory activity in neurons responsible for generating the rhythmic motor output necessary for swimming (Wallen and Grillner 1987). EPSPs with NMDA and non-NMDA components can be recorded from the motoneurons and excitatory interneurons (premotor neurons) in this spinal swimming circuit (Dale and Grillner 1986), and the differential activation of NMDA and non-NMDA receptors can determine its output frequency (Brodin et al., 1985). Singing is also a rhythmic, oscillatory behavior, particularly in the sense that it is integrated with respiration. Perhaps the pharmacological segregation of the MAN and HVc pathways plays an important role in determining the output patterns of RA neurons during song. Because of the different voltage dependence of synaptic currents mediated by NMDA and non-NMDA receptors, the weighting of HVc and MAN synapses will shift in a reciprocal fashion as a function of the postsynaptic membrane potential. These opposing synaptic inputs may set the phase of discharge across RA, and the inherent oscillatory properties of RA neurons may preserve this information over time periods that can exceed the length of individual synaptic currents. Interactions such as these may help pattern the temporal aspects of the bird's song.

Polysynaptic inhibition within nucleus RA

Inhibitory potentials were also evoked within RA by electrical stimulation of the MAN and HVc fiber pathways. The IPSP reversed when the somatic membrane potential was between -55 and -65 mV, and was reversibly blocked by bicuculline, consistent with a chloride current mediated by postsynaptic $GABA_a$ receptors. The IPSP could also be blocked by CNQX or kynurenic acid, however, suggesting that GABAergic interneurons might be driven by glutamatergic afferents. Although the present experiments cannot discriminate between feedback versus feedforward inhibition, other experiments may point to the latter mechanism. In parasagittal slices of zebra finch brain, electrical stimuli applied dorsal to RA evoked an increased release of tritiated-GABA from RA, whereas stimulation rostral to the nucleus, which would have antidromically activated spinous RA neurons, did not (Sakaguchi, Asano et al. 1987).

Additional evidence for GABAergic inhibition within comes from GAD immunohistochemistry, which has revealed dense, terminal staining within RA (Sue Volman, personal communication). The most likely candidate for a local GABAergic interneuron is an aspinous RA neuron described in Golgi studies (DeVoogd and Nottebohm 1981; Gurney 1981). The axons of aspinous RA neurons extend a dense plexus of collaterals within RA, which are studded with varicosities that could serve as part of an inhibitory network.

The extremely fast nature of the GABA-mediated IPSPs could serve to sharpen the temporal response properties of RA neurons. EPSPs within RA, which normally last several tens of milliseconds, can be reduced to only several milliseconds in duration when the IPSP is also evoked. Inhibitory networks are a major part of synaptic transmission within RA, and may help sculpt the output of this nucleus.

CHAPTER 4. SYNAPTIC POTENTIATION WITHIN THE SONG SYSTEM

INTRODUCTION

Synaptic modification within certain song control nuclei may underly the vocal plasticity that characterizes song learning. An elucidation of the synaptic mechanisms subserving song learning seems especially tractable because the song behavior is so well characterized, and the neural structures controlling song are so clearly delineated from surrounding brain regions. The present set of experiments builds on previous work I have performed to characterize the development of synaptic transmission between several song control nuclei. Anatomical tracing techniques demonstrated that MAN and HVc axons enter RA at different stages of development. In an *in vitro* brain slice preparation, the electrophysiological properties of synapses between MAN and HVC axons and RA neurons were examined at the intracellular level. These experiments suggested that MAN and HVc axons activate different subtypes of glutamate receptors on the same RA neurons, and that these synapses are first formed at different stages in development.

When HVc axons first enter RA late in development (see Chapter 1), they may have to locate and synapse with "appropriate" cellular or subcellular targets within the nucleus. The period of time required by HVc axons to properly identify their appropriate targets, and subsequently to refine their synaptic connections to them, may have a behavioral correlate in the rambling and variable vocal output that characterizes early song production. If the respecification of HVc synapses within RA is causally related to vocal plasticity, then one hypothesis is that auditory feedback information, perhaps provided by preexisting MAN terminals within RA, might stabilize connections

between HVc axons and RA neurons that generate song patterns closely matching the memorized tutor song. A physiological mechanism capable of mediating such synaptic stabilization might involve activity-dependent changes in synaptic strength similar to those described in various parts of the CNS, such as the mammalian hippocampus.

These experiments examine whether certain types of electrically evoked, afferent fiber stimulation can alter the strength of MAN and HVc synapses within RA. Coronal brain slices were prepared in which the MAN and HVc fiber tracts could be independently stimulated with bipolar tungsten electrodes, and the resultant EPSPs could be monitored with intracellular recordings made from individual RA neurons. Cells responding to one or both sets of inputs were examined. High-frequency, afferent fiber stimulation, as well as low-frequency stimulation paired with postsynaptic depolarization, was used to test to see if these inputs could be modified in a use-dependent fashion. After these manipulations, several different measurements were used to assess changes in the strength of the EPSPs.

METHODS

Slice preparation and intracellular recording

Brain slices containing nucleus RA were prepared from thirty to fifty day old birds according to the methods outlined in Chapter 2. All experiments used coronal brain slices, and bipolar tungsten stimulating electrodes were placed ≤1.0 mm lateral and dorsal to nucleus RA, in areas containing either the MAN or HVc axon tracts entering the nucleus. Electrical stimulation of each fiber tract was accomplished with pulses of 100 μsec duration, at 0.1 to 100 Hz in frequency (WPI Pulsemaster), at 0.5 to 20 Volts.

Intracellular recordings were performed as outlined in the Chapter 2 Methods section. EPSPs were analyzed as in Chapter 2, except that the onset slope was calculated from a straight line intersecting the EPSP onset and the EPSP at *two* milliseconds after onset. The EPSP slope and EPSP amplitude were normalized to their respective control values measured before the potentiating stimulus was delivered.

Two basic stimulation paradigms were used. In the high-frequency paradigm, electrical stimulation of the afferent fibers consisted of three pulses, each one second in duration, spaced evenly at thirty-second intervals. During each pulse, the MAN and/or HVc inputs (as specified below), were stimulated at a frequency of 100 Hz. In the low-frequency paradigm, one afferent input (only the HVc input has been tested to date) was electrically stimulated at 0.1 Hz, coincident with the injection of a large depolarizing current into the postsynaptic cell. The objective was to depolarize the postsynaptic membrane at the same time that the presynaptic element was active (Gustafsson et al., 1987).

Of the five experiments that yielded positive results, two used females masculinized with early testosterone implants; a third case used a male also treated with testosterone. The rationale for using steroid-treated birds was that this manipulation can hasten song crystallization (Mark Konishi, personal communication). Therefore, such treatment may increase the rate of synaptic reorganization, and render it more readily detectable in acute brain slice preparations.

RESULTS

Both MAN and HVc EPSPs recorded within RA could undergo large and long-lasting increases in strength following either high-frequency

afferent fiber stimulation, or after low-frequency afferent fiber stimulation in conjunction with postsynaptic depolarization. Sixteen RA neurons yielded recordings with enough stability that the synaptic potentials could be recorded for at least thirty minutes following application of the conditioning stimuli. Five of these cells exhibited pronounced and prolonged increases in the onset slope and the peak amplitude of either one or both EPSPs.

MAN and HVc EPSPs: high-frequency stimulation

The first set of experiments asked whether in dually innervated RA neurons, simultaneous, high-frequency stimulation of the MAN and HVc fiber pathways could produce detectable changes in the amplitude of either EPSP. In fact, the MAN and HVc EPSPs recorded from two dually innervated RA neurons both displayed long lasting increases in amplitude after high frequency stimulation was simultaneously applied to both inputs.

In the first cell subjected to high-frequency, afferent fiber stimulation, the EPSPs evoked by MAN and HVc fiber stimulation were examined at 15, 30, 35, 45, and 60 minutes after the test stimulus. Both EPSPs increased in onset slope and peak amplitude over this duration. Sixty minutes after stimulation, the HVc EPSP's onset slope measured 2.35 times, and its amplitude 2.19 times, the control values. The MAN EPSP increased less markedly, but at sixty minutes, its onset slope measured 1.42 times greater, and its peak amplitude, 1.80 times greater, than the control values. The input resistance, which was monitored throughout the experiment, did not change from its initial value of 80 MΩ.

The second cell tested in this manner was bathed in high divalent ACSF (4 mM calcium, 4 mM magnesium) in order to suppress polysynaptic transmission. Nevertheless, both the HVc and MAN EPSPs exhibited large and

persistent increases in onset slope and peak amplitude following simultaneous high-frequency stimulation of the two inputs (see Figure 29). The cell was monitored for a two-hour period after stimulation before the impalement was lost. Throughout this period, the input resistance as measured in the soma remained constant at 60 MΩ. Note that the onset slope and the amplitude of the MAN EPSP continued to increase for the first hour after stimulation (see top of Figure 30).

MAN EPSPs only: high-frequency stimulation

In the second set of experiments, an RA neuron in which only MAN fiber stimulation had evoked an EPSP was subjected to high-frequency stimulation of that pathway. The cell was bathed in high divalent ACSF (see above), and monitored for sixty minutes before delivering the test stimulation, then for two hours after stimulation. Throughout this control period, as well as the two hours following stimulation, the input resistance remained constant, although the resting potential shifted slightly from -59 to -55 mV. Despite its stability during the one-hour baseline period, the MAN EPSP increased in both onset slope and amplitude following stimulation (see Figure 31a). This increase persisted throughout the subsequent two-hour recording period.

HVc EPSPs only: low-frequency stimulation paired with postsynaptic depolarization

The third set of experiments utilized low-frequency stimulation of the HVc fiber tract in conjunction with postsynaptic depolarization. These experiments were intended to explore whether the postsynaptic membrane potential influenced the initiation of LTP in this pathway. In two RA neurons in which only stimulation of the HVc fiber tract had evoked a response, the EPSPs

displayed persistent increases in strength following the low-frequency stimulation paradigm.

In the first cell, the test paradigm consisted of electrically stimulating the HVc fiber tract once every ten seconds, for a total of sixteen times. Fifty milliseconds before each fiber stimulus was applied, a depolarizing current (+775 pA) was passed through the recording electrode for a duration of 100 milliseconds. This method insured that the postsynaptic cell was depolarized when the the afferent volley triggered the EPSP. The EPSPs were monitored for slightly more than sixty minutes before losing the impalement. Both the onset slope and the peak amplitude of the EPSP increased in a pronounced fashion within 5 minutes after delivering the test stimulation (see Figure 31b).

The second cell, which was bathed in high divalent ACSF (see above), also responded only to electrical stimulation of the HVc fiber tract. Varying the stimulus intensity produced a graded series of depolarizing synaptic potentials, and an intensity was chosen that produced an EPSP approximately half of the saturating (subthreshold) response. Throughout the experiment, the HVc fiber tract was stimulated once every ten seconds. After a stable period of ten minutes, the HVc fiber stimulus was paired with a depolarizing (+1000 pA) current pulse, 500 milliseconds in duration, that began one hundred milliseconds before each fiber stimulus. After a total of sixteen such pairings, the postsynaptic current injection was discontinued. The EPSP was monitored continuously for a total of forty-five minutes before the impalement was lost. The HVc EPSP onset slope and peak amplitude both increased markedly over the forty-five minute period following the test stimulation (see Figure 32).

Figure 29. MAN and HVc EPSPs recorded from a dually innervated RA neuron that sustained long-lasting increases in amplitude and onset slope after simultaneous, high-frequency stimuli were applied to both inputs (see Methods). The top figure shows the EPSP evoked by electrical stimulation of the MAN fiber tract, before high-frequency stimulation (*control*), and one hour after the potentiating stimuli were applied (*60' post stimulation*). The bottom traces, recorded from the same cell, show the EPSP evoked by stimulation of the HVc fiber pathway before stimulation (control), and one hour after the potentiating stimuli were applied (*60' post stimulation*). The slice was prepared from a forty day old female finch that had received testosterone implants twenty-four days after hatching. Recording was made in high divalent ACSF.

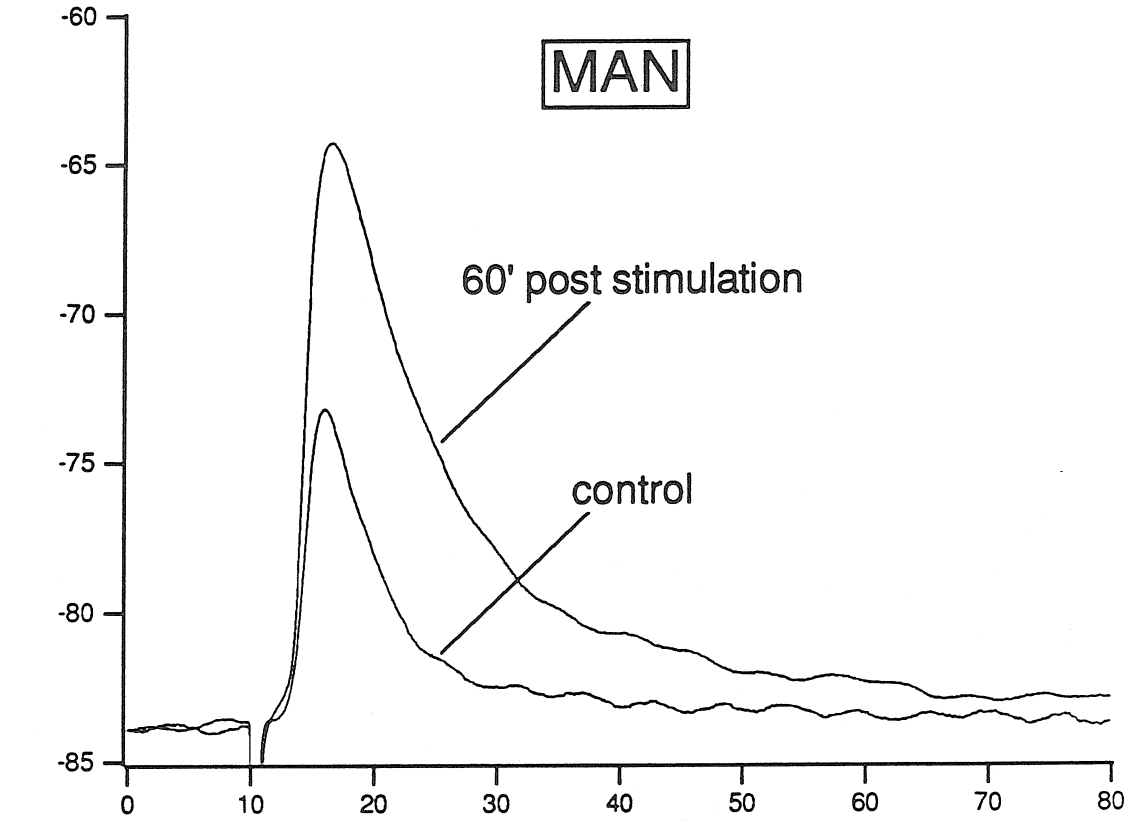
MAN
60' post stimulation
control
-60
-65
-70
-75
-80
-85
0
10
20
30
40
50
60
70
80

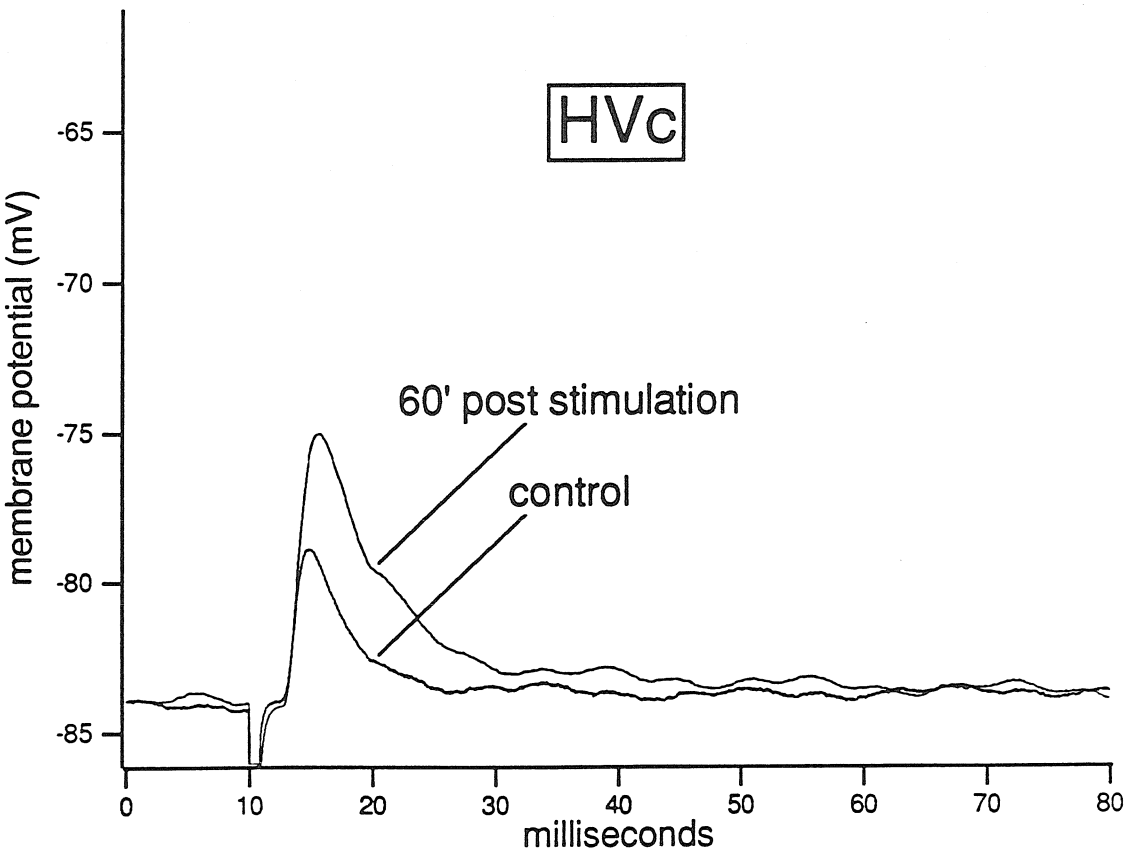
HVc
60' post stimulation
control
membrane potential (mV)
-65
-70
-75
-80
-85
0
10
20
30
40
50
60
70
80
milliseconds

Figure 30. Onset slope (*circles*) and peak amplitude (*squares*) of the MAN and HVc EPSPs shown in Figure 29 plotted as a function of time after stimulation. The upper graph plots these two parameters for the MAN EPSP; the lower graph plots these parameters for the HVc EPSP. Note the gradual increase of the MAN EPSP over the first sixty minutes.

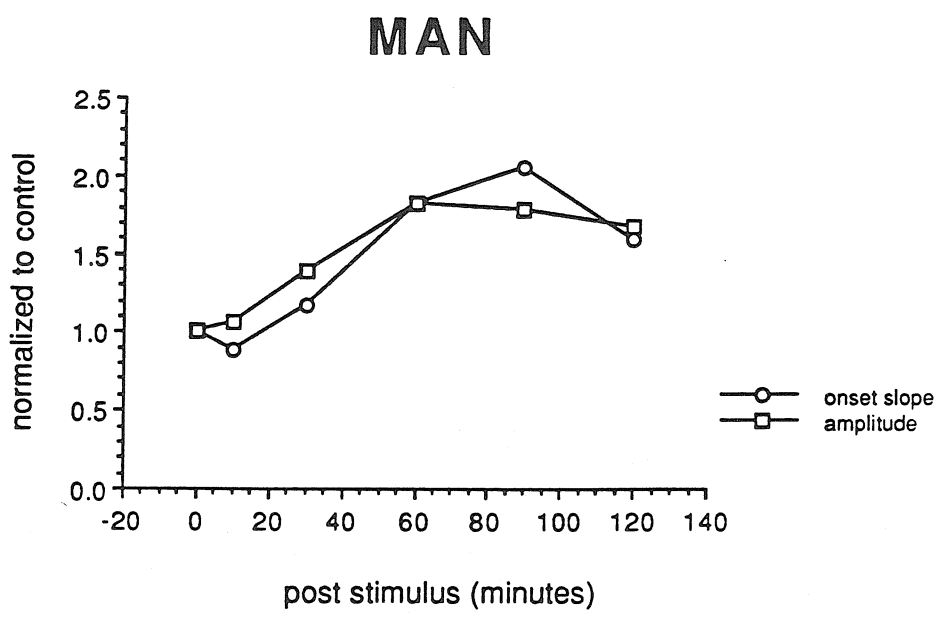
MAN
normalized to control
2.5
2.0
1.5
1.0
0.5
0.0
-20
0
20
40
60
80
100
120
140
post stimulus (minutes)
onset slope
amplitude

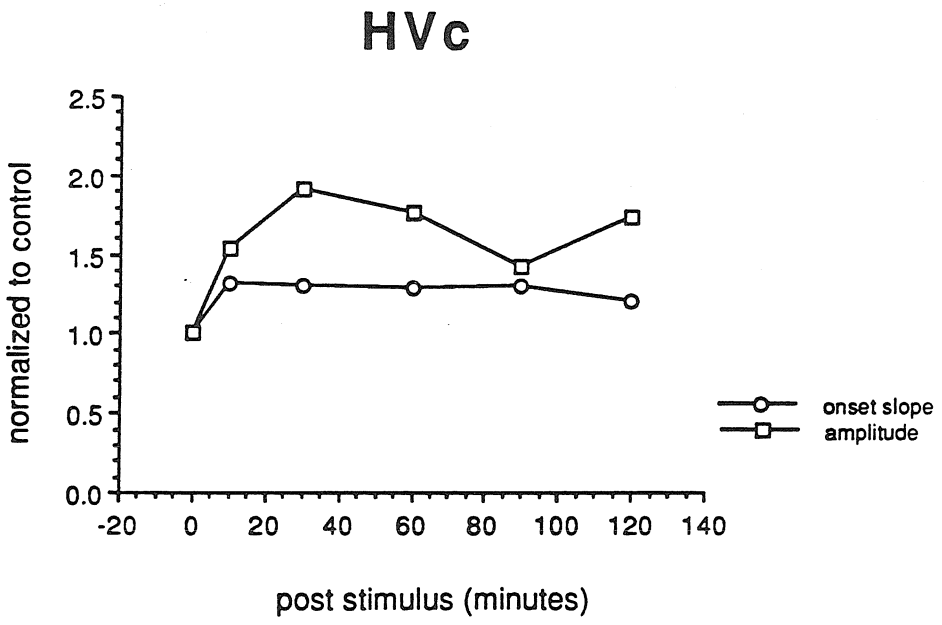
HVc
normalized to control
2.5
2.0
1.5
1.0
0.5
0.0
-20
0
20
40
60
80
100
120
140
post stimulus (minutes)
onset slope
amplitude

Figure 31. The onset slopes (*circles*) and peak amplitudes (*squares*) recorded from RA neurons responding only to MAN fiber tract stimulation (a)), or HVc fiber tract stimulation (b)), plotted as a function of the time after the potentiating stimuli were applied.

a) In an RA neuron responding only to MAN fiber stimulation, high-frequency stimulation of that pathway (see Methods) resulted in a large increase in the EPSP onset slope and amplitude, which persisted for the two-hour period before the impalement was lost. The EPSP had described a stable baseline for a one-hour period before stimulation (only the last ten minutes of which are shown). The slice was prepared from a thirty-five day old male finch.

b) In an RA neuron in which only stimulation of the HVc fiber pathway had evoked an EPSP, low-frequency (0.1 Hz) pairing of the EPSP with postsynaptic depolarization (see Methods) was followed by an almost twofold increase in onset slope and amplitude, which persisted for the one-hour period before the impalement was lost. Slice was prepared from a forty-four day old male finch that had been implanted with testosterone on day 38.

a

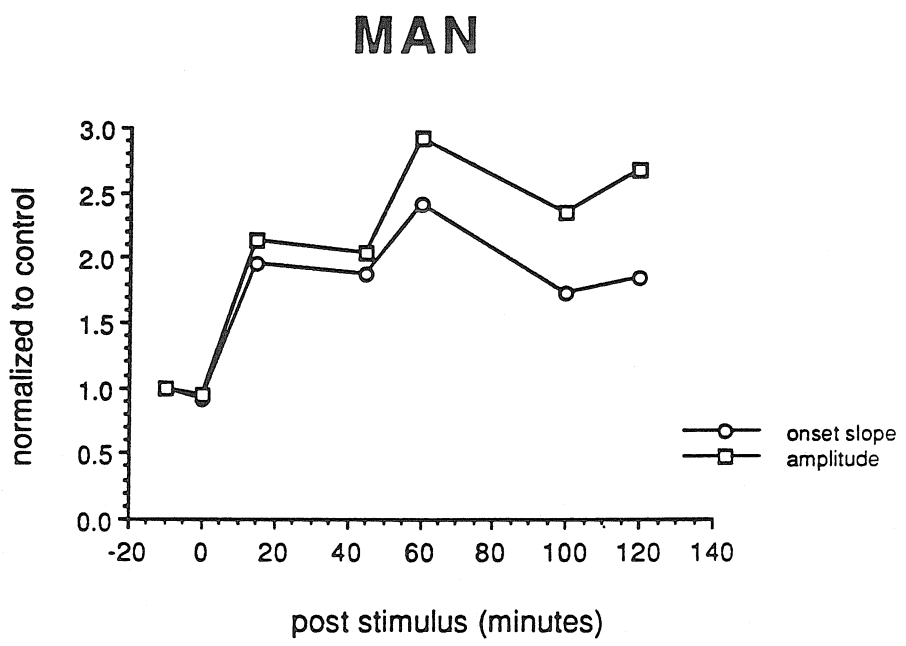
MAN
normalized to control
3.0
2.5
2.0
1.5
1.0
0.5
0.0
-20
0
20
40
60
80
100
120
140
post stimulus (minutes)
onset slope
amplitude

b

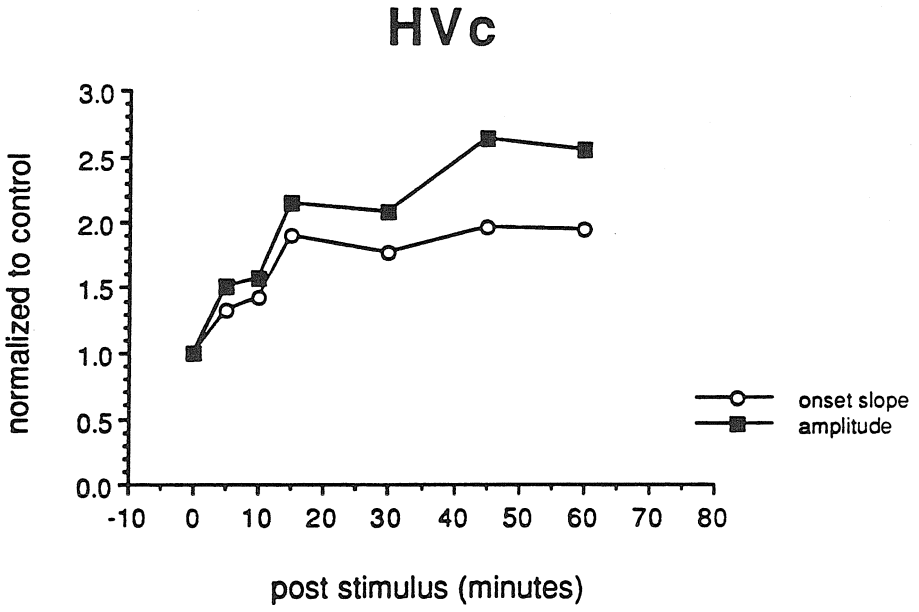
HVc
normalized to control
3.0
2.5
2.0
1.5
1.0
0.5
0.0
-10
0
10
20
30
40
50
60
70
80
post stimulus (minutes)
onset slope
amplitude

Figure 32. An HVc EPSP recorded from an RA neuron in which only stimulation of the HVc fiber pathway evoked a response. The two traces show the HVc EPSP before potentiation (*pre-stimulation*), and twenty-five minutes after the EPSP was paired at low frequency (0.1 Hz) with postsynaptic depolarization (*25' post stimulation*). Slice was prepared from a fifty day old male finch.

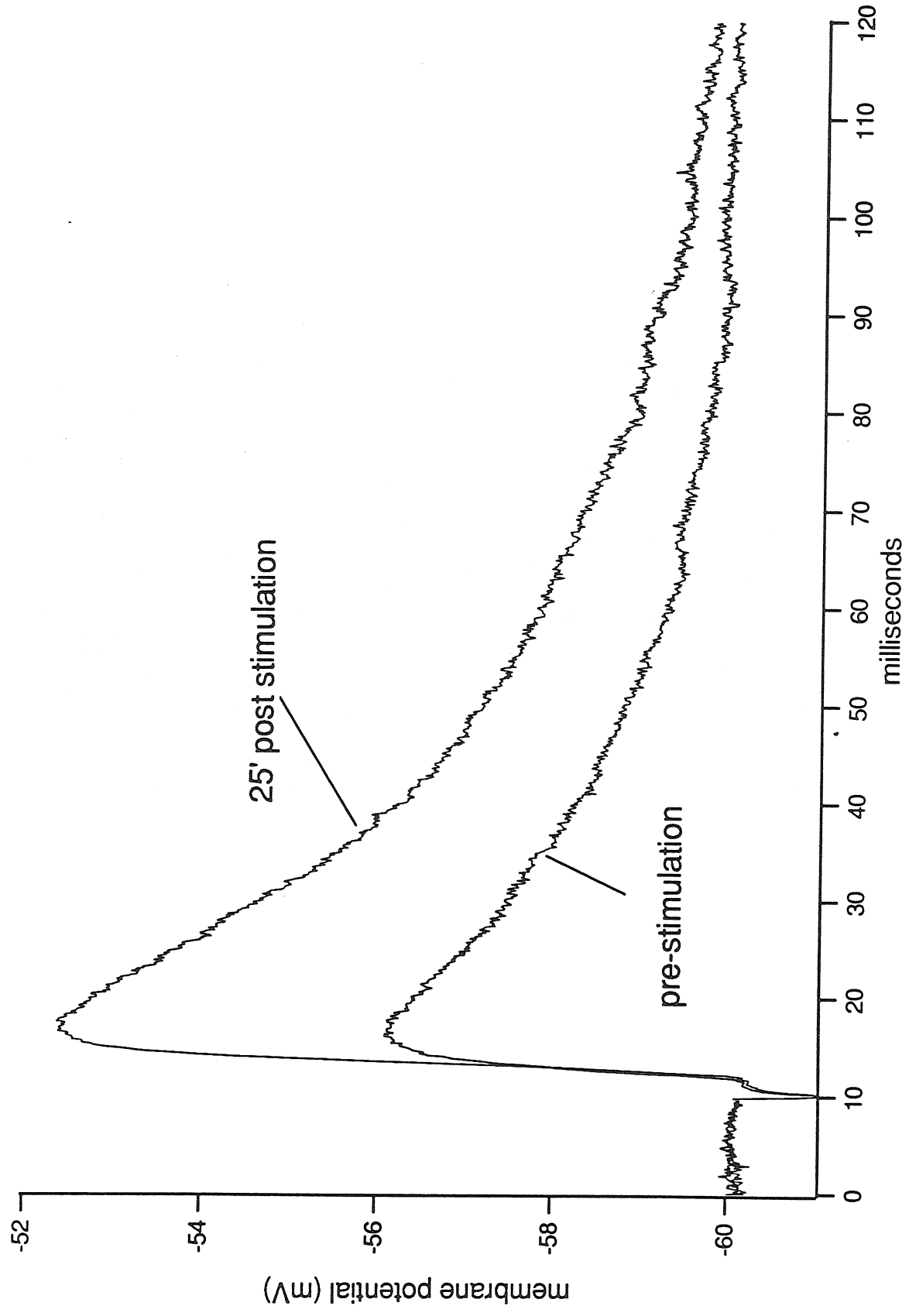
membrane potential (mV)
-52
-54
-56
-58
-60
0
10
20
30
40
50
60
70
80
90
100
110
120
milliseconds
25' post stimulation
pre-stimulation

DISCUSSION

These preliminary experiments demonstrate that the excitatory input provided to RA by MAN and HVc axons can be strengthened in an activity-dependent fashion. High-frequency stimulation of MAN and HVc axons, as well as low-frequency stimulation paired with postsynaptic depolarization, could produce long-lasting increases in synaptic strength within RA in slices prepared from birds of thirty to fifty days of age. Therefore, synapses strategically positioned in the descending vocal motor control pathway can be modified during a period when vocal plasticity is quite pronounced.

Since HVc and RA constitute a descending neural pathway that plays a motor role in singing (McCasland 1987; Nottebohm et al., 1976), one hypothesis is that faithful reproduction of the tutor song depends on the formation of specific connections between HVc axons and RA neurons. It is interesting to note that the earliest stages of song begin at the time that HVc axons first enter RA (Immelmann 1969; Konishi and Akutagawa 1985). Subsequent to axon ingrowth, the synapses that HVc axons make with RA neurons might be selectively reinforced, or removed, based on how closely the vocalizations that they engender match the auditory template. This model depends on a mechanism that could select for the "correct" synapses. Behaviorally, young songbirds use auditory feedback to match their own song to the tutor model memorized during sensory acquisition. Song-selective auditory neurons in MAN (Doupe and Konishi 1991), by virtue of their axonal projections to RA, might provide the cellular mechanism by which auditory feedback can provide error correction to the vocal motor system. The discovery that MAN lesions disrupt song production only when made during sensorimotor learning, and not after song crystallization (Bottjer et al., 1984), could reflect

MAN's transient role in guiding synapse formation within the developing vocal motor pathway.

One prediction of this model is that at the synaptic level within RA, certain interactions between MAN and HVc axon terminals might enhance synaptic transmission. In fact, the present experiments illustrate that *in vitro*, simultaneous high-frequency stimulation of MAN and HVc afferents can produce long lasting increases in EPSP amplitude. MAN and HVc synapses can be modified in an activity-dependent fashion, and this capacity might be utilized to select for certain patterns of connectivity within RA.

The most extensively studied form of plasticity in the vertebrate CNS is the long term potentiation of synaptic transmission (LTP) that can be elicited within the mammalian hippocampus (Bliss and Lomo 1973). In the CA1 region of hippocampus, NMDA receptor activation appears to be essential to LTP induced by high-frequency, afferent stimulation (Collingridge et al., 1983). In the CA3 region of hippocampus, both NMDA receptor-dependent and -independent forms of LTP can be induced. Pyramidal neurons in CA3 receive excitatory input from mossy fibers of the dentate gyrus, as well as from commissural-associational (CA) fibers (Amaral and Witter 1989). Although both inputs can support LTP, NMDA receptor antagonists block LTP induction only in the CA, but not mossy fiber, pathway (Harris and Cotman 1986). Conjunction, or the pairing of postsynaptic depolarization with low-frequency afferent stimulation, also elicits LTP, but only in those pathways where the induction of LTP by high-frequency stimulation is NMDA receptor-dependent. (Zalutsky and Nicoll 1990). The LTP induced by conjunction is also sensitive to D-APV blockade (Gustafsson et al., 1987; Zalutsky and Nicoll 1990).

Since HVc axons evoke EPSPs primarily through non-NMDA glutamate receptors (see Chapter 2), it was surprising that conjunction could

induce potentiation in this pathway. In some cases, small portions of the HVc EPSP appear to be mediated by NMDA receptors, and thus this minor NMDA component might be responsible for the changes in HVc synaptic strength when the EPSP is paired with postsynaptic depolarization.

Regardless of the actual mechanisms responsible for conjunction effects in the HVc pathway *in vitro*, postsynaptic depolarizations capable of potentiating the HVc pathway *in vivo* are probably generated by other synaptic afferents to RA. The dense intermixing of MAN and HVc terminals on RA dendrites (Canady et al., 1988) raises the possibility that the large NMDA receptor-mediated EPSPs evoked by MAN axons could provide the depolarization necessary to stabilize neighboring synapses. This model implies that within RA, certain vocalizations would be produced by activating specific HVc synapses within RA. Then, after the relevant auditory processing had occurred, MAN synapses in RA would be activated, and potentiate those HVc synapses that were recently active. One problem with this model is that the overall temporal delay between HVc and MAN synaptic activation within RA could be quite long. Transmission times from RA to the hypoglossal nerve approaches 10 milliseconds (Manogue and Paton 1982), and auditory response latencies in MAN are on the order of 50 milliseconds (Doupe and Konishi 1991), so that the delay between HVc and MAN EPSPs within RA might approach 75 to 100 milliseconds. However, in the CA1 region of hippocampus, conjunction experiments in which each pulse of the low frequency, afferent stimulus precedes the onset of each depolarizing current pulse to the postsynaptic cell have revealed a certain temporal window during which LTP can be induced. In fact, even when the EPSP is triggered as long as 100 milliseconds before the onset of each current pulse, significant LTP still occurs (Gustafsson et al., 1987). If the MAN EPSP is equivalent to the depolarizing

current pulse, then it might follow the HVc EPSP by many tens of milliseconds, and still be able to contribute to potentiation.

The role of postsynaptic depolarization in the formation of LTP in the HVc pathway might have some important functional consequences. First, on any given RA neuron (or dendrite), only those HVc synapses that are active just before or during the postsynaptic depolarization will be strengthened. Therefore, only certain subsets of HVc synapses will be potentiated out of the larger pool that are actually present. Additionally, it might be possible for a single HVc axon to strengthen its connections to several different RA neurons, if the relevant postsynaptic cells were simultaneously depolarized. Therefore, if certain RA neurons fire synchronously by virtue of local coupling mechanisms, then an HVc axon might reinforce its connections to all of these cells.

The basic cellular mechanisms necessary for synaptic modification are present within RA *in vitro*. A major issue still to be resolved is whether or not these mechanisms actually are utilized during vocal learning. One of the tremendous advantages that studies of synaptic potentiation within the song system have to offer is that song learning is such a well-described and robust process. Although other systems might be more tractable to intracellular analysis, none exist that are united with such an intriguing, yet well-defined learned behavior. The experiments described in this thesis suggest how the physiological properties of song control neurons might relate to the development and the production of learned song. The process of uniting the cellular and behavioral properties of the song system will ultimately transfer knowledge gained from *in vitro* analyses such as these into an appreciation of the cellular mechanisms controlling song learning.

CONCLUDING REMARKS

The song system can be divided into two functionally distinct pathways on the basis of both behavioral and electrophysiological experiments. The primary pathway is involved in vocal motor control, and includes the descending projection from HVc to RA, and from RA onto the hypoglossal motoneurons innervating the syringeal musculature. The accessory pathway contains several nuclei that do not have a clear motor role in adult song production, but are essential to normal song development. The developmental importance of the accessory song nuclei might reflect their transient involvement in vocal motor control, or their role in providing auditory feedback to the primary vocal motor control pathway. The recent discovery of song-selective auditory neurons within both MAN and area X of the accessory pathway is consistent with this latter role.

Many of the connections within the accessory pathway are formed earlier in development than are those within the primary vocal motor control pathway. I have shown with anatomical tracers that MAN axons project into RA, and HVc axons project to area X, as early as fifteen days after hatching. This contrasts with the development of connections between HVc and RA, which are not formed until twenty-five to thirty days after hatching. If the accessory nuclei in very young finches have song-selective auditory responses as have been described in the adult, then differences in when the accessory and primary pathways are formed might have special significance for song development. Specifically, the accessory pathway is interconnected during the early stages of sensory acquisition, whereas the connections between HVc and RA are not. Therefore, because young male finches learn songs that they hear before day twenty-five, this early auditory experience must be directly affecting other connections than those between HVc and RA, since these have yet to be made.

One site within the song system where early auditory experience could directly alter synaptic properties is within the accessory pathway. Such early auditory experience could lead to the formation of an auditory template, or memory of the tutor song, by shaping the auditory response properties of neurons within the accessory nuclei. If this is so, then neurons within the accessory pathway might become highly tuned to the tutor song during sensory acquisition.

The close coincidence of when HVc axons first enter RA and when subsong begins suggests that functional connections between these two nuclei are obligatory for song production. This is reasonable given that HVc and RA are clearly essential for the motor control of song in adult birds. If these nuclei perform a similar role in young finches, then song production could depend on the elaboration of functional synapses between HVc axons and RA neurons. Furthermore, the failure to form these connections in female finches could explain why they are incapable of producing song.

If the accessory pathway conveys song-related auditory information, and the primary pathway is involved in vocal motor control, then the convergence of these two functionally distinct pathways within RA is especially intriguing. The electrophysiological analyses presented here strongly suggest that spinous RA neurons, which provide the sole output of the entire forebrain vocal control pathway, initially receive extrinsic innervation only from MAN axons, but at later stages are innervated by both MAN and HVc axons. This pattern of convergent connectivity, developing as a result of the massive ingrowth of HVc axons into RA, could provide a cellular locus for the auditory-motor integration fundamental to song learning.

Presumably, one major obstacle facing HVc axons as they enter RA is the elaboration of specific sets of synapses with postsynaptic neurons. Perhaps the preexisting projection from MAN to RA could guide the formation of

HVc synapses on RA neurons. The rambling and highly variable quality of subsong suggests that the initial HVc axonal ingrowth into RA produces largely random, or at least imprecise, synaptic connections. If the precision of HVc axonal connectivity with RA neurons does determine the acoustical quality of the bird's song, then the vocal refinement observed during sensorimotor learning might depend on strengthening specific sets of connections between HVc and RA. Auditory feedback might selectively reinforce those "specific sets" of synapses between HVc and RA that generate vocalizations most closely matching the tutor song. The projection from MAN to RA could provide the means by which song-related auditory information impinges on the vocal motor connections from HVc to RA. The convergence of MAN and HVc axons onto individual RA neurons provides a discrete cellular site where auditory feedback could modulate synaptic transmission within the descending vocal motor control pathway.

If individual RA neurons are the locus of auditory-motor interaction within the song system, then the interactions of MAN and HVc synapses on these neurons might explain how auditory feedback actually provides "error-correction" to the vocal motor control system. By recording from individual RA neurons *in vitro*, I have shown that both HVc and MAN EPSPs sustain long-lasting increases in amplitude in response to repeated synaptic activation. Synaptic potentiation could serve to selectively strengthen specific connections between HVc axons and RA neurons, as is proposed to occur during sensorimotor learning.

With pharmacological techniques, I have shown that although HVc and MAN axons provide excitatory input to many of the same RA neurons, "HVc" EPSPs involve non-NMDA glutamate receptor activation, whereas "MAN" EPSPs are mediated primarily by NMDA receptors. The discovery of NMDA

receptors within the song system is especially important because these receptors are implicated in several forms of synaptic modification within the vertebrate CNS, including the induction of long-lasting changes in EPSP amplitude (i. e., synaptic potentiation). At present, it is unknown whether NMDA receptor activation is an essential requirement for synaptic potentiation within RA. However, the large NMDA-receptor mediated component of the MAN EPSP might render any NMDA-receptor dependent processes within RA extremely sensitive to MAN synaptic activation. The application of NMDA receptor antagonists could clarify the mechanism of synaptic potentiation within RA *in vitro*, and ultimately could be used to test whether NMDA receptor activation *in vivo* is an essential feature of sensorimotor learning.

The auditory-motor interaction proposed to occur on individual RA neurons has certain implications for the order of activation of HVc and MAN synapses. First, HVc axons would propagate a descending vocal motor command, activating synaptic inputs on RA neurons. HVc synaptic activation would alter the output patterns of RA neurons. Because of RA's direct projection onto hypoglossal motoneurons, this altered output pattern would influence syringeal muscle tone and modulate the acoustical properties of the bird's song. After some delay, auditory feedback processing within the accessory pathway would "compare" the vocal output with the template. Song-selective auditory units within the accessory pathway, and especially MAN, would fire when vocalizations closely matched the tutor model. Consequently, close matches between the bird's own song and the tutor model would lead to the activation of MAN synapses on RA neurons. HVc synapses on RA neurons would be potentiated if their activation was followed after some critical delay by the activation of adjacent MAN synapses.

Two predictions of this model are that synaptic potentiation will occur when HVc synaptic activation precedes MAN synaptic activation within RA, and when the delay between the activation of these two inputs falls within a certain time window. The critical delay between HVc and MAN synaptic activation might lie within a range of fifty to one hundred and fifty milliseconds, since the spike discharge rate increases within RA ten to fifteen milliseconds before the onset of the vocalization, and auditory units within MAN respond more than fifty milliseconds after stimulus presentation. It would be possible to test these two predictions by varying the order of HVc and MAN synaptic activation within RA, and by varying the delay between the activation of each input.

In fact, the potentiation experiments presented here do begin to address the issue of synaptic delay. The conjunction paradigm, in which the HVc pathway is stimulated at low frequency while simultaneously injecting depolarizing currents into the postsynaptic cell, can potentiate the HVc EPSP. In the mammalian hippocampus, conjunction can generate synaptic potentiation even when the depolarizing current injection follows each afferent fiber stimulus by as much as two hundred milliseconds. If the same holds true in RA, then the depolarizing current injection could follow activation of the HVc EPSP by fifty to two hundred milliseconds and still result in potentiation. If the depolarizing current injection is merely a substitute for the depolarization generated by the MAN EPSP, then the activation of the MAN input might follow that of the HVc input by fifty to two hundred milliseconds and still potentiate the HVc synapse.

A major issue is how the MAN input determines which HVc synapses to potentiate. Presumably, the vocal motor pathway must be in part spatially organized, because the syringeal muscles and their representations

within the hypoglossal nucleus and RA are topographically organized. In contrast, song-selective MAN neurons respond primarily to the temporal order of the vocal elements of the bird's song. It might not be necessary for the MAN input to have any "map" of *where* the correct HVc synapses should be made within RA, if their activation reinforces HVc synapses in a purely time-dependent manner. Song-selective units in MAN could activate synapses throughout all of RA, but would only potentiate those HVc synapses that were previously active within the critical time window. Consequently, even if HVc axons have to terminate at precise locations within RA, MAN axonal projections could be quite diffuse. In this context, it will be useful to learn more about how MAN and HVc axons map onto RA.

Finally, the activation of HVc and MAN synapses must influence the firing patterns of RA neurons in order to affect the bird's song. These studies have examined the subthreshold properties of HVc and MAN EPSPs within RA. However, it is not yet established how these subthreshold events pertain to the suprathreshold behavior of RA neurons. Potentiation of an excitatory synapse should increase the probability that its activation will bring the postsynaptic cell beyond spike threshold. Since RA neurons are often spontaneously active, however, activation of excitatory inputs might instead modulate the phase of the ongoing spike discharge. A critical issue is whether HVc and/or MAN inputs function to transform spiking activity within RA from an uncorrelated state to one in which the spiking phase of many RA neurons become highly correlated. Potentiation of specific synapses could then determine which subsets of RA neurons would be driven in a correlated fashion by a given input. This would be especially relevant if HVc premotor neurons are organized to command specific vocal "motions," and therefore have to simultaneously recruit many disparate RA neurons, which are organized myotopically.

A further possibility is that RA functions similarly to certain vertebrate pattern-generating circuits, such as the swimming circuit in the lamprey spinal cord, or the hindbrain pacemaker nucleus of weakly electric fish that controls electric organ discharge. These circuits' output patterns are modulated by the differential activation of NMDA and non-NMDA glutamate receptors. The differential activation of these two glutamate receptor subtypes on individual RA neurons might modulate RA's output patterns. During sensorimotor learning, varying numbers of HVc and MAN synapses would activate different ratios of NMDA and non-NMDA receptors on RA neurons, resulting in extensive variation in the vocal output. Synaptic potentiation via auditory feedback would preserve matches to the tutor song from this wide variety of vocal outputs. In this case, MAN might serve a transient motor role and to stabilize synaptic connections within RA through auditory feedback.

The potential to understand complex behaviors in the context of neuronal properties is one of the great attractions of modern neurobiology. Birdsong is an intriguing and elaborate learned behavior mediated by a discretely organized neural circuit. This project has provided a rewarding glimpse of neuronal properties within the song system, and has illuminated mechanisms that could subserve both song learning and vocal motor control. Future work will seek to establish how these cellular mechanisms contribute to the development of the song behavior.

BIBLIOGRAPHY

Alvarez-Buylla, A., M. Theelen and F. Nottebohm. (1988). "Birth of projection neurons in the higher vocal center of the canary forebrain before, during, and after song learning." PNAS USA. **85**: 8722-8726.

Amaral, D. G. and M. P. Witter. (1989). "The three-dimensional organization of the hippocampal formation- a review of anatomical data." Neurosci. **31**(3): 571-591.

Ascher, P. and L. Nowak. (1988). "The role of divalent cations in the N-methyl-D-aspartate responses of mouse central neurones in culture." J. Physiol. **399**: 247-266.

Ball, G. F. (1990). Chemical neuroanatomical studies of the steroid-sensitive songbird vocal control system: a comparative approach. Brain and Behavior in Vertebrates. 1. Sexual Differentiation, Neuroanatomical Aspects, Neurotransmitters and Neuropeptides. Basel, Karger, Comp. Physiol.

Ball, G. F., P. L. Faris, B. K. Hartman and J. C. Wingfield. (1988). "Immunohistochemical localization of neuropeptides in the vocal control regions of two songbird species." J. Comp. Neurol. **268**: 171-180.

Barclay, S. and C. Harding. (1988). "Androstenedione modulation of monoamine levels and turnover in hypothalamic and vocal control nuclei in the male zebra finch: steroid effects on brain monoamines." Brain Res. **459**: 333-343.

Barrionuevo, G. and T. H. Brown. (1983). "Associative long-term potentiation in hippocampal slices." PNAS USA. **80**: 7347-7351.

Bliss, T. V. P. and T. Lomo. (1973). "Long-lasting potentiation of synaptic transmission in the dentate area of the anesthetized rabbit following stimulation of the perforant path." J. Physiol. **232**: 331-356.

Bohner, J. (1983). "Song learning in the zebra finch (*Taeniopygia guttata*): selectivity in the choice of a tutor and accuracy of song copies." Anim. Behav. **31**: 231-237.

Bohner, J. (1990). "Early acquisition of song in the zebra finch, *Taeniopygia guttata*." Anim. Behav. **39**: 369-374.

Bottjer, S. W., K. A. Halsema, S. A. Brown and E. A. Miesner. (1989). "Axonal connections of a forebrain nucleus involved with vocal learning in zebra finches." J. Comp. Neurol. **279**: 312-326.

Bottjer, S. W., E. A. Miesner and A. Arnold. (1986). "Changes in neuronal number, density and size account for increases in volume of song-control nuclei during song development in zebra finches." Neurosci. Lett. **67**: 263-268.

Bottjer, S. W., E. A. Miesner and A. P. Arnold. (1984). "Forebrain lesions disrupt development but not maintenance of song in passerine birds." Sci. **224**: 901-903.

Brodin, L. and S. Grillner. (1985). "The role of putative excitatory amino acid neurotransmitters in the lamprey spinal cord. I. The effects of excitatory amino acid antagonists." Brain Res. **360**: 139-148.

Brodin, L., S. Grillner and C. M. Rovainen. (1985). "N-methyl-D-aspartate, kainate and quisqualate receptors and the generation of fictive locomotion in the lamprey spinal cord." Brain Res. **325**: 302-306.

Canady, R. A., G. D. Burd, T. J. DeVoogd and F. Nottebohm. (1988). "Effect of testosterone on input received by an identified neuron type of the canary song system: a Golgi/electron microscopy/degeneration study." J. Neurosci. **8**(10): 3770-3784.

Catchpole, C. K. (1982). The evolution of bird sounds in relation to mating and spacing behavior. Acoustic Communication in Birds. New York, Academic Press.

Clayton, N. and E. Prove. (1989). "Song discrimination in female zebra finches and bengalese finches." Anim. Behav. **38**: 352-354.

Collingridge, G. L., S. J. Kehl and H. McLennan. (1983). "Excitatory amino acids in synaptic transmission in the Schaffer collateral-commissural pathway of the rat hippocampus." J. Physiol. **334**: 33-46.

Crawford, A. C. and R. Fettiplace. (1981). "An electrical tuning mechanism in turtle cochlear hair cells." J. Physiol. **312**: 377-412.

Dale, N. and S. Grillner. (1986). "Dual-component synaptic potentials in the lamprey mediated by excitatory amino acid receptors." J. Neurosci. **6**(9): 2653-2661.

Dale, N. and A. Roberts. (1984). "Excitatory amino acid receptors in *Xenopus* embryo spinal cord and their role in the activation of swimming." J. Physiol. **348**: 527-543.

Dale, N. and A. Roberts. (1985). "Dual-component amino acid-mediated synaptic potentials: excitatory drive for swimming in *Xenopus* embryos." J. Physiol. **363**: 35-59.

Davies, J., A. A. Francis, A. W. Jones and J. C. Watkins. (1981). "2-amino-5-phosphonovalerate (2APV), a potent and selective antagonist of amino acid-induced and synaptic excitation." Neurosci. Lett. **21**: 77-81.

DeVoogd, T. J., H. Norden and C. Gould. (1986). Dendritic retraction and spine elimination in females contribute to sex dimorphisms in the avian song system. Society for Neuroscience Abstracts. **XVI:** 1214.

DeVoogd, T. J. and F. Nottebohm. (1981). "Sex differences in dendritic morphology of a song control nucleus in the canary: a quantitative Golgi study." J. Comp. Neurol. **196**: 309-316.

Doupe, A. J. and M. Konishi. (1991). in preparation.

Eales, L. A. (1985). "Song learning in zebra finches; some effects of song model availability on what is learnt and when." Anim. Behav. **33**: 1293-1300.

Forsythe, I. D. and G. L. Westbrook. (1988). "Slow excitatory postsynaptic currents mediated by N-methyl-D-aspartate receptors on cultured mouse central neurones." J. Physiol. **396**: 515-533.

Frankenhaeuser, B. and A. L. Hodgkin. (1957). "The action of calcium on the electrical properties of squid axons." J. Physiol. **137**: 218-244.

Gurney, M. E. (1981). "Hormonal control of cell form and number in the zebra finch song system." J. Neurosci. **1**(6): 658-673.

Gurney, M. E. (1982). "Behavioral correlates of sexual differentiation in the zebra finch song system." Brain Res. **231**: 153-172.

Gurney, M. E. and M. Konishi. (1980). "Hormone-induced sexual differentiation of brain and behavior in zebra finches." Sci. **208**: 1380-1383.

Gustafsson, B., H. Wigstrom, W. C. Abraham and Y.-Y. Huang. (1987). "Long-term potentiation in the hippocampus using depolarizing current pulses as the conditioning stimulus to single volley synaptic potentials." J. Neurosci. **7**(3): 774-780.

Hall, M. F. (1962). "Evolutionary aspects of estrildid song." Symp. Zool. Soc. Lond. **8**: 37-55.

Harris, E. W. and C. W. Cotman. (1986). "Long-term potentiation of guinea pig mossy fiber responses is not blocked by N-methyl D-aspartate antagonists." Neurosci. Lett. **70**: 132-137.

Herrmann, K. and A. P. Arnold. (1989). The development of afferent projections to RA in male zebra finches. Society for Neuroscience Abstracts XIX. **XIX:** 234.10.

Hestrin, S., R. A. Nicoll, D. J. Perkel and P. Sah. (1990). "Analysis of excitatory synaptic action in pyramidal cells using whole-cell recording from rat hippocampal slices." J. Physiol. **422**: 203-225.

Hille, B. (1984). Ionic Channels of Excitable Membranes. Sunderland, MA, Sinauer Associates, Inc.

Honore, T., S. N. Davies, J. Drejer, E. Fletcher, P. Jacobsen, D. Lodge and F. E. Nielsen. (1988). "Quinoxalinediones: potent competitive non-NMDA glutamate receptor antagonists." Sci. **241**: 701-703.

Horikawa, K. and W. E. Armstrong. (1988). "A versatile means of intracellular labeling: injection of biocytin and its detection with avidin conjugates." J. Neurosci. Methods. **25**(1): 1-11.

Hudspeth, A. J. and R. S. Lewis. (1988). "Kinetic analysis of voltage- and ion-dependent conductances in saccular hair cells of the bull frog, *Rana catesbeiana*." J. Physiol. **400**: 237-274.

Immelmann, K. (1969). Song development in the zebra finch and other estrildid finches. Bird Vocalizations. London, Cambridge University Press.

Jodkowski, J. S., F. Viana, T. E. Dick and A. J. Berger. (1988). "Repetitive firing properties of phrenic motoneurons in the cat." J. Neurophysiol. **60**(2): 687-702.

Karten, H. (1969). "The organization of the avian telencephalon and some speculations on the phylogeny of the amniote telencephalon." Ann. N. Y. Acad. Sci. **167**: 164-179.

Katz, L. C. and M. E. Gurney. (1981). "Auditory responses in the zebra finch's motor system for song." Brain Res. **211**: 192-197.

Kernell, D. (1965). "High-frequency repetitive firing of cat lumbrosacral motoneurones stimulated by long-lasting injected currents." Acta Physiol. Scand. **65**: 74-86.

Kirn, J. R. and T. J. DeVoogd. (1989). "Genesis and death of vocal control neurons during sexual differentiation in the zebra finch." J. Neurosci. **9**(9): 3176-3187.

Konishi, M. (1963). "The role of auditory feedback in the vocal behavior of the domestic fowl." Z. fur Tierpsychol. **20**: 349-367.

Konishi, M. (1965). "The role of auditory feedback in the control of vocalization in the white-crowned sparrow." Z. fur Tierpsychol. **22**: 770-783.

Konishi, M. (1985). "Birdsong: from behavior to neuron." Ann. Rev. Neurosci. **8**: 125-170.

Konishi, M. and E. Akutagawa. (1985). "Neuronal growth, atrophy and death in a sexually dimorphic song nucleus in the zebra finch." Nat. **315**: 145-147.

Konishi, M. and E. Akutagawa. (1987). Hormonal control of cell death in a sexually dimorphic song nucleus in the zebra finch. Selective Neuronal Death. Chichester, Wiley.

Konishi, M. and E. Akutagawa. (1988). "A critical period for estrogen action on neurons of the song control system in the zebra finch." PNAS USA. **85**: 7006-7007.

Konishi, M. and E. Akutagawa. (1990). "Growth and atrophy of neurons labeled at their birth in a song nucleus of the zebra finch." PNAS USA. **87**: 3538-3541.

Konishi, M. and F. Nottebohm. (1969). Experimental studies in the ontogeny of avian vocalization. Bird Vocalizations. London, Cambridge University Press.

Korsia, S. and S. W. Bottjer. (1989). "Developmental changes in the cellular composition of a brain nucleus involved with song learning in zebra finches." Neuron. **3**: 451-460.

Krebs, J. R. (1977). Song and territory in the Great tit *Parus major*. Evolutionary Ecology. New York, Macmillan.

Lund, R. D. and M. J. Mustari. (1977). "Development of the geniculocortical pathway in rats." J. Comp. Neurol. **173**: 289-306.

Luskin, M. B. and C. J. Shatz. (1985). "Neurogenesis of the cat's primary visual cortex." J. Comp. Neurol. **242**: 611-631.

Malenka, R., J. A. Kauer, R. S. Zucker and R. A. Nicoll. (1988). "Postsynaptic calcium is sufficient for potentiation of hippocampal synaptic transmission." Sci. **242**: 81-84.

Manogue, K. and F. Nottebohm. (1982). "Relation of medullary motor nuclei to nerves supplying the vocal tract of the budgerigar (*Melopsittacus undulatus*)." J. Comp. Neurol. **204**: 384-391.

Manogue, K. and J. A. Paton. (1982). "Respiratory gating of activity in the avian vocal control system." Brain Res. **247**: 383-387.

Marfurt, C., D. F. Turner and C. Adams. (1988). "Stabilization of tetramethylbenzidine (TMB) reaction product at the electron microscopic level by ammonium molybdate." J. Neurosci. Meth. **25**: 215-223.

Margoliash, D. (1983). "Acoustic parameters underlying the responses of song-specific neurons in the white-crowned sparrow." J. Neurosci. **3**: 1039-1057.

Marler, P. and S. Peters. (1981). "Sparrows learn adult song and more from memory." Sci. **213**: 780-782.

Mason, A. and A. Larkman. (1990). "Correlations between morphology and electrophysiology of pyramidal neurons in slices of rat visual cortex. II. Electrophysiology." J. Neurosci. **10**(5): 1415-1428.

McCasland, J. S. (1987). "Neuronal control of bird song production." J. Neurosci. **7**: 23-39.

McConnell, S. K., A. Ghosh and C. J. Shatz. (1989). "Subplate neurons pioneer the first axon pathway from the cerebral cortex." Sci. **245**: 978-982.

McCormick, D. A., B. W. Connors, J. W. Lightall and D. A. Prince. (1985). "Comparative electrophysiology of pyramidal and sparsely spiny stellate neurons of the neocortex." J. Neurophysiol. **54**(4): 782-806.

McDonald, M. V. (1989). "Function of song in Scott's seaside sparrow, *Ammodramus maritimus peninsulae*." Anim. Behav. **38**: 468-485.

Mesulam, M. (1978). "Tetramethylbenzidine for horseradish peroxidase neurochemistry: a non-carcinogenic blue reaction product with superior sensitivity for visualizing neural afferents and efferents." J. Histochem. Cytochem. **26**: 106-117.

Nordeen, K. W. and E. J. Nordeen. (1988). "Projection neurons within a vocal motor pathway are born during song learning in zebra finches." Nat. **334**: 149-151.

Nottebohm, F. and A. Arnold. (1976). "Sexual dimorphism in vocal control areas of the songbird brain." Sci. **194**: 211-213.

Nottebohm, F., D. B. Kelley and J. A. Paton. (1982). "Connections of vocal control nuclei in the canary telencephalon." J. Comp. Neurol. **207**: 344-357.

Nottebohm, F., T. M. Stokes and C. M. Leonard. (1976). "Central control of song in the canary, *Serinus canarius*." J. Comp. Neurol. **165**: 457-486.

Okuhata, S. and N. Saito. (1987). "Synaptic connections of thalamo-cerebral vocal control nuclei of the canary." Brain Res. Bull. **18**: 35-44.

Price, P. H. (1979). "Developmental determinants of structure in zebra finch song." J. Comp. Physiol. Psychol. **93**(2): 260-277.

Rall, W., R. E. Burke, T. G. Smith, P. G. Nelson and K. Frank. (1967). "Dendritic location of synapses and possible mechanisms for the monosynaptic EPSP in motoneurons." J. Neurophysiol. **30**: 1169-1193.

Regehr, W. G. and D. W. Tank. (1990). "Postsynaptic NMDA receptor-mediated calcium accumulation in hippocampal pyramidal cell dendrites." Nat. **345**: 807-810.

Ryan, S., A. P. Arnold and R. Elde. (1981). "Enkephalin-like immunoreactivity in vocal control regions of the zebra finch brain." Brain Res. **229**: 236-240.

Ryan, S. M. and A. P. Arnold. (1981). "Evidence for cholinergic participation in the control of bird song: acetylcholinesterase distribution and muscarinic receptor autoradiography in the zebra finch brain." J. Comp. Neurol. **202**: 211-219.

Sakaguchi, H., M. Asano, K. Yamamoto and N. Saito. (1987). "Release of GABA from vocalization nucleus, the robust nucleus of the archistriatum of zebra finch *in vitro*." Brain Res. **410**: 380-384.

Sakaguchi, H. and N. Saito. (1989). "The acetylcholine and catecholamine contents in song control nuclei of zebra finch during song ontogeny." Dev. Brain Res. **47**: 313-317.

Sandell, J. H. and R. H. Masland. (1988). "Photoconversion of some fluorescent markers to a diaminobenzidine product." J. Histochem. Cytochem. **36**(5): 555-559.

Scherer, W. J. and S. B. Udin. (1989). "N-methyl-D-aspartate antagonists prevent binocular interaction maps in *Xenopus* tectum." J. Neurosci. **9**(11): 3837-3843.

Shatz, C. J. (1983). "The prenatal development of the cat's retinogeniculate pathway." J. Neurosci. **3**: 482-499.

Shatz, C. J., J. J. Chun and M. B. Luskin. (1988). The role of the subplate in the development of the mammalian telencephalon. Cerebral Cortex. New York. Plenum.

Shatz, C. J. and M. B. Luskin. (1986). "The relationship between the geniculocortical afferents and their cortical target cells during the development of the cat's primary visual cortex." J. Neurosci. **6**: 3655-3668.

Silva, L. R., Y. Amitai and B. W. Connors. (in press). "Intrinsic oscillations of neocortex generated by layer 5 pyramidal neurons." Sci.

Simpson, H. B. and D. S. Vicario. (1990). "Brain pathways for learned and unlearned vocalizations in zebra finches." J. Neurosci. **10**(5): 1541-1556.

Sohrabji, F., E. J. Nordeen and K. W. Nordeen. (1990). "Selective impairment of song learning following lesions of a forebrain nucleus in the juvenile zebra finch." Behav. Neur. Biol. **53**: 51-63.

Stafstrom, C. E., P. C. Schwindt and W. E. Crill. (1984). "Repetitive firing in layer V neurons from cat neocortex in vitro." J. Neurophysiol. **52**(2): 264-277.

Stewart, W. W. (1978). "Functional connections between cells as revealed by dye-coupling with a highly fluorescent napthalimide tracer." Cell. **14**: 741-759.

Strichartz, G. R. (1973). "Inhibition of sodium currents in myelinated nerve by quaternary derivatives of lidocaine." J. Gen. Physiol. **62**: 37-57.

Thomson, A., D. Girdlestone and D. C. West. (1989). "A local circuit neocortical synapse that operates via both NMDA and non-NMDA receptors." Br. J. Pharmacol. **96**: 406-408.

Thomson, A. M. (1986). "A magnesium-sensitive post-synaptic potential in rat cerebral cortex resembles neuronal responses to N-methylaspartate." J. Physiol. **370**: 531-549.

Udin, S. B. and W. J. Scherer. (1990). "Restoration of the plasticity of binocular maps by NMDA after the critical period in *Xenopus*." Sci. **249**: 669-672.

Vicario, D. S. and F. Nottebohm. (1988). "Organization of the zebra finch song control system: I. Representation of syringeal muscles in the hypoglossal nucleus." J. Comp. Neurol. **271**: 346-354.

Vicario, D. S. and H. B. Simpson. (1988). "Control of syringeal muscles in nucleus RA of Zebra finches." Soc. Neurosci. Abs. **XIV**: 38.10.

Wallen, P. and S. Grillner. (1987). "N-methyl-D-aspartate receptor-induced, inherent oscillatory activity in neurons active during fictive locomotion in the lamprey." J. Neurosci. **7**(9): 2745-2755.

Watson, J. T., E. Adkins-Regan, P. Whiting, J. M. Lindstrom and T. R. Podleski. (1988). "Autoradiographic localization of nicotinic acetylcholine receptors in the brain of the zebra finch (*Poephila guttata*)." J. Comp. Neurol. **274**: 255-264.

Wigstrom, H., B. Gustafsson, Y.-Y. Huang and W. C. Abraham. (1986). "Hippocampal long term potentiation is induced by pairing single afferent volleys with intracellularly injected depolarizing current pulses." Acta Physiol. Scand. **126**: 317-319.

Williams, H. W. (1990). "Models for song learning in the zebra finch: fathers or others?" Anim. Behav. **39**: 745-757.

Zalutsky, R. A. and R. A. Nicoll. (1990). "Comparison of two forms of long-term potentiation in single hippocampal neurons." Sci. **248**: 1619-1624.

Zuschratter, W. and H. Scheich. (1990). "Distribution of choline acetyltransferase and acetylcholinesterase in the vocal motor system of zebra finches." Br. Res. **513**: 193-201.